Homeostasis-Bifurcation Singularities and Identifiability of Feedforward Networks

by

William Duncan

Department of Mathematics
Duke University

Date: _____

Approved:

_____
Michael Reed, Advisor

_____
Jonathan Mattingly

_____
Richard Durrett

_____
James Nolen

Dissertation submitted in partial fulfillment of the
requirements for the degree of Doctor of Philosophy
in the Department of Mathematics
in the Graduate School of
Duke University

2020

ABSTRACT

Homeostasis-Bifurcation Singularities and Identifiability of Feedforward Networks

by

William Duncan

Department of Mathematics
Duke University

Date: _____

Approved:

_____
Michael Reed, Advisor

_____
Jonathan Mattingly

_____
Richard Durrett

_____
James Nolen

An abstract of a dissertation submitted in partial fulfillment of the
requirements for the degree of Doctor of Philosophy
in the Department of Mathematics
in the Graduate School of
Duke University

2020

Copyright © 2020 by William Duncan
All rights reserved

Abstract

This dissertation addresses two aspects of dynamical systems arising from biological networks: homeostasis-bifurcation and identifiability.

Homeostasis occurs when a biological quantity does not change very much as a parameter is varied over a wide interval. Local bifurcation occurs when the multiplicity or stability of equilibria changes at a point. Both phenomena can occur simultaneously and as the result of a single mechanism. We show that this is the case in the feedback inhibition network motif. In addition we prove that longer feedback inhibition networks are less stable. Towards understanding interactions between homeostasis and bifurcations, we define a new type of singularity, the homeostasis-bifurcation point. Using singularity theory, the behavior of dynamical systems with homeostasis-bifurcation points is characterized. In particular, we show that multiple homeostatic plateaus separated by hysteretic switches and homeostatic limit cycle periods and amplitudes are common when these singularities occur.

Identifiability asks whether it is possible to infer model parameters from measurements. We characterize the structural identifiability properties for feedforward networks with linear reaction rate kinetics. Interestingly, the set of reaction rates corresponding to the edges of the graph are identifiable, but the assignment of rates to edges is not; Permutations of the reaction rates leads to the same measurements. We show how the identifiability results for linear kinetics can be extended to Michaelis-Menten kinetics using asymptotics.

For my parents.

Contents

Abstract **iv**

List of Figures **ix**

List of Tables **xi**

Acknowledgements **xii**

1 Introduction **1**

2 Background **3**

2.1 Homeostasis 3

2.1.1 Infinitesimal Homeostasis Points 5

2.2 Bifurcations 8

2.2.1 Steady State Bifurcation 9

2.2.2 Hopf Bifurcation 14

2.3 Identifiability 17

3 Homeostasis and Hopf Bifurcations in Feedback Inhibition **21**

3.1 The Feedback Inhibition Motif 21

3.2 Dependence of Stability on Network Length 23

3.2.1 Stability Properties for Small n 26

3.2.2 Stability Properties for General n 31

3.2.3 Stability Properties for Large I 33

3.3 Instability Regions with Piecewise Linear Feedback Inhibition 36

4 Homeostasis-Bifurcation Singularities **41**

4.1 Homeostasis-Bifurcation Singularities in Feedforward Networks 42

4.2 Reduction to a Scalar Equation: Steady State Bifurcation 44
4.2.1 Derivation of the reduction 45
4.2.2 Preservation of the desired properties 46
4.3 Reduction to a Scalar Equation: Hopf Bifurcation 47
4.3.1 Derivation of the Reduction 48
4.3.2 Preservation of the Desired Properties 52
4.3.3 Limit Cycle Periods Inherit Homeostasis Points 53
4.4 Universal Unfoldings of Homeostasis-Bifurcation Singularities 54
4.5 Transition varieties 55
4.6 Low Codimension Homeostasis-Bifurcation Points 61
4.7 Two Networks with Homeostasis-Bifurcation Points 93
4.7.1 A Network with a Chair-Hysteresis Point 93
4.7.2 A Network with a Chair-Isola Hopf Point 97
4.8 Biologically Relevant Persistent Phenomena 99
4.8.1 Multiple Homeostatic Plateaus in Chair-Hysteresis and Glycolysis 102
4.8.2 Homeostatic Amplitudes and Periods in Chair-Isola Hopf and Circadian Rhythms 103

5 Identifiability of Feedforward Networks 106

5.1 Linear Feedforward Networks 106
5.2 The Input-Output Equations 109
5.3 Identifiability Results 118
5.4 Michaelis-Menten Kinetics 129

6 Conclusion 135

Bibliography **136**

Biography **138**

List of Figures

2.1 A classic chair curve 4

2.2 Unperturbed simple homeostasis and chair points 6

2.3 Perturbations of the chair point, $x(\lambda) = \lambda^3 + a\lambda$ 7

2.4 Unperturbed diagrams of the limit point and simple bifurcation . . . 11

2.5 Persistent diagrams of the hysteresis point $-y^3 + \mu + b_1 y$ 12

2.6 Unperturbed diagrams of the simple and isola Hopf bifurcations . . . 16

2.7 Persistent perturbations of the isola Hopf point $-y^3 - \mu y + by$ 17

3.1 A simple biochemical chain with feedback inhibition 22

3.2 Instabilities in feedback inhibition 23

3.3 Contour used in the proof of Theorem 3.3 28

3.4 Instability regions as a function of network length 34

3.5 A piecewise linear feedback function 37

3.6 Parameter dependence of the instability region 40

3.7 Parameter dependence of the limit cycle amplitudes 40

4.1 A biochemical network with a chair-hysteresis point 94

4.2 The diagrams of x_3 and y_1 at the chair-hysteresis point 95

4.3 Behavior of the chair-hysteresis network of Figure 4.1 96

4.4 A biochemical network exhibiting a chair-isola Hopf point 98

4.5 Diagram of y_4 at the chair-isola Hopf point 98

4.6 Behavior of the chair-isola Hopf network in Figure 4.4 100

4.7 Examples of multiple homeostatic plateaus in chair-hysteresis 103

4.8 Bistability in cultured HeLa cells (reproduced from [MYDH14] 104

4.9 Examples of homeostatic amplitude and period in the chair-isola Hopf 105

5.1 The linear chain: a simple feedforward network 107

5.2 Two simple feedforward networks 107

5.3 Case 7 in the proof of Theorem 5.12 125

List of Tables

2.1 Universal unfoldings of low codimension homeostasis points 8

2.2 Universal unfoldings of low codimension steady state bifurcations . . 10

2.3 Universal unfoldings of low codimension Hopf bifurcations 15

4.1 Defining conditions 62

4.2 Universal unfoldings 63

4.3 The hysteresis and chair transition varieties 67

4.4 The bifurcation transition varieties 68

4.5 Persistent perturbations of homeostasis-steady state bifurcations . . . 69

4.6 Persistent perturbations of homeostasis-Hopf bifurcations 80

Acknowledgements

I would like to thank my advisor, Mike Reed, for his conscientious mentorship and support, for his advocacy for me as a professional mathematician, and for his advice both on mathematics and life.

I thank Jim Nolen, Jonathan Mattingly, and Rick Durrett for serving both on my prelim and defense committee.

I thank the professors at Carnegie Mellon whose mentorship led me to Duke: Bill Hrusa, who first made a PhD sound attainable, and David Kinderlehrer, whose guidance during graduate school applications was invaluable.

I thank Marty Golubitsky for his patient help and collaboration on the work involving singularity theory.

Many friends have made my time in Durham enjoyable. I would especially like to thank my roommates and office mates Matt Beckett and Kevin Stubbs for many conversations which found humor in math, Greg Herschlag for being a role model and climbing mentor, Jeremy Chiang for many late night crosswords, as well as Mike Bell, Ryan Gunderson, Erin Beckman, Josh Cruz, Orsola Capovilla-Searle, Gavin Ball, and Erica Ordog.

Lastly, I would like to thank my parents for their constant support without which this work would not have been possible.

Chapter 1

Introduction

Biological networks of chemical reactions are often modeled with systems of ordinary differential equations (ODEs). Biological questions about the networks can often be framed as mathematical questions about the properties of the ODE system. A biased sampling of some of the properties of interest include the existence of attracting equilibria or limit cycles, bistability, and how equilibria or limit cycle values vary with parameters. Additionally, experimentalists may be interested in which measurements in the biological system will allow them to infer the network's reaction rates.

This dissertation studies the first set of properties using tools from singularity theory. Existence of equilibria and limit cycles, bistability, and how these change as parameters are varied is typically studied using bifurcation theory, an instance of singularity theory. Bifurcation theory is concerned with how the multiplicity and stability of equilibria change as parameters are varied. In addition, it is of biological interest to know which quantities in the network are homeostatic – relatively insensitive to large changes in a parameter. Recently, Golubitsky and Stewart introduced a way to formalize homeostasis mathematically using singularity theory [GS16]. The work in this dissertation combines the two singularities into *homeostasis-bifurcation* singularities. These newly defined singularities allow the homeostasis to be studied simultaneously with multiplicity and stability of equilibria or limit cycles.

The ability to infer parameters from measurement data is known mathematically as identifiability. This dissertation studies the identifiability properties for a class of systems whose network is a directed tree. In particular, we characterize the minimal set of reactants which need to be measured or perturbed in order to infer reaction

rates. Interestingly, the set of reaction rates is identifiable, but which reaction rate is assigned to which reaction is in general not identifiable.

The structure of this document is as follows. In Chapter 2, we give background information that is used in the work of future chapters. In Chapter 3, we study a network with feedback inhibition which exhibits bifurcation and homeostasis produced through the same mechanism. This was the work that motivated the study of homeostasis-bifurcation singularities. In Chapter 4, homeostasis-bifurcation singularities are defined for feedforward networks and the behavior of dynamical systems near these points is characterized. Interestingly, these behaviors including multiple homeostatic plateaus and homeostatic limit cycle amplitudes and periods. Chapter 5 characterizes the identifiability properties for linear ODEs associated to directed trees and extends them to a partial result for when the linear reaction rates are replaced with Michaelis-Menten kinetics.

Chapter 2

Background

In this chapter, background for the three major topics of this dissertation – homeostasis, bifurcation, and identifiability – is reviewed. The material presented in this chapter is not novel, but provides motivation, inspiration, or context for the results of later chapters. In the first section of this chapter, the biological phenomenon of homeostasis is reviewed and mathematical formulations of homeostasis are presented. The formulation of homeostasis as a singularity is emphasized. The second section reviews bifurcation theory and is largely a summary of the relevant material found in [GS85]. The last section covers identifiability with an emphasis on the differential algebra perspective.

2.1 Homeostasis

Homeostasis gives name to the observation that many biologically relevant quantities do not change very much in the face of large environmental and/or genetic variation. A classic example of homeostasis is body temperature in warm-blooded mammals. Over a wide range of environmental temperatures, the body temperature of these organisms will not change very much. In humans, body temperature remains at 98.6°F in cold, temperate, and hot environments. Warm-blooded mammals have mechanisms to control body temperature because maintaining a stable body temperature is vital for the organism to function. As is typical of homeostatic variables, it is possible for these mechanisms to be overwhelmed; In very hot or very cold environment humans become hypo- or hyper- thermic. Fred Nijhout, Mike Reed, and Janet Best

call this phenomenon "escape from homeostasis" and the typical behavior is captured by the so called chair curve (Figure 2.1) [NBR14].

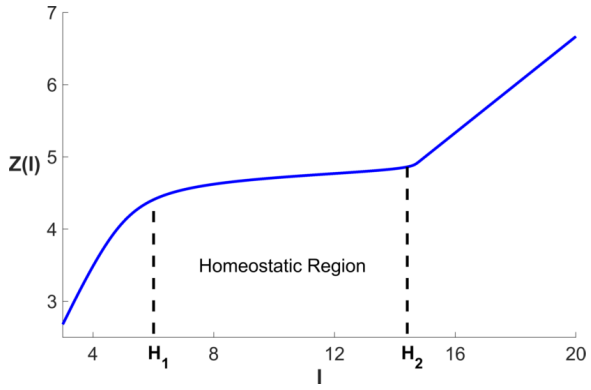

Figure 2.1: **A classic chair curve.** Z is homeostatic with respect to I when I is between H_1 and H_2. For $I < H_1$ or $I > H_2$, Z grows linearly in I so the behavior of Z is not homeostatic. This is the typical "escape from homeostasis behavior".

Towards formalizing homeostasis mathematically, suppose that the biological system of interest can be described by a system of ordinary differential equations depending on a parameter,

$$\dot{X} = G(X, \lambda) \tag{2.1.1}$$

where the dot indicates the time derivative. Roughly speaking, a component of the system, X_i, is homeostatic if the equilibrium value of X_i does not change very much as λ is varied over a wide interval. What "not very much" and "wide" mean will depend on the context and details of the system. Nevertheless, there have been at least two precise mathematical formulations of homeostasis. Note that there are examples of homeostasis that do not fit either definition. The first is known as absolute concentration robustness and is extensively studied by the chemical reaction theory community [SF10, AEJ14, EMKO$^+$16, KUAG17]. X_i is said to have absolute concentration robustness if the equilibrium concentration of X_i is the same for every steady state that (2.1.1) admits. This is a global definition for homeostasis. The

definition that this dissertation will use is a local definition for homeostasis and is discussed in detail in the following subsection.

2.1.1 Infinitesimal Homeostasis Points

This subsection is a summary of [GS16]. Assume that $X \in \mathbb{R}^m$ and $\lambda \in \mathbb{R}$ and suppose (2.1.1) admits a linearly stable equilibrium at (X_0, λ_0). Then we may apply the implicit function theorem to $G(X, \lambda) \equiv 0$ to obtain a curve of stable equilibria as a function of λ, say $X(\lambda)$ where $X(\lambda_0) = X_0$. In applications, we are concerned with the homeostatic properties of a distinguished variable x that we define to be X_i for some i. $x(\lambda)$ is called the input-output function.

Definition 2.1. $x(\lambda) := X_i(\lambda)$ has an *infinitesimal homeostasis point* at λ_0 if $x'(\lambda_0) = 0$. The homeostasis point is a *simple homeostasis point* if in addition $x''(\lambda_0) \neq 0$. It is a *chair point* if $x'(\lambda_0) = x''(\lambda_0) = 0$ and $x'''(\lambda_0) \neq 0$.

Under this formulation, homeostasis is treated as a singularity of the system. We will often drop the "infinitesimal" and call these singularities "homeostasis points". Simple homeostasis and the chair point are pictured in Figure 2.2.

Singularity theory studies the structure of singularities and their perturbations up to appropriate changes of coordinates. The appropriate changes of coordinates for homeostasis are those of elementary catastrophe theory:

$$\hat{G}(X, \lambda) = G(X - K, \Lambda(\lambda)) \tag{2.1.2}$$

where $\Lambda(\lambda_0) = \lambda_0, \Lambda'(\lambda_0) > 0$, and $K = (\kappa_1, \ldots, \kappa_m) \in \mathbb{R}^m$. These changes of coordinates are appropriate because they preserve homeostasis points as stated in the following theorem.

Theorem 2.1. *Let $\Lambda(\lambda)$ be a reparameterization of λ and $K = (\kappa_1, \ldots, \kappa_m) \in \mathbb{R}^m$ be a constant. Define $\hat{G}$ as in* (2.1.2)*. Then*

1. *The input-output function $x(\lambda)$ transforms to*

$$\hat{x}(\lambda) = x(\Lambda(\lambda)) + \kappa_i \tag{2.1.3}$$

2. *Simple homeostasis and chair points are preserved by the input-output transformation* (2.1.3). *That is, if λ_0 is a simple homeostasis point or chair point for x, then so is $\Lambda^{-1}(\lambda_0)$ for $\hat{x}$.*

These changes of coordinates allow use to transform away the properties of the input-output function we aren't interested and retain only the information that we are interested in–the number of consecutive vanishing derivatives at λ_0. Assuming that not all derivatives vanish at λ_0, homeostasis points can be classified by the first nonvanishing λ-derivative $x^{(k)}(\lambda_0)$.

Definition 2.2. Let $x^{(k)}(\lambda_0)$ be the first nonvanishing derivative of $x(\lambda)$ at λ_0. For $k \geq 2$, the *codimension* of x is $k-2$ which is denoted $\text{codim}_H(x) = k-2$.

If $\text{codim}_H(x) = k-2$, then the *normal form* for x is λ^k. This name is given because there is a change of variables of the form (2.1.2) that transforms $x(\lambda)$ to

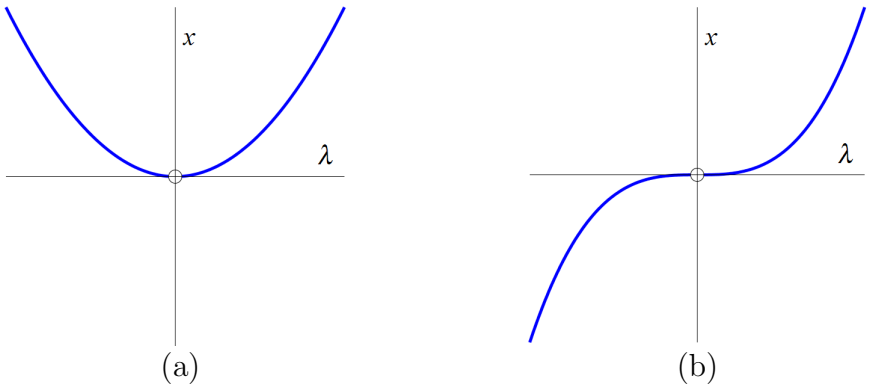

Figure 2.2: **Unperturbed homeostasis and chair points.** The curves are shown for $\varepsilon = 1$ and the singularity is marked in each case. **(a):** The simple homeostasis point. The simple homeostasis is its own unfolding so every perturbation is equivalent to this curve. **(b):** The chair point $x(\lambda) = \lambda^3$.

λ^k in this case. Another way to say this is that $x(\lambda)$ locally looks like λ^k when $\text{codim}_H(x) = k - 2$.

Definition 2.3. $\mathcal{X}(\lambda, a)$ is an *unfolding* of $x(\lambda)$ if $\mathcal{X}(\lambda, 0) = x(\lambda)$. $\mathcal{X}$ is a *universal unfolding* of x if every unfolding $\mathcal{Y}(\lambda, b)$ *factors through* $\mathcal{X}$. That is,

$$\mathcal{Y}(\lambda, b) = \mathcal{X}(\Lambda(\lambda, b), A(b)) + \kappa(b).$$

The universal unfolding of x captures all possible perturbations of x. This is important because in applications singularities of codimension one or greater are never observed because they require perfect choice of the external parameters (a in $\mathcal{X}(\lambda, a)$). Perturbations of high codimension singularities can be observed in applications, although low codimension phenomena are more common. Perturbations of the chair point can be seen in Figure 2.3. The number of external parameters in the universal unfolding of x is equal to the codimension of x.

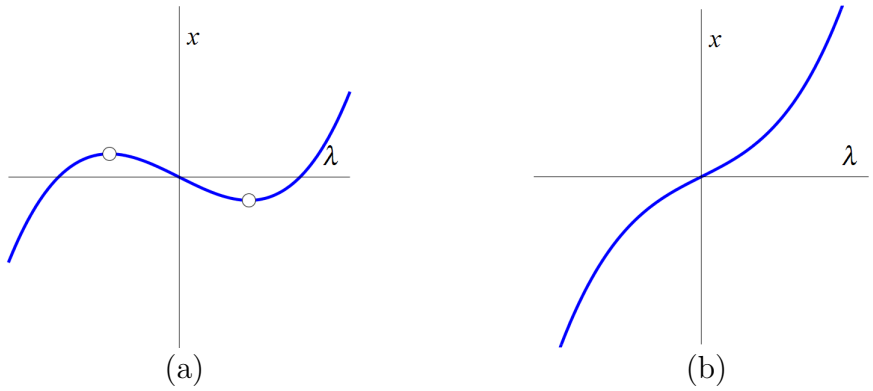

Figure 2.3: **Persistent perturbations of the chair point $x(\lambda) = \lambda^3 + a\lambda$.** Simple homeostasis points are marked. **(a):** $a = -\frac{1}{2}$. The two simple homeostasis points are separated. **(b):** $a = \frac{1}{2}$. The two homeostasis points collided at $a = 0$ and annihilated each other.

Theorem 2.2. *Let $x(\lambda)$ be an input-output function with a homeostasis point at λ_0 and $\text{codim}_H(x) = k - 2$. If $k = 2$ then the universal unfolding of x is $\mathcal{X}(\lambda, a) = \pm\lambda^2$.*

If $k \geq 3$, then the universal unfolding of x is given by

$$\mathcal{X}(\lambda, a) = \pm\lambda^k + a_{k-2}\lambda^{k-2} + a_{k-3}\lambda^{k-3} + \cdots + a_{21}\lambda$$

where $a = (a_{21}, \ldots, a_{k-2})$.

The normal forms and universal unfoldings for low codimension homeostasis points are summarized in Table 2.1.

Table 2.1: **Universal unfoldings of low codimension homeostasis points.** $\varepsilon = \pm 1$. The normal forms, $x(\lambda)$, can be recovered by setting $a_1 = 0$.

Universal Unfolding, $\mathcal{X}(\lambda, a)$	Nomenclature	$\text{codim}_H(x)$
$\varepsilon\lambda^2$	Simple Homeostasis	0
$\varepsilon\lambda^3 + a_1\lambda$	Chair Point	1

2.2 Bifurcations

In some ways bifurcation is the opposite of homeostasis. Near a homeostasis point, the equilibrium of a system is not quantitatively changing as a parameter is varied. At a bifurcation point, the equilibrium is not only quantitatively changing, it is qualitatively changing. The curve of equilibria may disappear, lose stability, split into multiple equilibria, become a limit cycle, or have a vertical tangent line. The property of interest for homeostasis singularities is number of nearby points were $x'(\lambda) = 0$ whereas for bifurcation points, the properties of interest are multiplicity and stability of equilibria or limit cycles.

There are two types of bifurcation points of interest for the purpose of this dissertation: steady state bifurcation and Hopf bifurcation. There is a subsection below devoted to each type. In either case, we consider a system of the form

$$\dot{Y} = F(Y, \mu) \tag{2.2.1}$$

where the dot indicates a time derivative, $Y \in \mathbb{R}^n$, and $\mu \in \mathbb{R}$ is a distinguished bifurcation parameter. This section is a summary of the relevant material from [GS85].

2.2.1 Steady State Bifurcation

Let (Y_0, μ_0) be an equilibrium of (2.2.1). If the Jacobian, $(D_Y F)_{(Y_0,\mu_0)}$, is non-singular, then by the implicit function theorem the equilibrium value of Y is locally a function of μ. Steady state bifurcation points are exactly those points where the implicit function theorem fails. Specifically, we consider the case that $D_Y F$ has a single 0 eigenvalue. In this case, solutions to $F(Y, \mu) = 0$ can locally be put into one-to-one correspondence to solutions of a scalar equation

$$f(y, \mu) = 0$$

where $y \in \mathbb{R}$ via the Lyapunov-Schmidt reduction (see Section 4.2 for details of this reduction). There is a relationship between derivatives of F at (Y_0, μ_0) and derivatives of f at the corresponding (y_0, μ_0). The zero eigenvalue of $(D_Y F)_{(Y_0,\mu_0)}$ means $f_y(y_0, \mu_0) = 0$. Bifurcations are a singularity exactly because $f = f_y = 0$. Rather than study the full system, (2.2.1), the scalar equation, $f = 0$, will be the main object of study.

The quantities of interest for steady state bifurcation are multiplicity and stability of solutions. This information is typically summarized by plotting the bifurcation diagram – the set (y, μ) of solutions to $f(y, \mu) = 0$ (see Figures 2.4 and 2.5 for examples of bifurcation diagrams). The change of coordinates which preserve these properties are given by

$$\hat{f}(y, \mu) = S(x, \mu) f(\mathcal{Y}(y, \mu), M(\mu)) \tag{2.2.2}$$

where S, Y, and M are smooth mappings satisfying $S > 0$, $\mathcal{Y}_y > 0$, and $M_\mu > 0$.

Definition 2.4. If $\hat{f}$ and f can be related by a change of coordinates as in (2.2.2), then $\hat{f}$ and f are *equivalent as bifurcations.*

Within each equivalence class, a representative called the normal form is chosen. Each function within the equivalence class is locally qualitatively the same as the normal form where "qualitatively the same" means that the multiplicity and stability of the solutions agree. As with homeostasis singularities, bifurcations and their normal forms can be classified by the codimension of the singularity. The codimension of a bifurcation is defined by its universal unfolding.

Definition 2.5. $h(y, \mu, b)$ where $b = (b_1, b_2, \ldots, b_k)$ is an *unfolding* of f if $h(y, \mu, 0) = f(y, \mu)$. h is a *versal unfolding* of f if every unfolding, g, of f factors through h. That is, there are smooth mappings $S, M, \mathcal{Y}$, and B such that

$$h(y, \mu, b) = S(y, \mu, b)g(\mathcal{Y}(y, \mu, b), M(\mu, b), B(b))$$

where $S(y, \mu, 0) \equiv 1$, $\mathcal{Y}(y, \mu, 0) \equiv y$, $M(\mu, 0) \equiv \mu)$, and $B(0) = 0$. h is a *universal unfolding* of f if h is a versal unfolding and k is the minimum number of parameters in any versal unfolding of f. In this case, k is the *codimension* of f and we write $\text{codim}_B(f) = k$.

Table 2.2: **Universal unfoldings of low codimension steady state bifurcations.** $\varepsilon = \pm 1$ and $\delta = \pm 1$. The normal forms of codimension 1 bifurcations can be recovered by setting $b_1 = 0$.

Universal Unfolding, $h(y, \mu)$	Nomenclature	$\text{codim}_B(f)$
$\varepsilon y^2 + \delta\mu$	Limit point	0
$\varepsilon(y^2 - \mu^2 + b_1)$	Simple bifurcation	1
$\varepsilon(y^2 + \mu^2 + b_1)$	Isola	1
$\varepsilon y^3 + \delta\mu + b_1 y$	Hysteresis	1

The universal unfolding captures all possible perturbations of the corresponding bifurcation point. As with homeostasis points, this is important because only perturbations of bifurcations are observed in applications. The universal unfoldings for

low codimension steady state bifurcations are listed in Table 2.2. The unperturbed diagrams for the limit point and hysteresis point are drawn in Figure 2.4. The persistent perturbations of the hysteresis point are pictured in 2.5. The limit point is its own universal unfolding and therefore persistent.

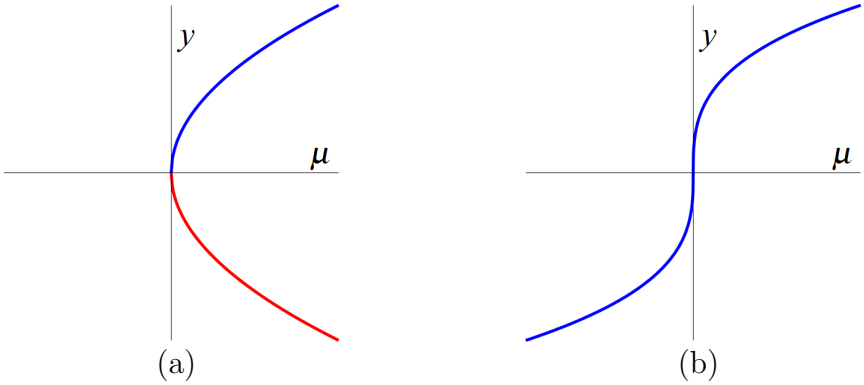

Figure 2.4: **Unperturbed diagrams of the limit point and simple bifurcation.** The diagrams are drawn with $\varepsilon = -1$ and $\delta = 1$. Blue (red) curves indicates stable (unstable) equilibria where we assume $f_y < 0$ implies stability. **(a):** The limit point bifurcation. The limit point is its own unfolding, so this diagram is equivalent to every perturbation of the limit point. **(b):** The hysteresis point.

The universal unfolding of a bifurcation can be used to enumerate all qualitative behaviors arising from perturbations of the bifurcation point that are themselves stable under perturbations. These behaviors are called persistent behavior, persistent phenomena, or persistent perturbations. To do so, we will need to compute another object related to the universal unfolding which describes when the bifurcation diagram qualitatively changes.

Definition 2.6. Define $\mathscr{B}$, $\mathscr{H}$, $\mathscr{D}$, and Σ by

$$\mathscr{B} = \{b \in \mathbb{R}^k \mid \exists (y, \mu) \in \mathbb{R} \times \mathbb{R} \text{ such that } h = h_y = h_\mu = 0 \text{ at } (y, \mu, b)\},$$

$$\mathscr{H} = \{b \in \mathbb{R}^k \mid \exists (y, \mu) \in \mathbb{R} \times \mathbb{R} \text{ such that } h = h_y = h_{yy} = 0 \text{ at } (y, \mu, b)\},$$

$$\mathscr{D} = \{b \in \mathbb{R}^k \mid \exists (y_1, y_2, \mu) \in \mathbb{R} \times \mathbb{R} \times \mathbb{R} \text{ such that } h = h_y \text{ at } (y_i, \mu, b), i = 1, 2\},$$

$$\Sigma = \mathscr{B} \cup \mathscr{H} \cup \mathscr{D}.$$

$\mathscr{B}$, $\mathscr{H}$, and $\mathscr{D}$ are the *bifurcation*, *hysteresis*, and *double limit point* transition varieties, respectively.

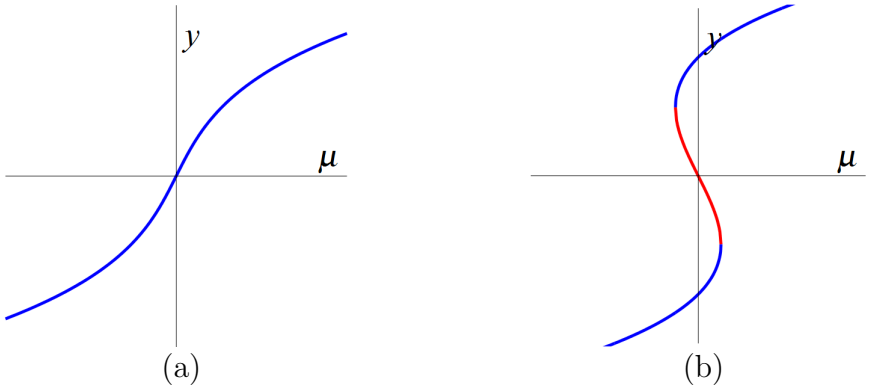

Figure 2.5: **Persistent diagrams of the hysteresis point** $-y^3 + \mu + b_1 y$**.** Blue (red) curves indicate stable (unstable) equilibria where we assume $f_y < 0$ implies stability. The transition variety is $\Sigma = \mathscr{H} = \{b_1 = 0\}$. **(a):** $b_1 = -\frac{1}{2}$. **(b):** $b_1 = \frac{1}{2}$.

Typically, we consider h on a finite domain $U \times L \times W$ where U and L are closed intervals and $W \subset \mathbb{R}^k$. The transition varieties defined above are local in that they contain the bifurcation point corresponding to $b = 0$. There are non-local transitions corresponding to transitions occurring on the boundary of $U \times L$. We do not consider these transitions.

Theorem 2.3. *Let U and L be closed intervals and $W \subset \mathbb{R}^k$. Let*

$$h : U \times L \times W \to \mathbb{R}$$

be an unfolding of a bifurcation point. Let b_1 *and* b_2 *be in the same connected component of* $W \setminus \Sigma$ *and suppose there are no boundary transitions. Then* $h(\cdot, \cdot, b_1)$ *and* $h(\cdot, \cdot, b_2)$ *are equivalent as bifurcations.*

In principle, Theorem 2.3 does not rule out equivalence between $h(\cdot, \cdot, b_1)$ and $h(\cdot, \cdot, b_2)$ when b_1 and b_2 are in different connected components but there are no known examples of this.

The subsection concludes with an important consequence of equivalence as bifurcations that is used in Chapter 4. Assume that $h(y, \mu, b) \neq 0$ for $(y, \mu, b) \in \partial U \times L \times W$. This assumption is not necessary, but simplifies the notation and exposition.

Definition 2.7. Fix $b \in W$. A *branch* of h is a continuous function $C : [L_1, L_2] \to U$ which is smooth on $(L_1, L_2) \subset L$ and satisfies

1. $h(C(\mu), \mu, b) = 0$ on $[L_1, L_2]$, and
2. either $L_i \in \partial L$ or $(C(L_i), L_i, b)$ is a bifurcation point of h for $i = 1, 2$.

Definition 2.8. Let $b_1, b_2 \in W \setminus \Sigma$. Define $f(y, \mu) = h(y, \mu, b_1)$ and $g(y, \mu) = h(y, \mu, b_2)$. f and g are *combinatorially equivalent* if

1. The mappings f and g have the same number of limit points, right-hand boundary points, and left-hand boundary points.
2. There is a natural bijection between branches of f and g induced by (1). If there is a branch of f, C^f, with end points L_1^f and L_2^f then there is a branch of g, C^g, with end points L_1^g and L_2^g such that L_i^f and L_i^g are end points of the same type for $i = 1, 2$. The same holds when the roles of f and g are switched.
3. The bijection of branches of f to branches of g preserves the ordering of branches.

Theorem 2.4. *Suppose b_1 and b_2 are in the same connected component of $W \setminus \Sigma$. Then $h(\cdot, \cdot, b_1)$ and $h(\cdot, \cdot, b_2)$ are combinatorially equivalent.*

2.2.2 Hopf Bifurcation

Hopf bifurcations occur when the Jacobian, $(D_Y F)_{(Y_0,\mu_0)}$ has a pair of purely imaginary eigenvalues, $\pm i\omega$. At a simple Hopf bifurcation, an equilibrium solution bifurcates into a limit cycle and an equilibrium as pictured in Figure 2.6(a). As with steady state bifurcations, we would like to reduce the system to a scalar equation. This is possible by applying the Lyapunov-Schmidt reduction to the operator defined by $Lu = \frac{d}{dt}u + F(u, \mu)$ and looking for periodic solutions (see Section 4.3 for details). Doing so results in a scalar equation

$$f(y, \mu) = 0, \quad y \geq 0$$

but in this case solutions are in one-to-one correspondence to periodic solutions of (2.2.1) and y is the amplitude of the limit cycle. Solutions with $y = 0$ are equilibrium solutions. There is a rotational symmetry in periodic solutions that manifests as a $\mathbb{Z}_2$ symmetry for the reduced equation:

$$f(-y, \mu) = -f(y, \mu).$$

The result is that f can be written as

$$f(y, \mu) = r(y^2, \mu)y$$

for some smooth function r. The change of coordinates that define equivalence for Hopf bifurcations need to respect this symmetry so the allowable transformations are of the form

$$\hat{f}(y, \mu) = S(y, \mu) f(\mathcal{Y}(y, \mu), M(\mu)) \tag{2.2.3}$$

where $S(-y, \mu) = S(y, \mu) > 0$, $\mathcal{Y}_y > 0$, $\mathcal{Y}(-y, \mu) = -\mathcal{Y}(y, \mu)$, and $M_\mu > 0$.

Definition 2.9. If $\hat{f}$ and f can be related by a change of coordinates of the form (2.2.3) then $\hat{f}$ and f are $\mathbb{Z}_2$-*equivalent as bifurcations.*

The definition for the universal unfolding for Hopf bifurcations is similar.

Definition 2.10. $h(y, \mu, b)$ where $b = (b_1, b_2, \ldots, b_k)$ is a $\mathbb{Z}_2$-*unfolding* of f if $h(y, \mu, 0) = f(y, \mu)$ and $h(-y, \mu, b) = -h(y, \mu, b)$. h is a $\mathbb{Z}_2$-*versal unfolding* of f if every $\mathbb{Z}_2$-unfolding, g, of f factors through h. That is, there are smooth mappings S, M, $\mathcal{Y}$, and B such that

$$h(y, \mu, b) = S(y, \mu, b)g(\mathcal{Y}(y, \mu, b), M(\mu, b), B(b))$$

where $S(y, \mu, 0) = 1$, $\mathcal{Y}(y, \mu, 0) = y$, $M(\mu, 0) = \mu$, $B(0) = 0$, $S(-y, \mu, b) = S(y, \mu, b)$, and $\mathcal{Y}(-y, \mu, b) = -\mathcal{Y}(y, \mu, b)$. h is a $\mathbb{Z}_2$-*universal unfolding* of f if h is $\mathbb{Z}_2$-versal and k is the minimum number of parameters in any versal unfolding of f. In this case, k is the $\mathbb{Z}_2$-codimension of f and we write $\text{codim}_B^{\mathbb{Z}_2}(f) = k$.

We will often drop the $\mathbb{Z}_2$ when the context is clear. As with steady state bifurcation, the universal unfolding captures all persistent perturbations of the singularity. The difference is that the perturbations allowed in the case of Hopf bifurcations are restricted to those that respect the $\mathbb{Z}_2$ symmetry. For this reason codimension and $\mathbb{Z}_2$-codimension often do not agree for the same f. The universal unfoldings for low $\mathbb{Z}_2$-codimension Hopf bifurcations are listed in Table 2.3.

Table 2.3: **Universal unfoldings of low codimension Hopf bifurcations.** $\varepsilon = \pm 1$ and $\delta = \pm 1$. The normal forms can be recovered by setting $b_1 = 0$.

Universal Unfolding, $h(y, \mu, b)$	Nomenclature	$\text{codim}_B^{\mathbb{Z}_2}(f)$
$\varepsilon y^3 + \delta y\mu$	Simple Hopf	0
$\varepsilon(y^3 + y\mu^2 + b_1 y)$	Isola Hopf	1
$\varepsilon(y^3 - y\mu^2 + b_1 y)$		1
$\varepsilon y^5 + \delta y\mu + b_1 y^3$		1

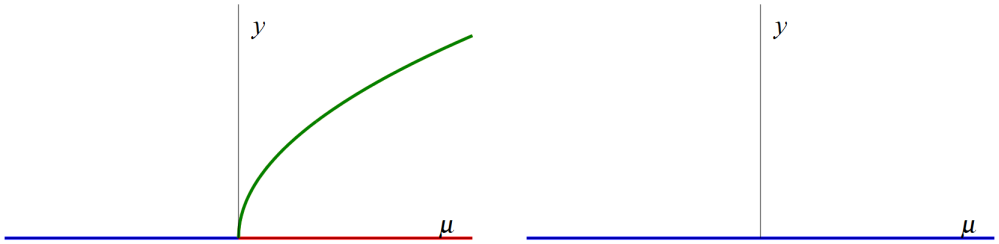

(a) (b)

Figure 2.6: **Unperturbed diagrams of the simple and isola Hopf bifurcations.** Blue (red) curves indicate stable (unstable) equilibria. **(a):** The green curve indicates amplitudes of stable limit cycles. The simple Hopf point is its own unfolding, so this diagram is equivalent to every perturbation of the simple Hopf point. **(b):** At the singular point, two simple Hopf points coincide. The result is that the two singularities annihilate each other.

Definition 2.11. Let $h(y, \mu, b) = r(y^2, \mu, b)y$ and define $u = y^2$. The $\mathbb{Z}_2$ *transition varieties* are defined by

$$\mathscr{B}_1 = \{b \in \mathbb{R}^k \mid \exists(u, \mu), u > 0 \text{ such that } r = r_u = r_\mu = 0 \text{ at } (u, \mu, b)\}$$

$$\mathscr{B}_0 = \{b \in \mathbb{R}^k \mid \exists(u, \mu), u > 0 \text{ such that } r = r_\mu = 0 \text{ at } (0, \mu, b)\}$$

$$\mathscr{H}_1 = \{b \in \mathbb{R}^k \mid \exists(u, \mu), u > 0 \text{ such that } r = r_u = r_{uu} = 0 \text{ at } (u, \mu, b)\}$$

$$\mathscr{H}_0 = \{b \in \mathbb{R}^k \mid \exists(u, \mu), u > 0 \text{ such that } r = r_u = 0 \text{ at } (0, \mu, b)\}$$

$$\mathscr{D}(\mathbb{Z}_2) = \{b \in \mathbb{R}^k \mid \exists(u_1, u_2, \mu), u_i > 0 \text{ such that } r = ur_u = 0 \text{ at } (u_i, \mu, b), i = 1, 2\}$$

$$\Sigma(\mathbb{Z}_2) = \mathscr{B}_1 \cup \mathscr{B}_0 \cup \mathscr{H}_1 \cup \mathscr{H}_0 \cup \mathscr{D}(\mathbb{Z}_2)$$

Theorem 2.5. *Let U and L be closed intervals and $W \subset \mathbb{R}^k$. Let $h : U \times L \times W \to \mathbb{R}$ be a $\mathbb{Z}_2$-unfolding of a Hopf bifurcation with $h(y, \mu, b) = r(y^2, \mu, b)y$. Let b_1 and b_2 be in the same connected component of $W \setminus \Sigma(\mathbb{Z}_2)$ and suppose there are no boundary transitions. Then*

1. *$h(\cdot, \cdot, b_1)$ and $h(\cdot, \cdot, b_2)$ are $\mathbb{Z}_2$-equivalent as bifurcations.*

2. *$r(\cdot,\cdot,b_1)$ and $r(\cdot,\cdot,b_2)$ are combinatorially equivalent.*

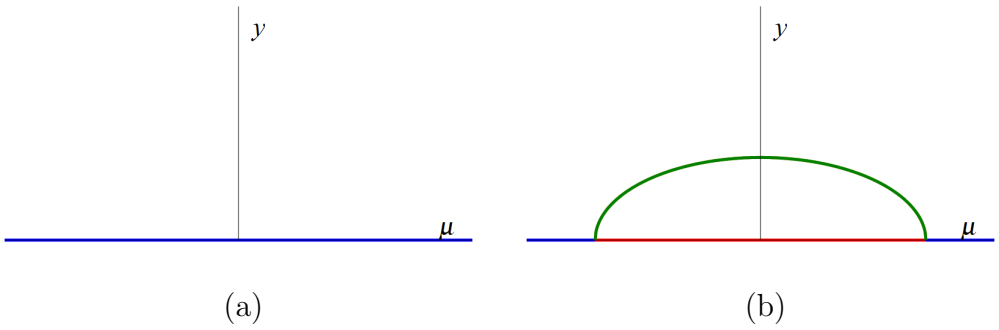

Figure 2.7: **Persistent perturbations of the isola Hopf point $-y^3 - \mu y + by$.** The transition variety is given by $\Sigma(\mathbb{Z}_2) = \mathscr{B}_0 = \{b = 0\}$. Blue (red) curves indicate stable (unstable) equilibria. **(a):** $b = -\frac{1}{2}$. The two simple Hopf points have annihilated each other. **(b):** $b = \frac{1}{2}$. The two simple Hopf points have separated and are connected by a curve of stable limit cycles.

2.3 Identifiability

A dynamical system with parameters is identifiable if, given measurements of the system, it is possible to determine the parameters which produced those measurements. There are two notions of identifiability: structural and practical. Practical identifiability is concerned with whether parameters can be inferred from realistic or actual data. Measurement noise and the finite number of measurements taken are major issues in practical identifiability. Structural identifiability asks whether it is possible to identify parameters given perfect and arbitrary number of measurements. Clearly structural identifiability is a necessary condition for practical identifiability. Additionally, structural identifiability analysis can give insights into what measurements would be useful to make. Chapter 5 is concerned with the structural identifiability of a class of differential equations which arise from feedforward networks. We

therefore review structural identifiability here, but not practical identifiability. For the remainder of this section, we use identifiability to mean structural identifiability. The material in this section is based on the exposition of [ERT13].

Consider a differential equation model $\dot{x} = f(x, u, a)$ where x is the vector of state variables, $u = u(t)$ is a vector of input functions controlled by the experimenter, and a is a vector of parameters. The experimentally observed vector of output variables is defined by $y = g(x, a)$. We will use Greek letters, α in this case, to denote the unobserved "true" value of the parameters.

Definition 2.12. Given an ODE model $\dot{x} = f(x, u, a)$ and output y, a parameter a_k is *globally identifiable* if for almost every value α the equation $y(x, a) = y(x, \alpha)$ implies $a_k = \alpha_k$. The parameter a_k is *locally identifiable* if for almost any α the equation $y(x, a) = y(x, \alpha)$ implies that a_k has a finite number of solutions. a_k is *unidentifiable* if $y(x, a) = y(x, \alpha)$ implies that a_k has an infinite number of solutions.

Definition 2.13. The model $\dot{x} = f(x, u, a)$, $y = g(x, a)$ is globally (locally) identifiable if every parameter is globally (locally) identifiable.

Example 2.1. Consider the system given by

$$\begin{aligned} \dot{x} &= u(t) - (a + b)x \\ y &= x \end{aligned} \tag{2.3.1}$$

where a and b are parameters. (2.3.1) is unidentifiable and the reason is simple: a and b only appears as the sum $a + b$ and it is only this sum which determines the behavior of y. If α and β are the true parameters, then $a = \alpha + c$ and $b = \beta - c$ is a solution for any choice of c.

We take the differential algebra approach to solving the identifiability problem. The method relies on using algebraic manipulations to rewrite the model as a monic polynomial in only the outputs variables y, the input variables u, and the derivatives

of y and u, with coefficients in the parameters a. If $y \in \mathbb{R}^m$ then the input-output equations will be a set of m equations. It is possible to write a single nth order differential equation as a system of n first order differential equations. Finding the input-output equation when $m = 1$ is similar to reversing this process – rewriting a system of n first order differential equations as a single nth order differential equation. The coefficients of the *input-output equations* are identifiable and we have the following theorem from [Eis13].

Theorem 2.6. *The parameters of a rational function ODE model $x(u, a)$, $y(x, a)$ are globally (locally) identifiable if and only if the map $c(a)$ from the parameters to the coefficients of a set of input-output equations is injective (the fibers contain finitely many elements), regardless of how the input-output equations are generated.*

Example 2.2. In (2.3.1), there is only one output and the input-output equation can be obtained by substituting $y = x$ into the differential equation: $\dot{y} = u(t) - (a + b)y$. Theorem 2.6 says that the coefficients of the input-output equation contain all identifiability information. $a + b$ is the only coefficient so the identifiability can be determined by solving

$$a + b = \alpha + \beta. \tag{2.3.2}$$

However, we cannot solve (2.3.2) for a or b individually, verifying the earlier claim that a and b are unidentifiable.

Example 2.3. Consider the system given by

$$\begin{aligned} \dot{x}_1 &= u(t) - a_{21}x_1 \\ \dot{x}_2 &= a_{21}x_1 - b_2x_2 \\ y &= x_2. \end{aligned} \tag{2.3.3}$$

The parameters a_{21} and b_2 are named to be consistent with the notation of Chapter 5. Substituting $y = x_2$ into the second equation we have

$$a_{21}x_1 = \dot{y} + b_2 y. \tag{2.3.4}$$

Differentiating (2.3.4),

$$a_{21}\dot{x}_1 = \ddot{y} + b_2\dot{y}. \tag{2.3.5}$$

Substituting (2.3.4) and (2.3.5) into the first equation of (2.3.3),

$$\frac{1}{a_{21}}\ddot{y} + \frac{b_2}{a_{21}}\dot{y} = u(t) - \dot{y} + b_2 y. \tag{2.3.6}$$

Multiplying by a_{21} to make the polynomial monic and rearranging gives the input-output equation

$$\ddot{y} + (a_{21} + b_2)\dot{y} + a_{21}b_2 y = a_{21}u(t). \tag{2.3.7}$$

The coefficients, $a_{21}+b_2$, $a_{21}b_2$, and a_{21} are identifiable so the question of identifiability is reduced to solving $a_{21} + b_2 = \alpha_{21} + \beta_2$, $a_{21}b_2 = \alpha_{21}\beta_2$, and $a_{21} = \alpha_{21}$. The only solution is $a_{21} = \alpha_{21}$ and $b_2 = \beta_2$ so this model is globally identifiable.

Chapter 3

Homeostasis and Hopf Bifurcations in Feedback Inhibition

This chapter is based on work published in Mathematical Biosciences [DBG+18] and was done in collaboration with Janet Best, Martin Golubitsky, Fred Nijhout, and Michael Reed. In this work, the behavior of the biochemical network motif of feedback inhibition is studied both analytically and numerically as a function of various parameters. In particular, it is shown that the same mechanisms that lead to Hopf bifurcations also contribute to homeostasis. This motivated the more general study of the interaction between homeostasis and bifurcations which is discussed in Chapter 4.

In Section 3.1, the feedback inhibition motif is introduced and basic properties are discussed. In Section 3.2, the dependence of stability of the equilibrium on the inhibition function and network length is studied both analytically and through numerics. In Section 3.3, a simple choice is made for the feedback function to facilitate understanding of how the details of the feedback function effect stability.

3.1 The Feedback Inhibition Motif

Feedback inhibition is a common control mechanism in biochemical networks in which the product of a series of chemical reactions inhibits one of the reactions involved in its production. One realization of the feedback inhibition motif is shown in Figure 3.1 and this is the network which is studied in this chapter. The last element in the

chain, X_n, inhibits the reaction that converts X_1 to X_2. This kind of feedback inhibition is one of the most common homeostatic mechanisms in biochemistry [RBG+17]. The homeostatic variable is X_n because as I increases, X_n tends to increase, which increases the inhibition by f, limiting how much X_n rises.

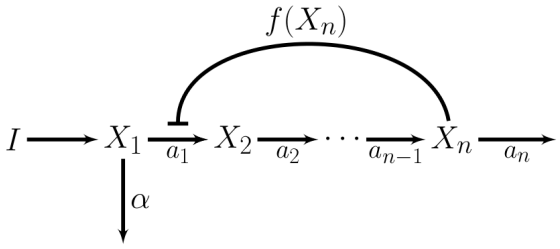

Figure 3.1: **A simple biochemical chain with feedback inhibition.** The variable X_n inhibits the reaction that takes X_1 to X_2 via the function $f(X_n)$. I is the input to the chain, α is a leakage parameter which determines the rate at which X_1 leaves the system, and a_j are the forward reaction rates.

For $n = 4$ and an appropriate choice of the inhibitory function, f, the system shows the behavior indicated in figure 3.2. For I small, the equilibrium is stable and $X_4(I)$ increases linearly in I. At the value I_1 there is a Hopf bifurcation and the equilibrium becomes unstable but shows homeostasis (the red curve). Finally at I_2, the equilibrium becomes stable again and shortly thereafter $X_4(I)$ shows escape from homeostasis by rising linearly with I. For I in the interval (I_1, I_2), the system has a stable limit cycle; the green curves show the maximum and minimum values of $X_4(I, t)$ as $X(I, t)$ traverses the limit cycle for fixed I.

If a different choice for f or α were made, then there may not be Hopf bifurcations in the homeostatic plateau, the equilibrium would be stable for all values of I, and $X_4(I)$ would be a classic chair curve as shown in Figure 2.1. Determining this dependence is the focus of the remainder of this chapter.

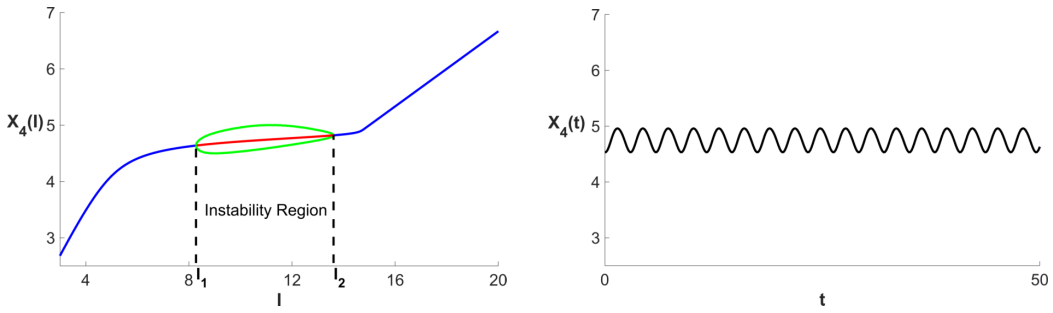

Figure 3.2: **Instabilities in feedback inhibition.** In the feedback chain of Figure 3.1, the equilibrium becomes unstable for I in the interval (I_1, I_2) for an appropriate choice of the feedback function f. We chose $n = 4$, $\alpha = 1$, $a_j = 1$ for each j, and $f(x) = 10e^{-1/(5-x)+1/5}\Theta\big(5-x\big)+1/2$, where $\Theta(x)$ is the Heaviside step function. **(a):** The blue (red) curves shows the values of $X_4(I)$ at the stable (unstable) equilibria. The green curves show the maximum and minimum values of X_4 as the dynamics traverses the limit cycle for fixed I. **(b):** The time course of the oscillations in X_4 for $I = 10$, where the maximum amplitude oscillations are obtained.

3.2 Dependence of Stability on Network Length

In this section, the dependence of stability of equilibrium solutions on n and f is studied. Throughout this section the following assumptions are made on f:

$$f \text{ is differentiable, } f > 0, \text{ and } f' \leq 0. \tag{3.2.1}$$

The assumption that $f > 0$ is made so that the backwards reaction of $X_2 \to X_1$ does not occur and the forward reaction of $X_1 \to X_2$ always occurs at some rate. The assumption that $f' \leq 0$ is made so that X_n inhibits the production of X_2 from X_1. Additionally, assume $a_j > 0$ for each j. Other hypotheses will be introduced as appropriate. Let $x_i(t)$ denote the concentration of X_i at time t. Each differential equation expresses that the rate of change of the variable is the rate at which it is made minus the rate at which it is consumed. We assume mass action kinetics for all reactions except for the rate from X_1 to X_2 that depends on inhibition from X_n expressed through f.

The dynamics are given explicitly by

$$\begin{aligned}
\dot{x}_1 &= I - (a_1 f(x_n) + \alpha) x_1 \\
\dot{x}_2 &= a_1 f(x_n) x_1 - a_2 x_2 \\
\dot{x}_3 &= a_2 x_2 - a_3 x_3 \\
&\vdots \\
\dot{x}_n &= a_{n-1} x_{n-1} - a_n x_n
\end{aligned} \tag{3.2.2}$$

where dot indicates a derivative in t. When $\alpha = a_2$, $\dot{x}_1 + \dot{x}_2 = I - a_2(x_1 + x_2)$ so that as $t \to \infty$, $x_1 + x_2 \to I/a_2$. This allows the reduction of the dimension of the steady state Jacobian by 1 and significantly simplifies the analysis. For $n = 2, 3, 4$, a necessary and sufficient condition for instability is given, and the same is done for $n = 5$ if $\alpha = 1$. For general n, we provide a necessary condition for instability and a sufficient condition for instability, but neither is necessary and sufficient.

First, we show that there is always a unique equilibrium solution. Using equation (3.2.2), it is easy to see that the steady state solutions satisfy

$$\begin{aligned}
\bar{x}_1 &= \frac{I}{a_1 f(\bar{x}_n) + \alpha} \\
\bar{x}_j &= \frac{1}{a_j} \frac{a_1 f(\bar{x}_n) I}{a_1 f(\bar{x}_n) + \alpha} \quad \text{for } j \geq 2.
\end{aligned} \tag{3.2.3}$$

Proposition 3.1. *Suppose f satisfies* (3.2.1)*. Then for each $I \in [0, \infty)$,* (3.2.3) *has a unique solution.*

Proof. Let $\ell(x) = (a_1 f(x) + \alpha)(a_n x)/(a_1 f(x))$ so that $\ell(\bar{x}_n) = I$. By the hypotheses on f, $\ell(x)$ is strictly monotone increasing, $\ell(0) = 0$ and $\ell(x) \to \infty$ as $x \to \infty$. Thus, $\ell : [0, \infty) \to [0, \infty)$ is invertible, so that $\bar{x}_n$ is determined by I. For $j < n$, each $\bar{x}_j$ is an explicit function of $\bar{x}_n$ and I and is thus determined. ■

From now on, we drop the overbar and denote $x_j = x_j(I)$ as the steady state concentration of X_j. Except in Theorem 3.2, we consider only $a_j = 1$ for each j.

We are interested in the value of x_n and the stability of the equilibrium. As (3.2.3) shows, x_n depends only on a_1 and a_n. The value of a_n scales x_n, so varying a_n leaves the range of homeostasis unchanged. Changing a_1 is equivalent to rescaling $f(x)$, so nothing is lost by setting $a_1 = 1$. We choose $a_j = 1$ for $j = 2, \ldots, n-1$ for simplicity. Choosing other values may change the stability of the equilibrium, but makes the proofs more complicated and the statements of some inequalities a little different while involving no new ideas. We will see later that the choice of α does make a difference.

Differentiating the steady state equation for x_n with respect to I and using (3.2.1), we have, for $a_j = 1$,

$$x_n'(I) = \frac{f(x_n)(f(x_n)+\alpha)}{(f(x_n)+\alpha)^2 - \alpha f'(x_n) I} \tag{3.2.4}$$

so that $x_n'(I) > 0$ for every I. Although $x_n'(I)$ is always nonzero, it may be small over a range of I so that x_n exhibits a homeostatic region. Indeed, feedback inhibition is one of the examples in [RBG+17] of a system exhibiting homeostasis but having no homeostasis points. We will show in the theorems below that if $|f'(x_n)I|$ is large, then the equilibrium is unstable and if $|f'(x_n)I|$ is small, then the equilibrium is stable. Together with (3.2.4), this suggests that the homeostatic region and region of instability overlap, as depicted in Figure 3.2.

The characteristic polynomial of the Jacobian when $a_j = 1$ is given by

$$P_n(\lambda) = (f(x_n)+\alpha+\lambda)(1+\lambda)^{n-1} - f'(x_n) I \left(\frac{\lambda+\alpha}{f(x_n)+\alpha} \right). \tag{3.2.5}$$

Expanding, this may also be written as

$$\begin{aligned} P_n(\lambda) =& \lambda^n + \sum_{k=2}^{n-1} \left[\binom{n-1}{k} (f(x_n)+\alpha) + \binom{n-1}{k-1} \right] \lambda^k \\ &+ \left[(n-1)(f(x_n)+\alpha) + 1 - \frac{f'(x_n) I}{f(x_n)+\alpha} \right] \lambda \\ &+ \left[f(x_n) + \alpha - f'(x_n) I \frac{\alpha}{f(x_n)+\alpha} \right]. \end{aligned} \tag{3.2.6}$$

Note that every coefficient of P_n is positive (since $f' \leq 0$), so that, by Descartes' rule of signs, there can be no real positive roots of P_n. In addition, $\lambda = 0$ is never a root, so a loss of stability must occur by a pair of eigenvalues crossing the imaginary axis, that is, via a Hopf bifurcation.

When $\alpha = 1$, $\lambda = -1$ is always a root of $P_n(\lambda)$. This is a reflection of the fact that $x_1 + x_2 = I$, mentioned above. Dividing out the factor of $(1 + \lambda)$ gives us the characteristic polynomial for the reduced Jacobian:

$$\widetilde{P}_n(\lambda) = (f(x_n) + 1 + \lambda)(1 + \lambda)^{n-2} - \frac{f'(x_n)I}{f(x_n) + 1}. \tag{3.2.7}$$

Expanded, this is

$$\widetilde{P}_n(\lambda) = \lambda^{n-1} + \sum_{k=1}^{n-2} \left[\binom{n-2}{k} (f(x_n) + 1) + \binom{n-2}{k-1} \right] \lambda^k + f(x_n) + 1 - \frac{f'(x_n)I}{f(x_n) + 1}. \tag{3.2.8}$$

3.2.1 Stability Properties for Small n

We first study the case when $n \leq 5$. Theorem 3.2 and Theorem 3.3 together show that $n = 4$ is the minimum network length for which instabilities can occur.

Theorem 3.2. *Let f satisfy* (3.2.1). *If $n = 2$ or 3 and $\alpha > 0$ then the equilibrium is locally asymptotically stable for every $I \in [0, \infty)$.*

Proof. Consider $n = 3$. Although the theorem is true for general $\alpha > 0$, we prove it in the case $\alpha = a_2$ only. The technique for the general case is the same as the technique for the $\alpha = 1, n = 4$ case used in the proof of Theorem 3.3.

When $n = 3$, $\alpha = a_2$, and using $x_1 = I/a_2 - x_2$, the reduced Jacobian is given by

$$J = \begin{pmatrix} -(a_1 f(x_3) + a_2) & a_1 f'(x_3)(I/a_2 - x_2) \\ a_2 & -a_3 \end{pmatrix}$$

Using $I/a_2 - x_2 > 0$ and (3.2.1), we see $\mathrm{Tr}(J) < 0$ and $\det(J) > 0$ for each choice of $I \geq 0$ so that the steady state is asymptotically stable for every $I \geq 0$. For the case $n = 2$, $\alpha > 0$, the proof is similar.

■

Theorem 3.3. *Fix $I > 0$. If $n = 4$ and $\alpha > 0$, or if $n = 5$ and $\alpha = 1$, then f can be chosen so that f satisfies* (3.2.1) *and the equilibrium is unstable.*

Proof. Taking $\alpha = 1$ simplifies the calculations because it allows us to consider the roots of $\widetilde{P}_n$, a degree $(n-1)$ polynomial, when determining stability rather than the roots of P_n, a degree n polynomial. So, in the case of $n = 4$ and $\alpha > 0$ as well as $n = 5$ and $\alpha = 1$, we need to localize the roots of a degree 4 polynomial. We may use the same techniques to do so in both cases. For this reason, the general case of $n = 4$, $\alpha > 0$ is similar to the case of $n = 5, \alpha = 1$ and, as in the proof of Theorem 3.2, we prove Theorem 3.3 only in the case $\alpha = 1$.

The main tool of the proof is the argument principle. Consider the contour in the complex plane shown in Figure 3.3. This contour forms a closed curve connecting the points Ri and $-Ri$ via a semi-circle and a line on the imaginary axis. For large R, the dominant term of $\widetilde{P}_n$ (equation (3.2.8))on the semi-circle is of the form $R^{n-1}e^{(n-1)i\theta}$. So, in the limit as $R \to \infty$, the change in the argument on the semi-circle is $(n-1)\pi$. For $z \in \mathbb{C}$, let $\mathrm{Re}(z)$ denote the real part of z and $\mathrm{Im}(z)$ denote the imaginary part. We may determine the change in the argument on the imaginary axis between Ri and $-Ri$ by computing the zeros and tracking the signs of $\mathrm{Re}(\widetilde{P}_n(iy))$ and $\mathrm{Im}(\widetilde{P}_n(iy))$.

For $n = 4$, the zeros of $\mathrm{Re}(\widetilde{P}_4(iy))$ satisfy

$$y^2 \;=\; \frac{(f(x_4)+1)^2 - f'(x_4)I}{(f(x_4)+3)(f(x_4)+1)} \;=:\; r_{Re} \;>\; 0$$

and the zeros of $\mathrm{Im}(\widetilde{P}_4(iy))$ satisfy

$$y \;=\; 0 \quad \text{or} \quad y^2 \;=\; 2f(x_4)+3 \;=:\; r_{Im} \;>\; 0.$$

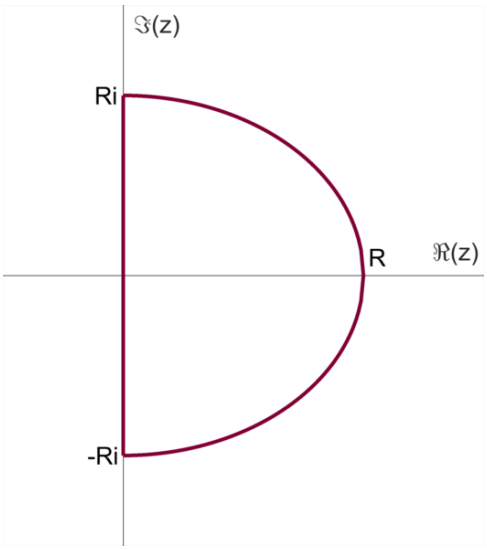

Figure 3.3: **Contour used in the proof of Theorem 3.3.**

To compute the the change in the argument of $\widetilde{P}_4$ on the imaginary axis, we track which quadrant of the complex plane $\widetilde{P}_4(iy)$ lies in as y varies from ∞ to $-\infty$. Note that $\mathrm{Re}(\widetilde{P}_4(iy)) = -C(y-\sqrt{r_{Re}})(y+\sqrt{r_{Re}})$ where C is a positive constant and $\mathrm{Im}(\widetilde{P}_4(iy)) = -y(y-\sqrt{r_{Im}})(y+\sqrt{r_{Im}})$. For y large, $\mathrm{Re}(\widetilde{P}_4(iy)) < 0$ and $\mathrm{Im}(\widetilde{P}_4(iy)) < 0$ so $\widetilde{P}_4(iy)$ lies in quadrant 3. $\mathrm{Re}(\widetilde{P}_4(iy))$ and $\mathrm{Im}(\widetilde{P}_4(iy))$ have only simple roots, so the quadrant changes exactly when y passes through one of the roots. The path $\widetilde{P}_4(iy)$ takes, and therefore the the change in the argument, depends on whether $r_{Re} < r_{Im}$ or $r_{Im} < r_{Re}$. We consider these two cases separately.

Case 1: $r_{Im} < r_{Re}$

The number line below shows which quadrant of the complex plane $\widetilde{P}_4(iy)$ lies in.

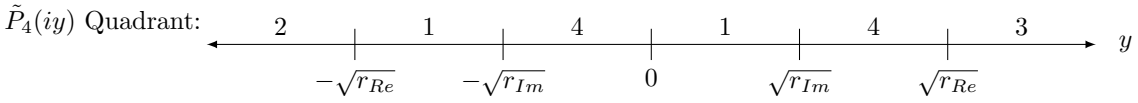

$\widetilde{P}_4(iy)$ goes from $-i\infty$ to $i\infty$ as y goes from ∞ to $-\infty$ and, as the number line shows, makes no additional revolutions in between. That is, the change in the argument of $\widetilde{P}_4$ on the imaginary axis is π. Along with the change of 3π on the arc of the semi-

circle, the total change in the argument of $\widetilde{P}_4$ on the whole contour is 4π, indicating that there are 2 roots with positive real part when $r_{Im} < r_{Re}$.

Case 2: $r_{Re} < r_{Im}$

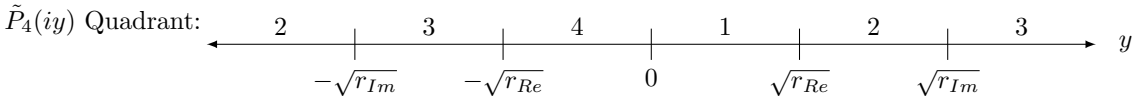

The change in the argument of $\widetilde{P}_4$ on the imaginary axis is -3π in this case. The total on the contour is then 0 revolutions and there are no roots inside the contour.

Let λ_4^* be a root of P_4 with largest real part. The analysis above shows that

$$\text{sign}(\text{Re}(\lambda_4^*)) = \text{sign}(r_{Re} - r_{Im}).$$

Simplifying this expression, we have

$$\text{sign}\left(\text{Re}(\lambda_4^*)\right) = \text{sign}\left(- f'(x_4)I - (2(f(x_4)+1)(f(x_4)+2)^2\right) \tag{3.2.9}$$

For $n = 5$ and $\alpha = 1$ we again compute the zeros of the real and imaginary parts of $\widetilde{P}_n$ in order to determine which quadrant it lies in as it traverses the imaginary axis The zeros of $\text{Re}(\widetilde{P}_5(iy))$ satisfy

$$2y^2 \;=\; (3f(x_5)+6) \pm \sqrt{(3f(x_5)+6)^2 - 4\left(f(x_5)+1 - \frac{f'(x_5)I}{f(x_5)+1}\right)} \;=:\; 2r_{\pm}$$

and the zeros of $\text{Im}(\widetilde{P}_5(iy))$ satisfy

$$y \;=\; 0 \quad \text{or} \quad y^2 \;=\; \frac{3f(x_5)+4}{f(x_5)+4} \;=:\; r_{Im}$$

It can be shown that the change in the argument of $\widetilde{P}_5(iy)$ as y goes from ∞ to $-\infty$ is -4π if and only if $r_{\pm} \in \mathbb{R}$ and $r_- < r_{Im} < r_+$. Further, if $r_{\pm} \in \mathbb{R}$, then $r_{Im} < r_+$ is always satisfied. Let λ_5^* be a root of P_5 with largest real part. Then, $\text{sign}(\text{Re}(\lambda_5^*))$ $\geq$ $\text{sign}(r_- - r_{Im})$ which is equal to the sign of

$$-4f'(x_5)I - (f(x_5)+1)\left[\frac{4(3f(x_5)+4)(3f(x)+6)}{f(x_5)+4} - 4(f(x_5)+1) - \left(\frac{6f(x_5)+8}{f(x_5)+4}\right)^2\right]. \tag{3.2.10}$$

Now, fix $I > 0$ and pick any f satisfying (3.2.1). The equilibrium value is independent of network length, so let $\bar{x} = x_4 = x_5$. Now, if we have $\text{sign}(\text{Re}(\lambda_4^*)) > 0$ and $\text{sign}(\text{Re}(\lambda_5^*)) > 0$ then the equilibrium is unstable and we are done. If not, then we may choose g satisfying (3.2.1) with $g(\bar{x}) = f(\bar{x})$ so that the equilibrium value with g as the feedback function is the same, but with $|g'(\bar{x})|$ large enough so that $\text{sign}(\text{Re}(\lambda_4^*)) > 0$ and $\text{sign}(\text{Re}(\lambda_5^*)) > 0$, which guarantees the equilibrium is unstable.

■

Theorem 3.4. *Let f satisfy* (3.2.1)*, $I > 0$, and $\alpha = 1$. Let λ_4^* and λ_5^* be the roots of $\widetilde{P}_4$ and $\widetilde{P}_5$ with largest real part. If $\text{Re}(\lambda_4^*) \geq 0$ then $\text{Re}(\lambda_5^*) > 0$.*

Note that in particular, Theorem 3.4 says that for $\alpha = 1$, if the network with length 4 is unstable, then the network with length 5 is unstable as well.

Proof of Theorem 3.4. The steady state value of x_n is independent of n. So, the theorem is proven if the expression in (3.2.10) is strictly larger than the expression in (3.2.9). Letting $x = x_4 = x_5$, this requires

$$-4f'(x)I - (f(x)+1)\left[\frac{4(3f(x)+4)(3f(x)+6)}{f(x)+4} - 4(f(x)+1) - \left(\frac{6f(x)+8}{f(x)+4}\right)^2\right]$$

$$> -f'(x)I - 2(f(x)+1)(f(x)+2)^2$$

Rearranging the inequality, we see this is true if and only if

$$-\left(\frac{6f(x)+8}{f(x)+4}\right)^2 < \frac{4}{f(x)+4}[2f(x)^3 + 8f(x)^2 + 15f(x) + 12]$$

The left hand side is negative and the right hand side is positive so the inequality is always satisfied.

■

3.2.2 Stability Properties for General n

We now study stability in the case of a general n. By applying Gershgorin's circle theorem (see, for example, [Var00]) to the Jacobian, we find a necessary condition for instability of the equilibrium, which is presented in the following proposition.

Proposition 3.5. *Let f satisfy* (3.2.1) *and fix I. Suppose the equilibrium is unstable. If $\alpha = 1$ then $-f'(x_n)I > f(x_n) + 1$. If $\alpha \neq 1$ then $-2f'(x_n)I > f(x_n) + \alpha$.*

The following theorem provides a sufficient condition for instability.

Theorem 3.6. *Let f satisfy* (3.2.1) *and fix I, $n \geq 4$, and $\alpha > 0$. Suppose that $-f'(x_n)I > 2(f(x_n) + \alpha)\left(\sec\left(\frac{3\pi}{2(n-1)}\right)\right)^{n-1}$ and $f(x_n) < \alpha$. Then for $m \geq n$, the equilibrium of the network with length m is unstable.*

Proof. We use notation and Theorems 1 and 2 of [Mos86]. First, consider the network of length n. Let $Q_n(\lambda) = P_n(\lambda - 1)$ where P_n defined as in (3.2.5). P_n has a root with positive real part when Q_n has a root with real part greater than 1. Define $\gamma := -\frac{f'(x_n)I}{f(x_n)+\alpha}$. We may write

$$Q_n(\lambda) = (\lambda - 1 + \alpha)\left(\lambda^{n-1} + \gamma\right) + f(x_n)\lambda^{n-1}$$

and view $Q_n(\lambda)$ as a perturbation of $p(\lambda) := (\lambda - 1 + \alpha)(\lambda^{n-1} + \gamma)$. A root of p with largest real part is given by

$$\lambda^* := \gamma^{1/(n-1)} e^{i\pi/(n-1)}.$$

Let $Z(p, \varepsilon)$ be the root neighborhoods of p under the metric $d(p, q) = \max |a_j - b_j|/m_j$ with $m_{n-1} = 1$ and $m_j = 0$ for $j \neq n - 1$ as defined in [Mos86]. Let $Z^*(p, \varepsilon)$ be the connected component of $Z(p, \varepsilon)$ containing λ^*. By Theorem 2 of [Mos86] there is at least one root of Q_n in $Z^*(p, f(x_n))$. So it is sufficient to show that

$$Z^*(p, f(x_n)) \subset \Omega := \left\{ z \in \mathbb{C} : \mathrm{Re}(z) > 1 \text{ and } \arg(z) \in \left(\frac{\pi}{2(n-1)}, \frac{3\pi}{2(n-1)}\right) \right\}.$$

First, I show that $\lambda^* \in \Omega$.

$$\begin{aligned}\mathrm{Re}(\lambda^*) &= \gamma^{1/(n-1)} \cos\left(\frac{\pi}{n-1}\right) \\ &> 2^{1/(n-1)} \sec\left(\frac{3\pi}{2(n-1)}\right) \cos\left(\frac{\pi}{n-1}\right) \\ &> \sec\left(\frac{3\pi}{2(n-1)}\right) \cos\left(\frac{\pi}{n-1}\right) > 1 \quad \text{for } n \geq 4\end{aligned}$$

We also have $\arg(\lambda^*) = \frac{\pi}{2(n-1)}$ and thus $\lambda^* \in \Omega$. As $Z^*(p, f(x_n))$ is connected, the above containment holds if $\partial\Omega \cap Z(p, f(x_n)) = \emptyset$. Let $g(z) = p(z)/|z|^{n-1}$. By Theorem 1 of [Mos86], $z \in Z(p, f(x_n))$ if and only if $|g(z)| \leq f(x_n)$.

Now suppose $z \in \partial\Omega$ with $\mathrm{Re}(z) = 1$ and $\arg(z) \in \left(\frac{\pi}{2(n-1)}, \frac{3\pi}{2(n-1)}\right)$. We have

$$|g(z)| = \frac{|z - 1 + \alpha|\,|z^{n-1} + \gamma|}{|z|^{n-1}}.$$

$\mathrm{Re}(z) = 1$ so $z - 1 = \mathrm{Im}(z)i$ and thus $|z - 1 + \alpha| > \alpha$. Using the reverse triangle inequality we have

$$\begin{aligned}|g(z)| &> \alpha \left|1 - |z|^{-(n-1)}\gamma\right| \\ &\geq \alpha \left|1 - \left(\sec\left(\frac{3\pi}{2(n-1)}\right)\right)^{-(n-1)} \gamma\right| \\ &> \alpha|1 - 2| = \alpha > f(x_n)\end{aligned}$$

and we have $z \notin Z(p, f(x_n))$.

Now suppose $\arg(z) = \frac{\pi}{2(n-1)}$ and $\mathrm{Re}(z) \geq 1$. Then $z = re^{\frac{\pi i}{2(n-1)}}$ for $r \in \left[\sec\left(\frac{\pi}{2(n-1)}\right), \infty\right)$ and

$$\begin{aligned}|g(re^{\frac{\pi i}{2(n-1)}})| &= r^{-(n-1)} \left|re^{\frac{\pi i}{2(n-1)}} - 1 + \alpha\right| \left|r^{n-1}i + \gamma\right| \\ &> \left|re^{\frac{\pi i}{2(n-1)}} - 1 + \alpha\right| \\ &> \left|r\cos\left(\frac{\pi}{2(n-1)}\right) - 1 + \alpha\right| \geq \alpha > f(x_n)\end{aligned}$$

so $z \notin Z(p, f(x_n))$.

Finally, suppose $\arg(z) = \frac{3\pi}{2(n-1)}$ and $\mathrm{Re}(z) \geq 1$. Then $z = re^{\frac{3\pi i}{2(n-1)}}$ for $r \in \left[\sec\left(\frac{3\pi}{2(n-1)}\right), \infty\right)$ and

$$\begin{aligned}
|g(re^{\frac{3\pi i}{2(n-1)}})| &= r^{-(n-1)} \left|re^{\frac{3\pi i}{2(n-1)}} - 1 + \alpha\right| \left|-ir^{n-1} + \gamma\right| \\
&> \left|re^{\frac{3\pi i}{2(n-1)}} - 1 + \alpha\right| \\
&> \left|r\cos\left(\frac{3\pi}{2(n-1)}\right) - 1 + \alpha\right| \geq \alpha > f(x_n)
\end{aligned}$$

so again, $z \notin Z(p, f(x_n))$ and we have shown the case of $m = n$. For $m > n$, note that $\left(\sec\left(\frac{3\pi}{2(n-1)}\right)\right)^{n-1}$ is decreasing in n so that if the hypotheses are satisfied for $m = n$, they must also be satisfied for $m > n$.

■

In practice, if we are given f, n, and α and we wish to know if there is an I for which the equilibrium is unstable, we may use (3.2.3) to solve for I as a function of x_n: $I = x_n(f(x_n) + \alpha)/f(x_n)$. Then the hypotheses of Proposition 3.5 and Theorem 3.6 can be written independent of I. Proposition 3.5 can then be used to find x_n for which stability is guaranteed and Theorem 3.6 can be used to find x_n for which instability is guaranteed. The corresponding values of I can be found by substituting x_n back into (3.2.3).

3.2.3 Stability Properties for Large I

We are able to get a quantitative idea for the relative stability of the network at different lengths by looking at the stability of the equilibrium as $I \to \infty$.

First, we show that if f is bounded away from zero, then the equilibrium must eventually stabilize. It will be convenient to define $\ell(x) = (f(x) + \alpha)x/f(x)$ so that $\ell(x_n) = I$.

Proposition 3.7. *Let f satisfy* (3.2.1) *and suppose $f(x) \to C > 0$ as and $f'(x) \ll x^{-1}$ as $x \to \infty$. Then for large enough I, the equilibrium is stable.*

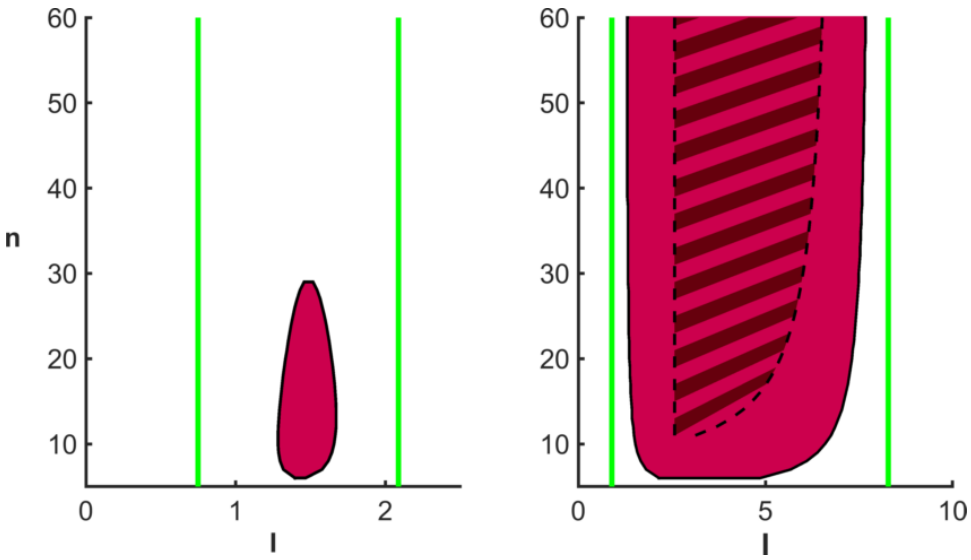

Figure 3.4: **Instability regions as a function of network length. (a):** The solid red area shows the instability region with $f(x) = \frac{10}{1+x^{10}} + 1/4$ and $\alpha = \frac{1}{50}$ computed numerically. $f(x) > \alpha$ for all x so Theorem 3.6 does not hold and if n is large enough the equilibrium is stable for every $I \in [0, \infty)$. Outside of the green lines, Proposition 3.5 applies so the equilibrium must be stable. **(b):** $f(x)$ as in A but $\alpha = 1$ so that there are I for which Theorem 3.6 applies. The dark striped area shows where Theorem 3.6 guarantees instability and the solid red area shows where we have numerically calculated instabilities to occur.

Proof. $f(x) \to C$, so $\ell(x) \sim (C+\alpha)x/C$ as $x \to \infty$. Therefore, $x_n \sim (1+\alpha/C)^{-1}I$ as $I \to \infty$. So, as $I \to \infty$, $f(x) \sim f((1+\alpha/C)^{-1}I) \to C$ and $f'(x) \sim f'((a+\alpha/C)^{-1}I) \ll I^{-1}$. By Proposition 3.5, the equilibrium is stable if $-f'(x_n)I < f(x_n)+\alpha$. The above relationships show that $-f'(x_n)I \to 0$ and $f(x_n)+\alpha \to C+\alpha > 0$ as $I \to \infty$, so the inequality must be satisfied in the limit. ■

Remark 3.8. The proof shows that if f satisfies (3.2.1) and $f(x)$ is bounded away from 0, then x_n grows linearly for I large enough. This is the classic escape from homeostasis behavior.

If instead $f \to 0$ as $x \to \infty$, then the stability of the equilibrium depends on how fast f approaches 0.

Proposition 3.9. *Let f satisfy* (3.2.1) *and suppose $f(x) \sim Ax^{-k}$ as $x \to \infty$ for some $A > 0$. For $n \geq 4$, the equilibrium is unstable for large enough I if $k > 2\left(\sec\left(\frac{3\pi}{2(n-1)}\right)\right)^{n-1}$. If $\alpha = 1$, then for large enough I the equilibrium is stable (unstable) for $n = 4$ if $k < 8$ ($k > 8$) and is stable (unstable) for $n = 5$ if $k < 4$ ($k > 4$).*

Proof. The value of A does not effect the proof and without loss of generality we may assume $A = 1$. If $f(x) \sim x^{-k}$ then $\ell(x) \sim x^{k+1}$. Using $\ell(x_n) = I$, we have $x_n \sim I^{\frac{1}{k+1}}$. Plugging this into f, $f(x_n) \sim f(I^{\frac{1}{k+1}}) \sim I^{-k}k + 1$ and $f'(x_n) \sim -kI^{-1}$. Therefore, $-f'(x_n)I \sim k$.

Now, for $n = 4$, the equilibrium is stable if and only if

$$-f'(x_4)I < (2(f(x_4)+1)(f(x_4)+2)^2 \tag{3.2.11}$$

by equation (3.2.9) in the proof of Theorem 3.3. As $f(x_n) \to 0$, the right hand side of (3.2.11) goes to 8 as $I \to \infty$, which proves the stated result for $n = 4$.

For $n = 5$, the proof of Theorem 3.3 shows that the equilibrium is stable if and only if

$$0 < (3f(x_5) + 6)^2 - 4\left(f(x_5) + 1 - \frac{f'(x_5)I}{f(x_5) + 1}\right) \tag{3.2.12}$$

and

$$-4f'(x_5)I < (f(x_5) + 1)\left[\frac{4(3f(x_5) + 4)(3f(x) + 6)}{f(x_5) + 4} - 4(f(x_5) + 1) - \left(\frac{6f(x_5) + 8}{f(x_5) + 4}\right)^2\right] \tag{3.2.13}$$

The right side of (3.2.12) goes to $32 + k$ and is thus always satisfied for large I. Noting that the right hand side of (3.2.13) approaches 16 while the left hand side approaches $4k$ completes the proof.

Applying $-f(x_n)I \sim k$ to the inequality in the statement of Theorem 3.6 and using $f(x_n) \to 0$ gives the result for $n \geq 4$ and general α.

■

In practice of course, large I is not achieved by a real system. However, these results, combined with numerical computations, provide some intuition about the system. Explicitly, let $f(x) = \frac{A}{1+x^k} + C$ for $A, k, C > 0$. Then numerical computation shows that instabilities can only exist for $n = 4$ when $k > 8$, even though f does not approach 0 and the equilibrium is stable for large I. Similarly, instabilities can only exist for $n = 5$ when $k > 4$. Said another way, Proposition 3.9 seems to provide the smallest k required for instabilities for $n = 4$ and $n = 5$ when f is in the above form. As C increases, a larger k is necessary for instabilities to appear.

3.3 Instability Regions with Piecewise Linear Feedback Inhibition

To better understand how the properties of the inhibition function effect the system, consider $n = 4$ and a piecewise linear form for the feedback function. Let f be defined

by

$$f(x) = \begin{cases} A + C, & x < 0 \\ A + C - sx, & 0 \leq sx \leq A \\ C, & sx > A \end{cases} \tag{3.3.1}$$

where $A > C$, $s > 0$, and $C \geq 0$. We define the feedback inhibition function, f_h, by horizontal shifts of f: $f_h(x) = f(x-h)$ for $h \geq 0$. C parameterizes the minimum value of f_h, A is the distance between the maximum and minimum value, s parameterizes the slope of f_h over the interval it is non-constant, and h is the value at which f_h begins to decrease (see Figure 3.5). This section studies how varying C, s, and h effect the instability region and amplitude of limit cycles when $n = 4$ and $\alpha = 1$. As in the previous section, given a value of I, we denote the equilibrium value of X_4 as $x_4(I)$ or simply x_4.

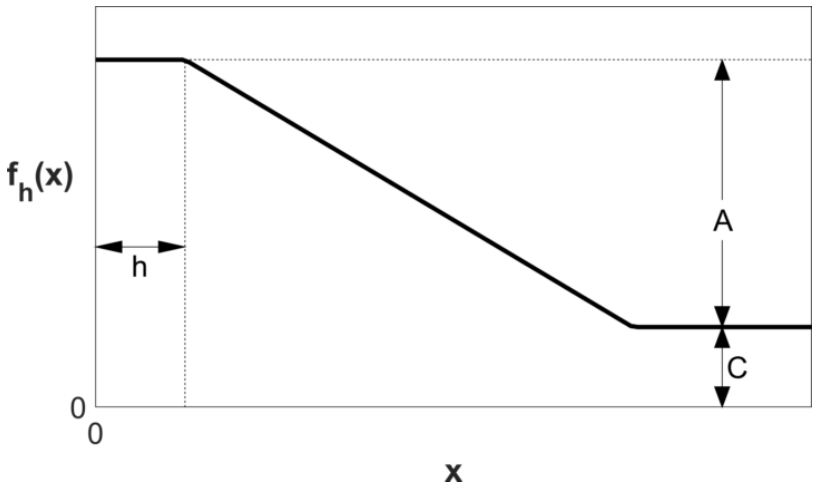

Figure 3.5: **A piecewise linear feedback function.**

Two theorems are provided. To state the theorems, we define

$$I_1 = \inf\{I > 0 : x_4(I) \text{ is unstable}\}$$

and

$$I_2 = \sup\{I > 0 : x_4(I) \text{ is unstable}\}$$

and note that (I_1, I_2) is the instability region. The first theorem relates the parameters of f_h with the existence of the instability region. The second theorem shows that when the instability region is not empty, $|x_4(I_2) - x_4(I_1)|$ must be relatively small. The purpose of the second theorem is to show that the region of instability is contained in the homeostatic region.

Theorem 3.10. *Define $f_h(x)$ as above, let $n = 4$ and $\alpha = 1$. Let $C^* > 0$ satisfy $2C^*(C^*+2)^2 = A+sh$. If $C > C^*$ then the equilibrium is stable for every $I \in [0, \infty)$. If $0 < C < C^*$, then the instability region is nonempty and $I_2 < \infty$. If $C = 0$ then the instability region is nonempty and $I_2 = \infty$.*

Proof. First note that if $x_4 < h$ or $x_4 > A/s + h$ then $f_h'(x_4) = 0$ and by Proposition 3.5, the equilibrium is stable. Let $g(x) = sx - 2(A+C-s(x-h))(A+C+2-s(x-h))^2$. For $x_4 \in (h, A/s+h)$, applying equation (3.2.9) from the proof of Theorem 3.3 shows that the equilibrium is stable if $g(x_4) < 0$ and unstable if $g(x_4) > 0$. Note that g is strictly monotone increasing and $g(A/s + h) = (A + sh) - 2C(2 + C)^2$.

Suppose $C > C^*$. Then $g(x) < g(A/s + h) < 0$ for all $x \in (h, A/s + h)$ so that the equilibrium is stable for every $I \geq 0$.

Now suppose $C < C^*$. Then $g(A/s+h) > 0$ so there is an interval $U \subset (h, A/s+h)$ so that if $x_4 \in U$ then $g(x_4) > 0$ and the equilibrium is unstable. If, in addition, $C > 0$, then the proof of Proposition 3.1 still works and $x_4 \to \infty$ as $I \to \infty$ so that there is an I for which $x_4 > A/s + h$ and stability is regained. In this case I_2 satisfies $x_4(I_2) = A/s + h$.

On the other hand, if $C = 0$, then as in the proof of Proposition 3.1, x_4 satisfies $\ell(x_4) := (f(x_4) + 1)x_4/f(x_4) = I$. Because $f(x) \to 0$ as $x \to A/s + h$, $\ell(x) \to \infty$ as $x \to A/s + h$. Thus $\ell : [0, A/s + h) \to [0, \infty)$ is invertible and x_4 is a function of I. In particular, $x_4 < A/s + h$ is satisfied for all I, so stability is not regained and $I_2 = \infty$.

■

Theorem 3.11. *Define $f_h(x)$ as above, let $n = 4$ and $\alpha = 1$. Suppose the instability region is nonempty. Then $x_4(I_1) > \frac{8}{9}x_4(I_2)$.*

Proof. Define $g(x, C) = sx - 2(A + C - s(x - h))(A + C + 2 - s(x - h))^2$. This is the same g as in the proof of Theorem 3.10 except that we make the dependence on C explicit. We have that the equilibrium is stable when $g < 0$ and unstable when $g > 0$. Note that g is decreasing in C, so that $g(x, C) < g(x, 0)$. We also have $x_4(I_2) = A/s + h$. Letting $\kappa = \frac{1}{9}$, we have

$$\begin{aligned} g\left(\frac{8}{9}x_4(I_2), 0\right) &= g((1-\kappa)(A/s+h), 0) \\ &= (1-\kappa)A + (1-\kappa)sh - 2(\kappa A + \kappa sh)(\kappa A + \kappa sh + 2)^2 \\ &\leq (1-\kappa)A - 2\kappa A(\kappa A + 2)^2 \\ &= (1-\kappa)A - 2(\kappa A)^3 - 8\kappa A^2 - 8\kappa A \\ &< A - 9\kappa A = 0 \end{aligned}$$

The instability region is nonempty so I_1 exists and $x_4(I_1)$ satisfies $g(x_4(I_1), C) = 0$. However, g is increasing in x and we have shown that $g(\frac{8}{9}x_4(I_2), C) < 0$ so we must have $x_4(I_1) \in \left(\frac{8}{9}x_4(I_2), x_4(I_2)\right)$ as claimed. ■

Theorem 3.11 says that although $|I_2 - I_1|$ may be large, the value of x_4 doesn't change very much on that interval. This indicates that the instability region lies on the homeostatic plateau. For example, Figure 3.6(a) shows that for $C = 1/5$, $I_1 \approx 25$ while $I_2 \approx 100$, but $x_4(I_1)$ and $x_4(I_2)$ are still close to each other.

Finally, we present numerical calculations of the instability regions and limit cycle amplitudes as C, s, and h are individually varied. Figure 3.6 shows the instability regions. Figure 3.7 shows the maximum limit cycle amplitude over the instability region. A is chosen so that $x_4(I_1) > h$.

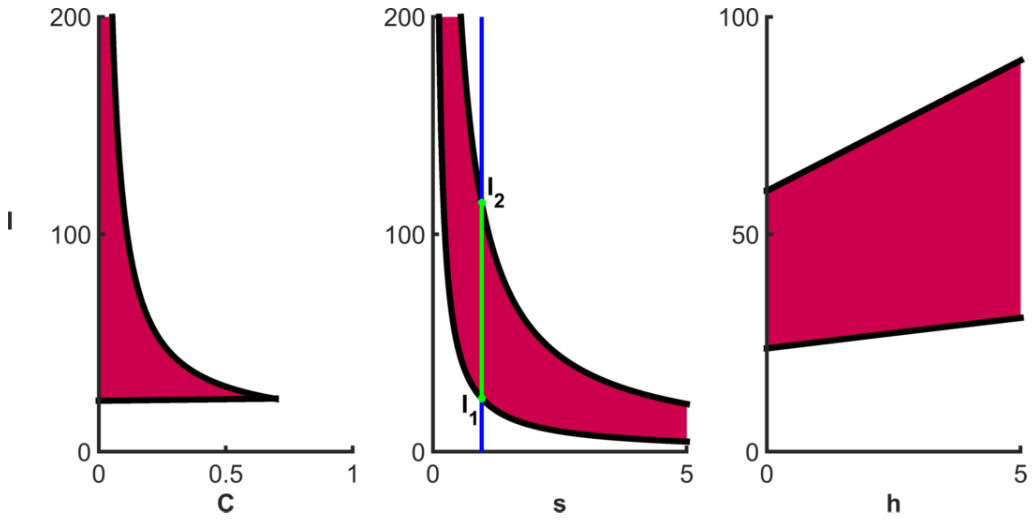

(a) (b) (c)

Figure 3.6: **Parameter dependence of the instability region.** $f_h(x)$ is chosen as above with $A = 10$, $C = 1/5$, $s = 1$, and $h = 0$ except when they are varied. The solid red regions shows the numerically calculated instability regions. **(a):** When $A = 10$ and $h = 0$, $C^* \approx .69$. As $C \to 0$, $I_2 \to \infty$. **(b):** Increasing s decreases both I_1 and I_2. The line $s = 0.96$ has been plotted and indicates for which values of I the equilibrium is stable (blue), and for which values of I there is a limit cycle (green). **(c):** Increasing h increases the size of the instability region.

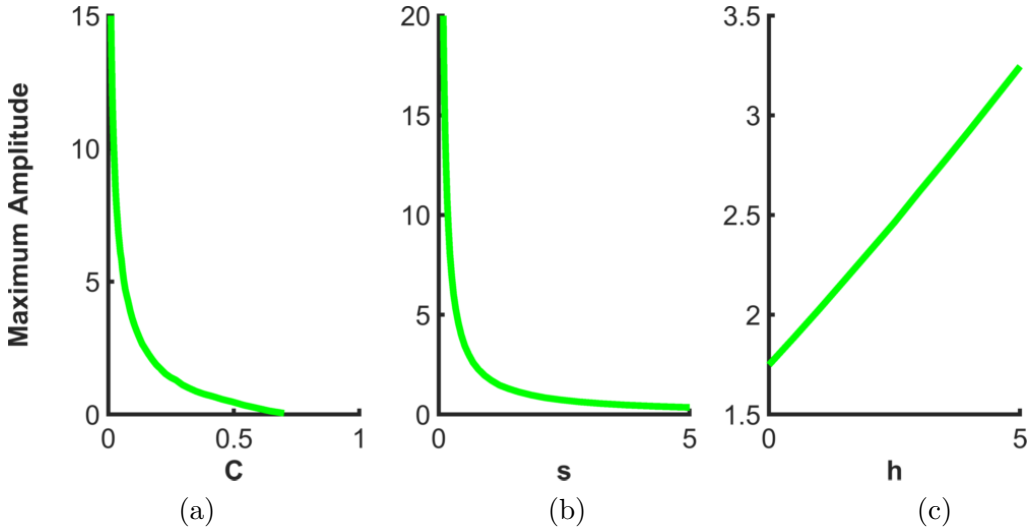

(a) (b) (c)

Figure 3.7: **Parameter dependence of the limit cycle amplitudes.** The maximum amplitude of the limit cycles over the instability region calculated numerically and plotted as a function of C, s, and h. The parameters are fixed at $A = 10$, $s = 1$, $C = 1/5$, and $h = 0$ when they are not varied.

Chapter 4

Homeostasis-Bifurcation Singularities

This chapter is based on work published in the International Journal of Bifurcation and Chaos [DG19] and was done in collaboration with Martin Golubitsky. In the work of Chapter 3, a network with a single mechanism contributing to both homeostasis and (Hopf) bifurcation was studied. This observation motivated the work of this chapter, which studies the behavior of systems in which homeostasis points and bifurcation points coincide. Near such *homeostasis-bifurcation* points, these systems can exhibit homeostatic plateaus separated by hysteretic switches (in the case of steady state bifurcation) and limit cycles with homeostatic periods and amplitudes (in the case of Hopf bifurcation).

In Section 4.1, we introduce the homeostasis-bifurcation singularity for feedforward networks and motivate the definition. In Sections 4.2 and 4.3, we show how to reduce a system of ordinary differential equations at a homeostasis-bifurcation singularity to a single scalar equation while preserving all the qualitative information of interest. The content in both of these sections is similar with the former dealing with steady state bifurcations and the latter with Hopf bifurcations. The separation is made because the reduction for Hopf bifurcations is more technical. In Section 4.4, the unfoldings of homeostasis-bifurcation points are derived. The transition varieties are defined in Section 4.5. In Section 4.6, low codimension homeostasis-bifurcation singularities are given with their transition varieties and an enumeration of their persistent behavior. Section 4.7 constructs two networks, each with a homeostasis-bifurcation singularity, and the persistent behavior is found numerically. Examples of biological systems which exhibit homeostasis-bifurcation type phenomena are given

in Section 4.8.

4.1 Homeostasis-Bifurcation Singularities in Feedforward Networks

This section introduces the feedforward system that is studied in this chapter and defines homeostasis-bifurcation points for this system. This section further gives a high level overview of the content of proceeding sections.

There is a technical difficulty in defining homeostasis-bifurcation singularities. Homeostasis points are defined in terms of an input-output function which relies on application of the implicit function theorem at a stable equilibrium. On the other hand, bifurcation points are exactly those points at which the implicit function theorem fails. As a result, homeostasis points are not well defined at bifurcation points. It is possible to construct systems in which a homeostasis point collides with a bifurcation point, but it is not straightforward to recognize the resulting singularity as arising from such a collision. The approach used in this chapter is to assume a feedforward structure which decouples the two singularities. The system studied is one in which the bifurcation parameter in a bifurcating system is replaced by the input-output function of a homeostatic system.

The first equation describes the homeostatic system and has the form

$$\dot{X} = G(X, \lambda) \tag{4.1.1}$$

where $X \in \mathbb{R}^m$ and $x \equiv X_i \in \mathbb{R}$ is the distinguished, homeostatic variable of (4.1.1) as a function of $\lambda \in \mathbb{R}$. The second equation describes the bifurcating system and has the form

$$\dot{Y} = F(Y, x) \tag{4.1.2}$$

where $Y \in \mathbb{R}^n$. Next suppose $x(\lambda)$ has a homeostasis point at λ_0 (that is, $x'(\lambda_0) = 0$) and $x(\lambda_0) = x_0$. Suppose also that $F(Y_0, x_0) = 0$, but F does not have a steady-state bifurcation at (Y_0, x_0). Then we may apply the implicit function theorem to obtain a curve of equilibria $Y(x(\lambda)) \in \mathbb{R}^n$ for (4.1.2) when λ near λ_0. Differentiating at λ_0, we have

$$\frac{d}{d\lambda} Y(x(\lambda))\bigg|_{\lambda=\lambda_0} = \frac{dx}{d\lambda}(\lambda_0)\frac{dY}{dx}(x_0) = 0 \tag{4.1.3}$$

so that all Y variables inherit homeostasis points from x. If F has a bifurcation point, one could vary parameters so that the inherited homeostasis point and the bifurcation point coincide.

We call points λ_0 where infinitesimal homeostasis points $x(\lambda_0)$ coincide with bifurcation points in $F(Y, x)$ at $x(\lambda_0)$ *homeostasis-bifurcation* points. We are interested in multiplicity and stability of solutions as well as homeostasis points in a particular Y variable, Y_k. In the case of steady-state bifurcation, we study homeostasis-bifurcation points by reducing the steady-state equation of (4.1.2),

$$F(Y, x) = 0, \tag{4.1.4}$$

to a scalar equation,

$$f(y, x) = 0 \tag{4.1.5}$$

that preserves the above properties. This can be done if we assume the non-degeneracy condition $e_k \notin (\ker(D_Y F)_{(Y_0,x_0)})^\perp$ where e_k is the unit vector in the kth direction (see Section 4.2). In the case that (4.1.2) undergoes a Hopf bifurcation at (Y_0, x_0), a reduction to (4.1.5) is still possible, but the non-degeneracy condition becomes $e_k \notin (\text{span}\{\text{Re}(v), \text{Im}(v)\})^\perp$ where v is an eigenvector of $(D_Y F)_{(Y_0,x_0)}$ whose eigenvalue is purely imaginary.

We define the codimension of a homeostasis-bifurcation point, $\text{codim}(x, f)$ or $\text{codim}(f(y, x(\lambda))$ as the number of parameters needed in its unfolding. Intuitively,

$$\text{codim}(x, f) = \text{codim}_H(x) + \text{codim}_B(f) + 1 \tag{4.1.6}$$

as we need enough parameters to unfold $x(\lambda)$ and f individually and then an additional parameter to bring the two singularities together. This formula will be justified in section 4.4.

4.2 Reduction to a Scalar Equation: Steady State Bifurcation

In this section, we use the Lyapunov-Schmidt method to reduce (4.1.4) to a scalar equation. We show that the reduced equation preserves homeostasis points of a chosen state variable Y_k as well as the multiplicity and stability of solutions. This is an important step because it allows us to consider only scalar equations in the classification of homeostasis-bifurcation singularities (given in Section 4.6) without losing the information we are interested in. As in the study of bifurcations, the reduction is a theoretical tool that is not typically performed in applications. In applications, the derivatives of the system at the singularity are used to recognize the corresponding scalar normal form. For low codimension singularities, the tables in Section 4.6 can then be used to determine the behavior the system can have when the singularity is perturbed.

Consider the equation

$$F(Y, \mu, b) = 0 \tag{4.2.1}$$

where $Y \in \mathbb{R}^n$, $\mu \in \mathbb{R}$ is a distinguished parameter, and $b \in \mathbb{R}^p$ is a vector of auxiliary parameters. We begin by explaining what we mean by Y_k homeostasis points.

Suppose that $F = 0$ and $D_Y F$ is nonsingular at (Y_0, μ_0, b_0). Then we may apply the implicit function theorem to obtain a function $Y(\mu, b) \in \mathbb{R}^n$ where, near (μ_0, b_0), $F(Y(\mu, b), \mu, b) = 0$. However, we will soon assume that F undergoes a bifurcation, so it is possible that there is another value of Y, say $\widetilde{Y}_0$, so that $F(\widetilde{Y}_0, \mu_0, b_0) = 0$. For this reason it will be useful to specify the value of Y when describing the homeostasis point.

Definition 4.1. The function $\rho : \mathbb{R} \times \mathbb{R} \times \mathbb{R}^p \to \mathbb{R}$ has a homeostasis point at (ρ_0, μ_0, b_0) if $\rho(\mu_0, b_0) = \rho_0$ and $\rho_\mu(\mu_0, b_0) = 0$.

4.2.1 Derivation of the reduction

Suppose F undergoes a simple 0 eigenvalue bifurcation at $(Y, \mu, b) = (0, 0, 0)$. We perform a Lyapunov-Schmidt reduction on F at the bifurcation point to get a scalar function, $f : \mathbb{R} \times \mathbb{R} \times \mathbb{R}^p \to \mathbb{R}$ so that, locally, solutions to $f(y, \mu, b) = 0$ are in one-to-one correspondence with solutions of (4.2.1). Let $L = (D_Y F)_{(0,0,0)}$. Lyapunov-Schmidt reduction requires making a choice of complementary subspaces M to $\ker(L) = \mathbb{R}\{v_0\}$ in $\mathbb{R}^n$ and N to $\text{range}(L) = \mathbb{R}\{v_0^*\}$ in $\mathbb{R}^n$. In order for Lyapunov-Schmidt reduction to preserve homeostasis of the k^{th} coordinate in the original equation $F = 0$ to the reduced equation $f = 0$, we must also assume the nondegeneracy condition on L at the origin

$$\langle v_0, e_k \rangle \neq 0$$

or $e_k \notin (\ker L)^\perp$. It follows that we can split the domain of L via $\mathbb{R}^n = \ker L \oplus M$ by choosing $M = \text{span}\{e_i \mid i \neq k\}$. We additionally split the codomain of L via $\mathbb{R}^n = \text{range}\, L \oplus N$. The choice of N is arbitrary.

Let E denote projection onto range L with $\ker E = N$. We may solve $F(Y, \mu, b) =$

0 by simultaneously solving

$$EF(Y, \mu, b) = 0$$
$$(I - E)F(Y, \mu, b) = 0$$

where I denotes the $n \times n$ identity.

The reduction continues by decomposing Y as $Y = v + w$ where $v \in \ker L$ and $w \in M$. Applying the implicit function theorem to $EF(v + w, \mu, b) = 0$ yields $w \equiv w(v, \mu, b)$. Define $\phi : \ker L \times \mathbb{R} \times \mathbb{R}^p \to N$ by $\phi(v, \mu, b) = (I - E)F(v + w(v, \mu, b), \mu, b)$. So that our reduction preserves stability, we require $\langle v_0, v_0^* \rangle > 0$, where $\langle \cdot, \cdot \rangle$ is the standard inner product on $\mathbb{R}^n$. This is called a consistent choice of v_0 and v_0^* (see [GS85] for more details). The reduction is now given by

$$f(y, \mu, b) = \langle v_0^*, \phi(yv_0, \mu, b) \rangle. \tag{4.2.2}$$

Note that if (y, μ, b) solves $f(y, \mu, b) = 0$ then Y in the corresponding solution of $F(Y, \mu, b) = 0$ can be recovered via

$$Y = yv_0 + w(yv_0, \mu, b). \tag{4.2.3}$$

4.2.2 Preservation of the desired properties

Solutions of $f = 0$ and $F = 0$ are in one-to-one correspondence so multiplicity of solutions is automatically preserved. Let $\lambda_1, \ldots, \lambda_n$ denote the eigenvalues of $D_Y F_{(0,0,0)}$ with $\lambda_1 = 0$. Note that we have assumed $\mathrm{Re}(\lambda_i) \neq 0$ for $i \neq 1$. The following proposition shows that stability of solutions is preserved if we make an additional assumption on λ_i.

Proposition 4.1. *Suppose* $\mathrm{Re}(\lambda_i) < 0$ *for* $i \neq 1$. *Then the equilibria of* $\dot{Y} = F(Y, \mu, b)$ *corresponding to a solution,* (y, μ, b), *of* $f(y, \mu, b) = 0$ *is asymptotically stable if* $f_y(y, \mu, b) < 0$ *and unstable if* $f_y(y, \mu, b) > 0$.

Proof. See chapter 1, Theorem 4.1 of [GS85]. ■

Now, given $f(y_0, \mu_0, b_0) = 0$ and $f_y(y_0, \mu_0, b_0) \neq 0$ we may apply the implicit function theorem to obtain a curve $y(\mu, b)$ where $f(y(\mu, b), \mu, b) = 0$ and $y(\mu_0, b_0) = y_0$. The one-to-one correspondence of f and F gives a corresponding curve of equilibria, $Y(\mu, b)$ with $Y(\mu_0, b_0) = Y_0$.

Definition 4.2. If y has a homeostasis point at (y_0, μ_0, b_0) if and only if Y_k has a homeostasis point at $((Y_0)_k, \mu_0, b_0)$ where Y_0 is the corresponding solution to y_0, then f is Y_k homeostasis preserving.

Proposition 4.2. *f is Y_k homeostasis preserving.*

Proof. Suppose $y(\mu, b)$ satisfies $f(y(\mu, b), \mu, b) = 0$. The corresponding solutions to $F = 0$ are given by (4.2.3):

$$Y(\mu, b) = y(\mu, b)v_0 + w(yv_0, \mu, b).$$

However, $w(yv_0, \mu, b) \in M$ so $w_k(y(\mu, b)v_0, \mu, b) \equiv 0$ and we have $Y_k(\mu, b) = y(\mu, b)(v_0)_k$. Therefore $(Y_k)_\mu(\mu, b) = y_\mu(\mu, b)(v_0)_k$ and f preserves Y_k homeostasis. ■

4.3 Reduction to a Scalar Equation: Hopf Bifurcation

There are some significant differences to the reduction when Hopf bifurcations are considered. This is primarily because $\dot{y}$ does not vanish for non-constant solutions so we have to consider the linearization of an operator in infinite dimensions rather than a finite dimensional one. Time translations of periodic solutions to (4.1.2) are still periodic solutions, so S^1 symmetries will also play a role.

Consider the equation

$$\dot{Y} = F(Y, \mu, b) \tag{4.3.1}$$

where $Y \in \mathbb{R}^n$, $\mu \in \mathbb{R}$ is a distinguished parameter, and $b \in \mathbb{R}^p$ is a vector of auxiliary parameters. We will be reducing (4.3.1) to a scalar equation that preserves periodic solutions, stability of limit cycles, and homeostasis points of the amplitude near points were $D_Y F$ has simple $\pm i\omega$ eigenvalues and no other eigenvalues on the imaginary axis. To simplify notation, it is convenient to assume that the Hopf bifurcation occurs at $(Y, \mu, b) = (0, 0, 0)$, $F(0, \mu, b) \equiv 0$, and the purely imaginary eigenvalues are exactly $\pm i$. This section is largely informed by chapters 7 and 8 of [GS85], but there is a modification in the reduction to ensure homeostasis points of the amplitude are preserved.

4.3.1 Derivation of the Reduction

First, we explicitly define the operator, Φ, to which we will apply the Lyapunov-Schmidt reduction. Φ should act on a space of periodic functions, but this space is not linear: the sum of two periodic functions with different periods is in general not periodic. To circumvent this problem, we introduce a parameter τ to rescale time:

$$s = (1 + \tau)t. \tag{4.3.2}$$

We will define Φ by

$$\Phi(u, \mu, b, \tau) = (1 + \tau)\frac{du}{ds} - F(u, \mu, b) \tag{4.3.3}$$

so that 2π-periodic solutions to $\Phi = 0$ correspond to periodic solutions to (4.3.1) with period $2\pi/(1 + \tau)$. Near the bifurcation, we will show that $\tau \approx 0$.

To be specific about the domain and range of Φ, let $C_{2\pi}$ be the Banach space of

continuous, 2π-periodic function from $\mathbb{R} \to \mathbb{R}^n$ with the norm

$$||u|| = \max_s |u(s)|$$

and $C^1_{2\pi}$ be the Banach space of 2π-periodic functions that are continuously differentiable with the norm

$$||u||_1 = ||u|| + \left|\left|\frac{du}{ds}\right|\right|.$$

Define $\Phi : C^1_{2\pi} \times \mathbb{R} \times \mathbb{R}^p \times \mathbb{R} \to C_{2\pi}$ by (4.3.3). S^1 acts on Φ through the change of phase action. For $\theta \in S^1$ and $u \in C_{2\pi}$ define

$$(\theta \cdot u)(s) = u(s - \theta). \tag{4.3.4}$$

Φ commutes with this group action:

$$\Phi(\theta \cdot u, \mu, b, \tau) = \theta \cdot \Phi(u, \mu, b, \tau). \tag{4.3.5}$$

The linearization of Φ at the bifurcation is given by

$$\mathscr{L}u = \frac{du}{ds} - Lu \tag{4.3.6}$$

where $L = D_Y F$ is the Jacobian of F at the bifurcation. The following proposition is Proposition 2.2 in Chapter 8 of [GS85].

Proposition 4.3. *Assume L has simple $\pm i$ eigenvalues and no other purely imaginary eigenvalues. Then*

1. $\dim \ker \mathscr{L} = 2$
2. *There is a basis, v_1, v_2 for $\ker \mathscr{L}$ with $|v_1| = |v_2| = 1$ and the following property: If we identify $\ker \mathscr{L}$ with $\mathbb{R}^2$ via the mapping*

$$(y_1, y_2) \mapsto y_1 v_1 + y_2 v_2, \tag{4.3.7}$$

then the action of S^1 *on* $\ker \mathscr{L}$ *is given by*

$$\theta \cdot \begin{pmatrix} y_1 \\ y_2 \end{pmatrix} = \begin{pmatrix} \cos(\theta) & -\sin(\theta) \\ \sin(\theta) & \cos(\theta). \end{pmatrix} \begin{pmatrix} y_1 \\ y_2 \end{pmatrix} \tag{4.3.8}$$

That is, θ *acts on* $\mathbb{R}^2$ *by rotation counterclockwise through the angle* θ*.*

3. *There is an invariant splitting of* $C_{2\pi}$ *given by*

$$C_{2\pi} = \ker \mathscr{L} \oplus \operatorname{range} \mathscr{L}. \tag{4.3.9}$$

This splitting induces a splitting of $C^1_{2\pi}$

$$C^1_{2\pi} = \ker \mathscr{L} \oplus ((\operatorname{range} \mathscr{L}) \cap C^1_{2\pi}). \tag{4.3.10}$$

We begin the Lyapunov-Schmidt reduction by defining $E : C_{2\pi} \to \operatorname{range} \mathscr{L}$ to be the projection onto the range $\mathscr{L}$ with $\ker E = \ker \mathscr{L}$. This is taking advantage of the splitting of $C_{2\pi}$ given by (4.3.9). We then have $\Phi = 0$ if and only if

$$E\Phi(u, \mu, b, \tau) = 0 \tag{4.3.11}$$

$$(I - E)\Phi(u, \mu, b, \tau) = 0 \tag{4.3.12}$$

where I is the identity operator on $C_{2\pi}$. When comparing to the reduction for steady state bifurcation, we have chosen N to be $\ker \mathscr{L}$. The choice in [GS85] for the splitting of the domain as $C^1_{2\pi} = \ker \mathscr{L} \oplus M$ was taken to be given by (4.3.10): $M = (\operatorname{range} \mathscr{L}) \cap C^1_{2\pi}$. However, to preserve homeostasis points of the amplitude, we take

$$M = \{w \in C^1_{2\pi} \mid w_k(t) \equiv 0\}. \tag{4.3.13}$$

We write $u = v + w$ where $v \in \ker \mathscr{L}$ and $w \in M$ and apply the implicit function theorem to $E\Phi(v + w, \mu, b, \tau) = 0$ so that $w = w(v, \mu, b, \tau)$. We now define the coordinate free reduced mapping $\phi : \ker \mathscr{L} \times \mathbb{R} \times \mathbb{R}^p \times \mathbb{R}$ by

$$\phi(v, \mu, b, \tau) = (I - E)\Phi(v + w(v, \mu, b, \tau), \mu, b, \tau). \tag{4.3.14}$$

Because M is invariant under the action of S_1 on $C^1_{2\pi}$, Proposition 2.3 in Chapter 8 of [GS85] still holds.

Proposition 4.4. *In the coordinates on* $\ker \mathscr{L}$ *defined by* (4.3.7)*, the reduced mapping* ϕ *has the form*

$$\phi(y_1, y_2, \mu, b, \tau) = p(y_1^2 + y_2^2, \mu, b, \tau) \begin{pmatrix} y_1 \\ y_2 \end{pmatrix} + q(x^2 + y^2, \mu, b, \tau) \begin{pmatrix} -y_2 \\ y_1 \end{pmatrix} \quad (4.3.15)$$

where p *and* q *are smooth functions satisfying*

$$\begin{aligned} &\text{(a)} \quad p(0,0,0,0) = 0, \qquad &&\text{(b)} \quad q(0,0,0,0) = 0, \\ &\text{(c)} \quad p_\tau(0,0,0,\tau) = 0, \qquad &&\text{(d)} \quad q_\tau(0,0,0,\tau) = -1. \end{aligned} \quad (4.3.16)$$

To complete the reduction, notice that $\phi = 0$ if and only if

$$y_1 = y_2 = 0, \text{ or} \quad (4.3.17)$$

$$p = q = 0. \quad (4.3.18)$$

Solutions satisfying (4.3.17) correspond to the trivial, steady state solutions $u = 0$, while solutions satisfying (4.3.18) correspond to 2π-periodic solutions which are nonconstant when $y_1^2 + y_2^2 > 0$. There is a redundancy in solutions corresponding to $p = q = 0$ due to the action of S_1. we eliminate this redundancy by assuming $y_2 = 0$ and $y_1 \geq 0$, as any vector can be rotated into this form. Setting $y = y_1$, equations (4.3.17) and (4.3.18) then take the form

$$y = 0, \text{ or} \quad (4.3.19)$$

$$p(y^2, \mu, b, \tau) = q(y^2, \mu, b, \tau) = 0. \quad (4.3.20)$$

Now, by Proposition 4.4, we may apply the implicit function theorem to $q(y^2, \mu, b, \tau) = 0$ to get $\tau = \tau(y^2, \mu, b)$ near the origin. In particular, $\tau(0,0,0) = 0$. Define

$$r(z, \mu, b) = p(z, \mu, b, \tau(z, \mu, b)) \quad (4.3.21)$$

and

$$f(y, \mu, b) = r(y^2, \mu, b)y. \tag{4.3.22}$$

Then the equation $\phi(y_1, y_2, \tau, \alpha) = 0$ has solution if and only if $f(y, \mu, b) = 0$. The solutions to $\phi = 0$ are in one-to-one correspondence with periodic solutions to (4.3.1), so solutions to $f(y, \mu, b) = 0$ are as well. $f = 0$ is the desired scalar equation.

Note that if y is a solution to $f(y, \mu, b) = 0$ then $yv_1 + w(yv_1, \mu, b, \tau(y, \mu, b))$ is a solution to $\Phi = 0$. To first order, y is the amplitude of the solution because $|v_1| = 1$. At the origin, $\tau = 0$ and τ is smooth so that near the origin $\tau \approx 0$. Therefore, small amplitude solutions are approximately 2π periodic.

4.3.2 Preservation of the Desired Properties

Multiplicity of periodic solutions is automatically preserved because solutions to $\Phi = 0$ are in one-to-one correspondence to $f = 0$. Let $\lambda_1, \ldots, \lambda_n$ denote the eigenvalues of $D_Y F$ at the bifurcation point with $\lambda_1 = i$ and $\lambda_2 = -i$. Note that we have assumed $\mathrm{Re}(\lambda_i) \neq 0$ for $i > 2$. As with the steady state reduction, stability is preserved if we make an additional assumption on λ_i.

Proposition 4.5. *Suppose* $\mathrm{Re}(\lambda_i) < 0$ *for* $i > 2$. *Then the periodic solution corresponding to a solution* (y, μ, b) *of* $f(y, \mu, b) = 0$ *is asymptotically stable if* $f_y(y, \mu, b) < 0$ *and unstable if* $f_y(y, \mu, b) > 0$.

Proof. See Theorem 4.1 in Chapter 8 of [GS85]. ■

Proposition 4.6. *f preserves homeostasis in the amplitudes of Y_k.*

Proof. Suppose $y(\mu, b)$ satisfies $f(y, \mu, b), \mu, b) = 0$. The corresponding periodic solution to (4.3.1) up to translations in time is given by $y(\mu, b)v_1 + w(y(\mu, b)v_1, \mu, b, \tau(y(\mu, b)v_1, \mu, b))$. Now, $w \in M$ so that $w_k \equiv 0$ and the kth component is given by $y(\mu, b)(v_1)_k$. The

amplitude of Y_k is thus precisely $y(\mu, b)$. So, there is a homeostasis point in $y(\mu, b)$ if and only if there is a homeostasis point in the amplitudes of Y_k. ■

4.3.3 Limit Cycle Periods Inherit Homeostasis Points

In this subsection, we digress to show that in addition to limit cycle amplitudes inheriting homeostasis points from $x(\lambda)$, the period of limit cycles do as well. The period P is controlled by the additional parameter τ introduced in (4.3.2):

$$\widetilde{P}(\tau) = \frac{2\pi}{1+\tau}. \tag{4.3.23}$$

In the previous subsection, we applied the implicit function theorem to show that $\tau = \tau(y, \mu, b)$ where μ is the distinguished bifurcation parameter. Suppose $y(\mu, b)$ is a branch of $f(y, \mu, b) = 0$ so that $f(y(\mu, b), \mu, b) = 0$. Replacing μ with the input-output function $x(\lambda)$ we have that the period is a function of λ and b:

$$P(\lambda, b) = \widetilde{P}(\tau(y(x(\lambda), b), x(\lambda), b)) = \frac{2\pi}{1+\tau(x(\lambda), b)}. \tag{4.3.24}$$

If $x(\lambda)$ has a homeostasis point at λ_0 then differentiating $P(\lambda, b)$ in λ at λ_0 shows that the period also has a homeostasis point.

Of course this analysis does not rule out that there are homeostasis points of the period independent of homeostasis points in $x(\lambda)$. This is possible, but not generic. Either there is a homeostasis point in the period occurring exactly at the Hopf point (the one sided derivative of the period vanishes), or there is a homeostasis point occurring away from the Hopf point. The former case is not stable to perturbations while the latter case can be excluded by shrinking the domain of study to a smaller neighborhood around the origin.

4.4 Universal Unfoldings of Homeostasis-Bifurcation Singularities

In this section, we characterize the universal unfolding of homeostasis-bifurcation points. The allowable perturbations are those which respect the feedforward structure of (4.1.1)-(4.1.2). That is, (4.1.1) and (4.1.2) can be independently perturbed, but the input-output function can never depend on the state variables of (4.1.2). For this reason, we can independently unfold the input-output function, x, and the bifurcation problem, f, and then link them together to obtain the unfolding of the homeostasis-bifurcation point, (x, f).

First, we unfold the homeostasis point. Let $x(\lambda, a)$ be a family of input-output functions where λ is the input parameter and a parameterizes the family. $a \neq 0$ represents a perturbation away from the homeostasis point. Specifically, suppose x has a λ-homeostasis point at $(\lambda, a) = (0, 0)$ with $x(0, 0) = 0$. By Theorem 2.2, $x(\lambda, a)$ factors through $\pm\lambda^k + a_{k-2}\lambda^{k-2} + \cdots + a_1\lambda$ where k is the first non-vanishing λ-derivative of x and $\text{codim}_H(x) = k - 2$. In particular we have

$$x(\lambda, a) = \pm\Lambda(\lambda, a)^k + A_{k-2}(a)\Lambda(\lambda, a)^{k-2} + \cdots + A_1(a)\Lambda(\lambda, a) - C(a) \qquad (4.4.1)$$

where $\Lambda(0, 0) = 0$, $A(0) = 0$, $C(0) = 0$, and $\Lambda_\lambda > 0$.

Next, we unfold the bifurcation point. Let $f(y, \mu, b)$ be a family of functions with a bifurcation point at $(y, \mu, b) = (0, 0, 0)$. As before, b parameterizes the family and $b \neq 0$ indicates a perturbation from the bifurcation. Define $\ell := \text{codim}_B(f)$. By the universal unfolding theorem for bifurcations, $f(y, \mu, b)$ factors through a normal form, say $N(y, \mu, B)$ where $B \in \mathbb{R}^\ell$. That is,

$$f(y, \mu, b) = S(y, \mu, b)N(Y(y, \mu, b), M(\mu, b), B(b)) \qquad (4.4.2)$$

where $S(0, 0, 0) > 0$, $Y(0, 0, 0) = 0$, $M(0, 0) = 0$, $B(0) = 0$, $Y_y(0, 0, 0) > 0$, and $M_\mu(0, 0) > 0$ [GS85].

A homeostasis-bifurcation point is created by linking the input-output function, $x(\lambda)$, with the bifurcation problem, $f(y,\mu)$, to form $h(y,\lambda) := f(y, x(\lambda))$. Replacing x and f with their normal form shows that h factors as

$$h(y,\lambda,a,b,c) = S(x(\lambda,a),y,b)N(Y(x(\lambda,a),y,b),X(x(\lambda,a),b),B(b)). \tag{4.4.3}$$

Therefore a universal unfolding for h is given by

$$N(y, \pm\lambda^k + a_{k-2}\lambda^{k-2} + \cdots a_1\lambda - c, b). \tag{4.4.4}$$

Noting that there are $(k-2)+\ell+1 = \text{codim}_H(x) + \text{codim}_B(f) + 1$ parameters in this unfolding justifies formula (4.1.6).

4.5 Transition varieties

In this section we define the transition varieties of a homeostasis-bifurcation point. These are the set of points in parameter space across which the diagram qualitatively changes. Knowledge of these transition varieties allows us to find all possible behaviors near the homeostasis-bifurcation point.

Consider a perturbed version of (4.1.1)-(4.1.2):

$$\dot{X} = G(X,\lambda,a) \tag{4.5.1}$$

$$\dot{Y} = F(Y, x-c, b) \tag{4.5.2}$$

where we recall $X \in \mathbb{R}^m$, $Y \in \mathbb{R}^n$, $x = X_i$ is the distinguished, homeostatic variable of (4.5.1), and Y_k is the variable of interest. We assume (4.5.2) undergoes a steady-state or Hopf bifurcation at $(Y,x,b,c) = (0,0,0,0)$. Let $x(\lambda,a)$ be the input output function of (4.5.1) and $f(y,\mu,b)$ be an appropriate scalar reduction of (4.5.2) at the bifurcation point. Define $h(y,\lambda,a,b,c) = f(y, x(\lambda,a)-c, b)$. Let $U,\ L \subset \mathbb{R}$ be closed intervals and $(a,b,c) \in W \subset \mathbb{R}^p$. We take $U \times L \times W$ to be the domain of h. Solutions

to $f = 0$ correspond to equilibria or amplitudes of limit cycles according to whether F undergoes a steady state or Hopf bifurcation, respectively.

As discussed in Section 2.2.2, (4.5.2) has a Hopf bifurcation, phase-shift symmetry forces f to be odd in y and that symmetry must be respected by perturbations. As a result, the transition varieties will differ depending on whether (4.5.2) has a steady-state or Hopf bifurcation. We first define the transition varieties for a steady-state bifurcation.

The transition varieties for homeostasis-steady state bifurcation can be defined by conditions on h or by conditions on (x, f). Defined by conditions on h they are as follows.

$$\mathcal{B} = \{(a,b,c) | \exists (y,\lambda) \text{ such that } h = h_\lambda = h_y = 0\}$$

$$\mathcal{H} = \{(a,b,c) | \exists (y,\lambda) \text{ such that } h = h_y = h_{yy} = 0\}$$

$$\mathcal{D} = \{(a,b,c) | \exists (y_1,y_2,\lambda) \text{ such that } h = h_y = 0 \text{ at } (y_i,\lambda), i = 1,2\}$$

$$\mathcal{C} = \{(a,b,c) | \exists (y,\lambda) \text{ such that } h = h_\lambda = h_{\lambda\lambda} = 0\}.$$

Note that $\mathcal{B}$, $\mathcal{H}$, and $\mathcal{D}$ are the bifurcation, hysteresis, and double limit point transition varieties for h as a bifurcation point (see Section 2.2.1). $\mathcal{C}$ is the parameter set where a branch of h has a chair point.

In terms of x and f the transition varieties are

$$\begin{aligned}
CH_x =&\{(a,b,c)|\exists(x,y,\lambda) \text{ such that } \mu - x = f = x_\lambda = x_{\lambda\lambda} = 0\}\\
\mathscr{B} =&\{(a,b,c)|\exists(x,y,\lambda) \text{ such that } \mu - x = f = f_\mu = f_y = 0\}\\
HYS =&\{(a,b,c)|\exists(x,y,\lambda) \text{ such that } \mu - x = f = f_y = f_{yy} = 0\}\\
\mathscr{D} =&\{(a,b,c)|\exists(x,\lambda,y_1,y_2), y_1 \neq y_2 \text{ such that}\\
&\quad \mu - x = f = f_y = 0 \text{ at } (x,y_i,\lambda), i = 1,2\}\\
CH_f =&\{(a,b,c)|\exists(x,y,\lambda) \text{ such that } \mu - x = f = f_\mu = f_{\mu\mu} = 0\}\\
\mathscr{C} =&\{(a,b,c)|\exists(x,y,\lambda) \text{ such that } \mu - x = f = f_y = x_\lambda = 0\}\\
HH =&\{(a,b,c)|\exists(x,y,\lambda) \text{ such that } \mu - x = f = x_\lambda = f_\mu = 0\}.
\end{aligned}$$

CH_x is the set of parameters where x has a chair point. $\mathscr{B}$, HYS, and $\mathscr{D}$ are the transition varieties of f as a bifurcation point. CH_f is where f has a branch with a chair point. $\mathscr{C}$ and HH are due to interactions between x and f. $\mathscr{C}$ is the coincidence transition variety consisting of points where homeostasis in x coincides with bifurcation in f. HH is where homeostasis in x coincides with homeostasis on a branch of f.

Proposition 4.7. *The two above definitions for the transition varieties are equivalent. That is,* $CH_1 \cup \mathscr{B} \cup HYS \cup \mathscr{D} \cup \mathscr{C} \cup HH \cup CH_2 = \mathcal{B} \cup \mathcal{H} \cup \mathcal{D} \cup \mathcal{C}$.

Proof. It is clear that $\mu - x(\lambda, a) = f(y, \mu - c, b) = 0$ if and only if $h(y, \lambda, a, b, c) = f(y, x(\lambda, a) - c, b) = 0$. Next, notice $h_\lambda = f_\mu x_\lambda$, $h_y = f_y$, $h_{yy} = f_{yy}$, and $h_{\lambda\lambda} = f_{\mu\mu}x_\lambda^2 + f_\mu x_{\lambda\lambda}$ so that we have

1. $h_\lambda = h_y = 0$ if and only if $(f_x = 0$ or $x_\lambda = 0)$ and $f_y = 0$,
2. $h_y = h_{yy} = 0$ if and only if $f_y = f_{yy} = 0$,

3. $h_y = 0$ if and only if $f_y = 0$,

4. $h_\lambda = h_{\lambda\lambda} = 0$ if and only if $(x_\lambda = f_\mu = 0)$ or $(f_\mu = f_{\mu\mu} = 0)$ or $(x_\lambda = x_{\lambda\lambda} = 0)$.

Each of these, respectively, imply $\mathcal{B} = \mathscr{B} \cup \mathscr{C}$, $\mathcal{H} = HYS$, $\mathcal{D} = \mathscr{D}$, and $\mathcal{C} = HH \cup CH_2 \cup CH_1$.

■

In addition to these transition varieties, there are transitions which correspond to singularities occurring on the boundary of $U \times L$. For bifurcations, these are described in chapter 4 of [GS85]. In the case of homeostasis-bifurcation, there are additional transitions corresponding to homeostasis points on the boundary. Dealing with these transitions is not difficult, but only serves to obscure the ideas, so we will assume that these boundary transitions do not occur.

Now suppose (4.5.2) undergoes a Hopf bifurcation at $(Y, x, b, c) = (0, 0, 0, 0)$. In this case we make an additional non-degeneracy assumption. We may apply the implicit function theorem to $F(Y, x, 0) = 0$ to obtain a curve of equilibria, $Y(x)$. We assume $Y'(x) \neq 0$. This assumption guarantees that locally the only equilibrium homeostasis points (either stable or unstable) of Y_k are inherited by x. The reduction of (4.5.2) yields $f(y, \mu, b) = \rho(y^2, \mu, b)y$ for some function $\rho(u, \mu, b)$. Define $r(u, \lambda, a, b, c) = \rho(u, x(\lambda, a) - c, b)$. h is then given by $h(y, \lambda, a, b, c) = r(y^2, \lambda, a, b, c)y$. The transition varieties can be defined by conditions on r and x only. They are as

follows.

$$\begin{aligned}
\mathcal{B}_H =&\{(a,b,c)|\exists(u,\lambda), u>0 \text{ such that } r=r_\lambda=r_u=0\}\\
\mathcal{B}_0 =&\{(a,b,c)|\exists\lambda \text{ such that at } u=0, r=r_\lambda=0\}\\
\mathcal{H}_H =&\{(a,b,c)|\exists(u,\lambda), u>0 \text{ such that } r=r_u=r_{uu}=0\}\\
\mathcal{H}_0 =&\{(a,b,c)|\exists\lambda \text{ such that at } u=0, r=r_u=0\}\\
\mathcal{D}_H =&\{(a,b,c)|\exists(u_1,u_2,\lambda)u\geq 0 \text{ such that } r=r_u=0 \text{ at } (u_i,\lambda), i=1,2\}\\
\mathcal{C}_H =&\{(a,b,c)|\exists(u,\lambda), u>0 \text{ such that } r=r_\lambda=r_{\lambda\lambda}=0\}\\
CH_H =&\{(a,b,c)|\exists\lambda \text{ such that } x_\lambda=x_{\lambda\lambda}=0\}.
\end{aligned}$$

These are the standard transition varieties for h treated as a bifurcation with the addition of $\mathcal{C}_H$, which accounts for chair points of the amplitude, and CH_H which accounts for chair points on the equilibria.

We use the definition involving h for the steady-state transitions in what follows. Define

$$\Sigma=\mathcal{B}\cup\mathcal{H}\cup\mathcal{D}\cup\mathcal{C} \quad \text{or} \quad \Sigma=\mathcal{B}_H\cup\mathcal{B}_0\cup\mathcal{H}_H\cup\mathcal{H}_0\cup\mathcal{D}_H\cup\mathcal{C}_H\cup CH_H$$

as appropriate. To simplify notation, collect the parameters into a single variable $\alpha=(a,b,c)\in W$. We will show that if $\alpha,\beta\in W\setminus\Sigma$ are in the same connected component of $W\setminus\Sigma$, then $h(y,\lambda,\alpha)$ and $h(y,\lambda,\beta)$ have the same diagram. Because Σ is a superset of the bifurcation transition varieties (Definitions 2.6 and 2.11) we immediately have the following proposition as a consequence of Theorems 2.3, 2.4, and 2.5.

Proposition 4.8. *Let α and β be in the same connected component of $W\setminus\Sigma$ and suppose that there are no boundary transitions. Then $h(\cdot,\cdot,\alpha)$ and $h(\cdot,\cdot,\beta)$ are equivalent as bifurcations. If f is the unfolding of a steady state bifurcation, then $h(\cdot,\cdot,\alpha)$ and*

$h(\cdot,\cdot,\beta)$ are combinatorially equivalent. If f is the unfolding of a Hopf bifurcation, then $r(\cdot,\cdot,\alpha)$ and $r(\cdot,\cdot,\beta)$ are combinatorially equivalent.

In particular, combinatorial equivalence allows us to identify branches of $h(\cdot,\cdot,\alpha)$ and $h(\cdot,\cdot,\beta)$ with each other. This identification allows us to determine if the branches have the same number of homeostasis points.

Theorem 4.9. *Let α and β be in the same connected component of $W \setminus \Sigma$ and suppose there are no boundary transitions. Then if C^α and C^β are corresponding branches of $h(\cdot,\cdot,\alpha)$ and $h(\cdot,\cdot,\beta)$ with homeostasis points $\nu_1 < \nu_2 < \cdots < \nu_i$ and $\sigma_1 < \sigma_2 < \cdots < \sigma_j$ respectively, then $i = j$ and $\operatorname{sign}(C^{\alpha\,\prime\prime}(\nu_m) = \operatorname{sign}(C^{\beta\,\prime\prime}(\sigma_m))$ for each m.*

Proof. Differentiating $h(C^\alpha(\lambda),\lambda,\alpha)$ in λ and using $\alpha \notin \mathcal{C}$ or $\alpha \notin \mathcal{C}_H$ shows that $C^{\alpha\,\prime}$ and $C^{\alpha\,\prime\prime}$ cannot simultaneously vanish. The same statement is true for C^β. This fact and the compactness of the domains of C^α and C^β together implies that there are only a finite number of homeostasis points on each branch. Therefore the enumeration in the statement of the theorem is well defined.

Let $\alpha(t)$ be a path in a connected component of $W \setminus \Sigma$ with $\alpha(0) = \alpha$ and $\alpha(1) = \beta$. For each $t \in [0,1]$, we can identify a branch of $h(\cdot,\cdot,\alpha(t))$ with C^α because the reduced functions are equivalent as bifurcations by Proposition 2. Name this branch C^t. Note that $C^0 = C^\alpha$ and $C^1 = C^\beta$.

Let $t_0 \in [0,1]$ and $\lambda_1 < \lambda_2 < \cdots < \lambda_\ell$ be the set of points where $\phi(\lambda,t_0) := C^{t_0\,\prime}(\lambda)$ vanishes. For each i, $\phi(\lambda_i,t_0) = 0$ and $\phi_\lambda(\lambda_i,t_0) = C^{t_0\,\prime\prime}(\lambda_i) \neq 0$. So, by the implicit function theorem, there is a smooth curve, $\Lambda_i(t)$ so that $\phi(\Lambda_i(t),t) = 0$ for t near t_0. We can construct such a function for any $t_0 \in [0,1]$. By the compactness of $[0,1]$ we can patch together these curves and define $\Lambda_i(t)$ globally on $[0,1]$. Uniqueness, implied by the implicit function theorem, then guarantees that $\ell = i = j$ and the ordering is preserved as the curves can't cross.

For each t, $C^t{}'(\Lambda_i(t)) = 0$ and $C^t{}''(\Lambda_i(t)) \neq 0$. So by continuity, $\text{sign}(C_k^t{}''(\Lambda_i(t)))$ is constant and in particular $\text{sign}(C^\alpha{}''(\nu_i)) = \text{sign}(C^\beta{}''(\sigma_i))$.

■

Proposition 4.8 and Theorem 4.9 together imply that the diagrams of h are qualitatively the same on connected components of $W \setminus \Sigma$ in the case of steady-state bifurcation. For Hopf bifurcation, this does not rule out homeostasis transitions for the equilibria solutions. Our assumption that the equilibria $Y_k'(x) \neq 0$ at the Hopf bifurcation means homeostasis in $Y_k(x(\lambda))$ can only be inherited from x. CH_H thus accounts for these transitions. It is possible that (4.5.1)-(4.5.2) have the same diagram on different connected components. Indeed Section 4.6 contains examples of this.

4.6 Low Codimension Homeostasis-Bifurcation Points

In this section we provide all information for the homeostasis-bifurcation points arising from the singularities in Tables 2.1, 2.2, and 2.3. The information is organized into the tables within this section with the numbers in parentheses indicating how to link the information between tables. When plotting the diagrams of persistent phenomena, we do not plot the period of limit cycle solutions. However, homeostasis points of the period which are inherited by x can be recovered by noting that these coincide with homeostasis points on the branch of unstable equilibria (see Figure 4.9 for an example). We assume that $f_y < 0$ indicates a stable equilibrium.

Table 4.1: **Defining Conditions**
For Hopf bifurcations $\rho(u,\mu)$ is defined by $f(y,\mu) = \rho(y^2,\mu)y$. The numbers link information between tables. * We always assume $x_\lambda = 0$ and $f = f_y = 0$. For Hopf bifurcations, we assume $\rho = 0$.

	Normal Form	Defining Conditions*	Nondegeneracy Conditions
	Homeostasis-steady state bifurcations		
(1)	$x(\lambda) = \eta\lambda^2$ $f(y,\mu) = \varepsilon y^2 + \delta\mu$		$\eta = \text{sign}(x_{\lambda\lambda})$ $\varepsilon = \text{sign}(f_{yy})$, $\delta = \text{sign}(f_\mu)$
(2)	$x(\lambda) = \eta\lambda^2$ $f(y,\mu) = \varepsilon(y^2 + \delta\mu^2)$	$f_\mu = 0$	$\eta = \text{sign}(x_{\lambda\lambda})$ $\varepsilon = \text{sign}(f_{yy})$, $\delta = \text{sign}(\det\ d^2 f)$
(3)	$x(\lambda) = \eta\lambda^2$ $f(y,\mu) = \varepsilon y^3 + \delta\mu$	$f_{yy} = 0$	$\eta = \text{sign}(x_{\lambda\lambda})$ $\varepsilon = \text{sign}(f_{yyy})$, $\delta = \text{sign}(f_\mu)$
(4)	$x(\lambda) = \eta\lambda^3$ $f(y,\mu) = \varepsilon y^2 + \delta\mu$	$x_{\lambda\lambda} = 0$	$\eta = \text{sign}(x_{\lambda\lambda\lambda})$ $\varepsilon = \text{sign}(f_{yy})$, $\delta = \text{sign}(f_\mu)$
(5)	$x(\lambda) = \eta\lambda^3$ $f(y,\mu) = \varepsilon(y^2 + \delta\mu^2)$	$x_{\lambda\lambda} = 0$ $f_\mu = 0$	$\eta = \text{sign}(x_{\lambda\lambda\lambda})$ $\varepsilon = \text{sign}(f_{yy})$, $\delta = \text{sign}(\det\ d^2 f)$
(6)	$x(\lambda) = \eta\lambda^3$ $f(y,\mu) = \varepsilon y^3 + \delta\mu$	$x_{\lambda\lambda} = 0$ $f_{yy} = 0$	$\eta = \text{sign}(x_{\lambda\lambda\lambda})$ $\varepsilon = \text{sign}(f_{yy})$, $\delta = \text{sign}(f_\mu)$
	Homeostasis-Hopf bifurcations		
(7)	$x(\lambda) = \eta\lambda^2$ $f(y,\mu) = (\varepsilon y^2 + \delta\mu)y$		$\eta = \text{sign}(x_{\lambda\lambda})$ $\varepsilon = \text{sign}(\rho_u)$, $\delta = \text{sign}(\rho_\mu)$
(8)	$x(\lambda) = \eta\lambda^2$ $f(y,\mu) = (\varepsilon y^2 + \delta\mu^2)y$	$\rho_\mu = 0$	$\eta = \text{sign}(x_{\lambda\lambda})$ $\varepsilon = \text{sign}(\rho_u)$, $\delta = \text{sign}(\rho_{\mu\mu})$
(9)	$x(\lambda) = \eta\lambda^2$ $f(y,\mu) = (\varepsilon y^4 + \delta\mu)y$	$\rho_u = 0$	$\eta = \text{sign}(x_{\lambda\lambda})$ $\varepsilon = \text{sign}(\rho_{uu})$, $\delta = \text{sign}(\rho_\mu)$
(10)	$x(\lambda) = \eta\lambda^3$ $f(y,\mu) = (\varepsilon y^2 + \delta\mu)y$	$x_{\lambda\lambda} = 0$	$\eta = \text{sign}(x_{\lambda\lambda\lambda})$ $\varepsilon = \text{sign}(\rho_u)$, $\delta = \text{sign}(\rho_\mu)$
(11)	$x(\lambda) = \eta\lambda^2$ $f(y,\mu) = (\varepsilon y^2 + \delta\mu^2)y$	$x_{\lambda\lambda} = 0$ $\rho_\mu = 0$	$\eta = \text{sign}(x_{\lambda\lambda\lambda})$ $\varepsilon = \text{sign}(\rho_u)$, $\delta = \text{sign}(\rho_{\mu\mu})$
(12)	$x(\lambda) = \eta\lambda^2$ $f(y,\mu) = (\varepsilon y^4 + \delta\mu)y$	$x_{\lambda\lambda} = 0$ $\rho_u = 0$	$\eta = \text{sign}(x_{\lambda\lambda\lambda})$ $\varepsilon = \text{sign}(\rho_{uu})$, $\delta = \text{sign}(\rho_\mu)$

Table 4.2: **Universal unfoldings**

Blue (red) curves indicate stable (unstable) equilibria. The numbers link information between tables.

	Universal Unfolding	Unperturbed Diagrams ($\varepsilon = -1,\ \eta = 1$) $\delta = 1$	$\delta = -1$
(1)	$x(\lambda) = \eta\lambda^2$ $f(y, \mu, c) = \varepsilon y^2 + \delta(\mu - c)$	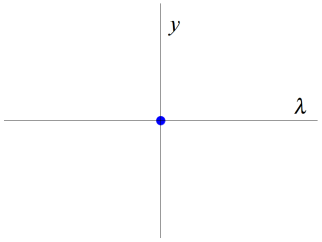	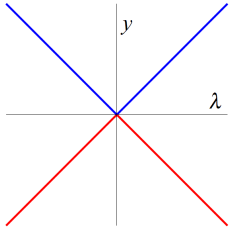
(2)	$x(\lambda) = \eta\lambda^2$ $f(y, \mu, c) = \varepsilon(y^2 + \delta(\mu - c)^2 + b)$	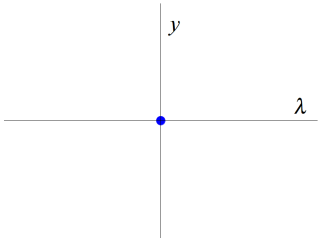	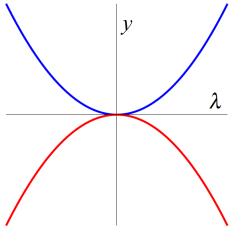
(3)	$x(\lambda) = \eta\lambda^2$ $f(y, \mu, c) = \varepsilon y^3 + \delta(\mu - c) + by$	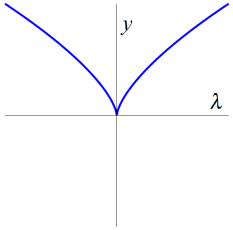	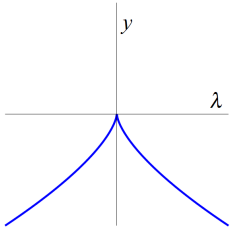

	Universal Unfolding	Unperturbed Diagrams ($\varepsilon = -1,\ \eta = 1$) $\delta = 1$	$\delta = -1$
(4)	$x(\lambda) = \eta\lambda^3 + a\lambda$ $f(y, \mu, c) = \varepsilon y^2 + \delta(\mu - c)$	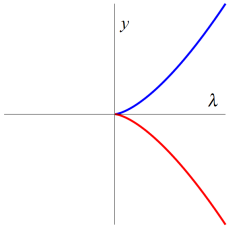	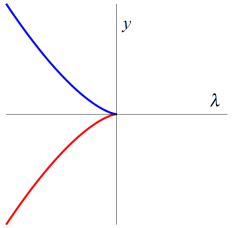
(5)	$x(\lambda) = \eta\lambda^3 + a\lambda$ $f(y, \mu, c) = \varepsilon(y^2 + \delta(\mu - c)^2 + b)$	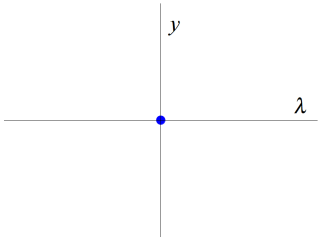	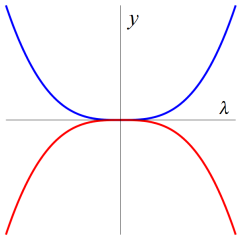
(6)	$x(\lambda) = \eta\lambda^3 + a\lambda$ $f(y, \mu, c) = \varepsilon y^3 + \delta(\mu - c) + by$	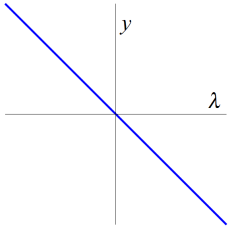	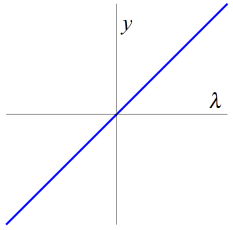

	Universal Unfolding	Unperturbed Diagrams ($\varepsilon = -1,\ \eta = 1$) $\delta = 1$	$\delta = -1$
(7)	$x(\lambda) = \eta\lambda^2$ $f(y, \mu, c) = \varepsilon y^3 + \delta(\mu - c)y$	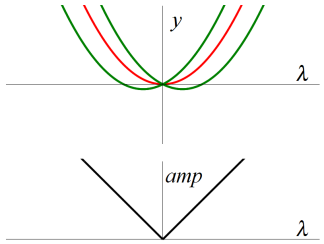	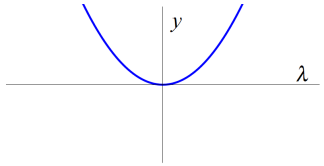
(8)	$x(\lambda) = \eta\lambda^2$ $f(y, \mu, c) = \varepsilon y^3 + \delta(\mu - c)^2 y + by$	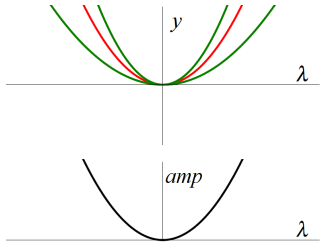	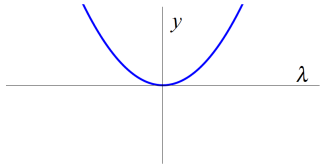
(9)	$x(\lambda) = \eta\lambda^2$ $f(y, \mu, c) = \varepsilon y^5 + \delta(\mu - c)y + by^3$	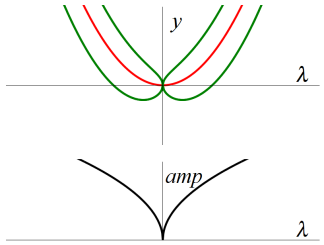	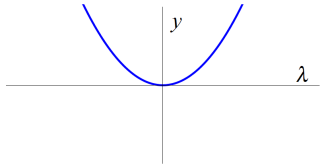

	Universal Unfolding	Unperturbed Diagrams ($\varepsilon = -1,\ \eta = 1$) $\delta = 1$	$\delta = -1$
(10)	$x(\lambda) = \eta\lambda^3 + a\lambda$ $f(y, \mu, c) = \varepsilon y^3 + \delta(\mu - c)y$	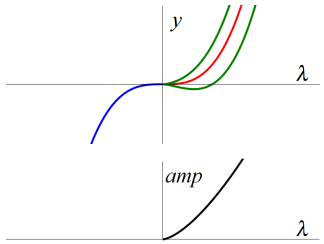	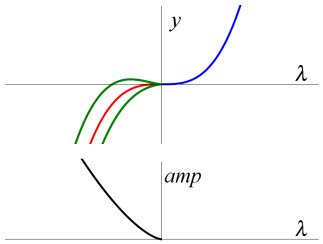
(11)	$x(\lambda) = \eta\lambda^3 + a\lambda$ $f(y, \mu, c) = \varepsilon y^3 + \delta(\mu - c)^2 y + by$	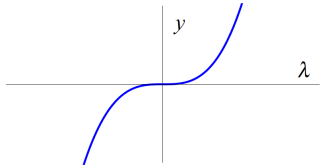	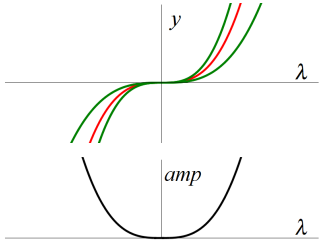
(12)	$x(\lambda) = \eta\lambda^3 + a\lambda$ $f(y, \mu, c) = \varepsilon y^5 + \delta(\mu - c)y + by^3$	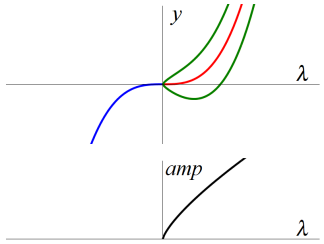	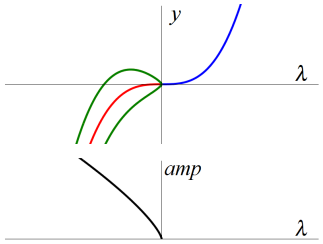

Table 4.3: **The hysteresis and chair transition varieties**
$\theta = 1$ or -1. $\mathcal{D} = \emptyset$ for each homeostasis-bifurcation point considered here. The numbers link information between tables with $(+)$ or $(-)$ indicating the sign of δ where appropriate. $\delta = 1$ otherwise. We choose $\varepsilon = -1$ and $\eta = 1$.

	Normal Form, h	$\mathcal{H}$	$\mathcal{C}$
$(1)^+$	$-y^2 + \lambda^2 - c$	$\emptyset$	$\emptyset$
$(1)^-$	$-y^2 - \lambda^2 + c$	$\emptyset$	$\emptyset$
$(2)^+$	$-y^2 - (\lambda^2 - c)^2 + b$	$\emptyset$	$\{c = 0 \mid b \geq 0\}$
$(2)^-$	$-y^2 + (\lambda^2 - c)^2 + b$	$\emptyset$	$\{c = 0 \mid b \geq 0\}$
(3)	$-y^3 + \lambda^2 - c + by$	$\{b = 0 \mid c \geq 0\}$	$\emptyset$
(4)	$-y^2 + \lambda^3 + a\lambda - c$	$\emptyset$	$\{a = 0 \mid c \leq 0\}$
$(5)^+$	$-y^2 + (\lambda^3 + a\lambda - c)^2 + b$	$\emptyset$	$\{2\theta\left(\frac{-a}{3}\right)^{\frac{3}{2}} = c \mid a \leq 0,\ b \leq 0\}$ $\cup$ $\{a = 0 \mid c^2 = -b\}$
$(5)^-$	$-y^2 - (\lambda^3 + a\lambda - c)^2 + b$	$\emptyset$	$\{2\theta\left(\frac{-a}{3}\right)^{\frac{3}{2}} = c \mid a \leq 0,\ b \leq 0\}$ $\cup$ $\{a = 0 \mid c^2 \geq b\}$
(6)	$-y^3 + \lambda^+ a\lambda - c + by$	$\{b = 0\}$	$\{a = 0\}$
$(7)^+$	$-y^3 + (\lambda^2 - c)y$	$\emptyset$	$\emptyset$
$(7)^-$	$-y^3 - (\lambda^2 - c)y$	$\emptyset$	$\emptyset$
$(8)^+$	$-y^3 + (\lambda^2 - c)^2 y + by$	$\emptyset$	$\{c = 0 \mid b \geq 0\}$
$(8)^-$	$-y^3 - (\lambda^2 - c)^2 y + by$	$\emptyset$	$\{c = 0 \mid b \leq 0\}$
$(9)^+$	$-y^5 + (\lambda^2 - c)y + by^3$	$\{b = 0 \mid c \geq 0\}$	$\emptyset$
$(9)^-$	$-y^5 - (\lambda^2 - c)y + by^3$	$\{b = 0 \mid c \leq 0\}$	$\emptyset$
(10)	$-y^3 + (\lambda^3 + a\lambda - c)y$	$\emptyset$	$\{a = 0\}$
(11)	$-y^3 + (\lambda^3 + a\lambda - c)^2 y + by$	$\emptyset$	$\{2\theta\left(\frac{-a}{3}\right)^{\frac{3}{2}} = c \mid a \leq 0,\ b \leq 0\}$ $\cup$ $\{a = 0\}$
(12)	$-y^5 + (\lambda^3 + a\lambda - c)y + by^3$	$\{b = 0\}$	$\{a = 0\}$

Table 4.4: **The bifurcation transition varieties**
$\theta = 1$ or -1. $\mathcal{D} = \emptyset$ for each homeostasis-bifurcation point considered here. The numbers link information between tables with $(+)$ or $(-)$ indicating the sign of δ where appropriate. $\delta = 1$ otherwise. We choose $\varepsilon = -1$ and $\eta = 1$.

	Normal Form, h	$\mathcal{B}$
$(1)^+$	$-y^2 + \lambda^2 - c$	$\{c = 0\}$
$(1)^-$	$-y^2 - \lambda^2 + c$	$\{c = 0\}$
$(2)^+$	$-y^2 - (\lambda^2 - c)^2 + b$	$\{b = 0 \vert c \geq 0\} \cup \{b = c^2\}$
$(2)^-$	$-y^2 + (\lambda^2 - c)^2 + b$	$\{b = 0 \vert c \geq 0\} \cup \{b = -c^2\}$
(3)	$-y^3 + \lambda^2 - c + by$	$\{-\theta \left(\frac{b}{3}\right)^{\frac{3}{2}} + \theta b \left(\frac{b}{3}\right)^{\frac{1}{2}} = c\}$
(4)	$-y^2 + \lambda^3 + a\lambda - c$	$\{2\theta \left(\frac{-a}{3}\right)^{\frac{3}{2}} = c \mid a \leq 0\}$
$(5)^+$	$-y^2 + (\lambda^3 + a\lambda - c)^2 + b$	$\{-(2\theta \left(\frac{-a}{3}\right)^{\frac{3}{2}} - c)^2 = b \mid a \leq 0\}$ $\cup$ $\{b = 0\}$
$(5)^-$	$-y^2 - (\lambda^3 + a\lambda - c)^2 + b$	$\{(2\theta \left(\frac{-a}{3}\right)^{\frac{3}{2}} - c)^2 = b \; a \leq 0\}$ $\cup$ $\{b = 0\}$
(6)	$-y^3 + \lambda^+ a\lambda - c + by$	$\{\theta_1 \left(\frac{-a}{3}\right)^{\frac{3}{2}} + \theta_2 \left(\frac{b}{3}\right)^{\frac{3}{2}} = 0 \; \vert a \leq 0, \; b \geq 0\}$
$(7)^+$	$-y^3 + (\lambda^2 - c)y$	$\{c = 0\}$
$(7)^-$	$-y^3 - (\lambda^2 - c)y$	$\{c = 0\}$
$(8)^+$	$-y^3 + (\lambda^2 - c)^2 y + by$	$\{b = 0 \mid c \geq 0\} \cup \{c^2 = -b\}$
$(8)^-$	$-y^3 - (\lambda^2 - c)^2 y + by$	$\{b = 0 \mid c \geq 0\} \cup \{c^2 = -b\}$
$(9)^+$	$-y^5 + (\lambda^2 - c)y + by^3$	$\{\frac{b^2}{4} = c\} \cup \{c = 0\}$
$(9)^-$	$-y^5 - (\lambda^2 - c)y + by^3$	$\{\frac{b^2}{4} = -c\} \cup \{c = 0\}$
(10)	$-y^3 + (\lambda^3 + a\lambda - c)y$	$\{2\theta \left(\frac{-a}{3}\right)^{\frac{3}{2}} = c \mid a \leq 0\}$
(11)	$-y^3 + (\lambda^3 + a\lambda - c)^2 y + by$	$\{(2\theta \left(\frac{-a}{3}\right)^{\frac{3}{2}} - c)^2 = b \mid a \leq 0\}$ $\cup$ $\{b = 0\}$
(12)	$-y^5 + (\lambda^3 + a\lambda - c)y + by^3$	$\{(2^{\frac{2}{3}} - 1) \left(\frac{b}{2}\right)^{\frac{4}{3}} + 2\theta \left(\frac{-a}{3}\right)^{\frac{3}{2}} = c \mid a \leq 0, \; b \geq 0\}$ $\cup$ $\{2\theta \left(\frac{-a}{3}\right)^{\frac{3}{2}} = c \mid a \leq 0\}$

Table 4.5: **Persistent perturbations of homeostasis-steady state bifurcations**
Blue (red) curves indicate stable (unstable) equilibria. Homeostasis points are marked. Diagrams with particularly interesting features are noted within the table. The numbers link information between tables with (+) or (−) indicating the sign of δ where appropriate. $\delta = 1$ otherwise. We choose $\varepsilon = -1$ and $\eta = 1$.

Transition Variety Σ	Persistent Perturbations
$(1)^+$ Simple homeostasis - limit point: $-y^2 + \lambda^2 - c$	
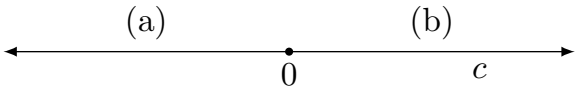	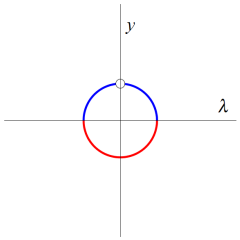 No solutions.
	(a) (b)
$(1)^-$ Simple homeostasis - limit point: $-y^2 - \lambda^2 + c$	
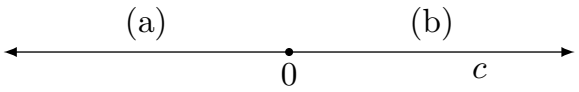	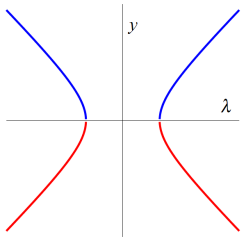 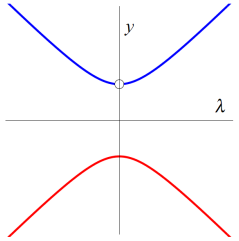
	(a) (b)

Transition Variety Σ	Persistent Perturbations

$(2)^+$ Simple homeostasis - isola: $-y^2 - (\lambda^2 - c)^2 + b$

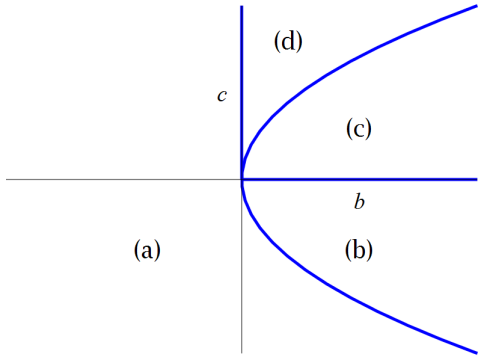

No solutions.

(a)

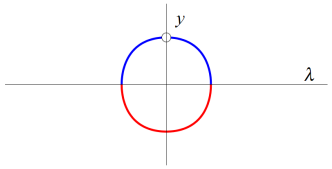

(b)

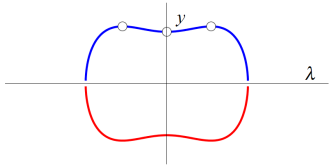

(c)

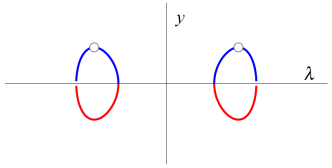

(d)

Region $(2)^+$(c) has a homeostatic plateau for which leaving the plateau is marked by a loss of steady-state.

$(2)^-$ Simple homeostasis - simple bifurcation: $-y^2 + (\lambda^2 - c)^2 + b$

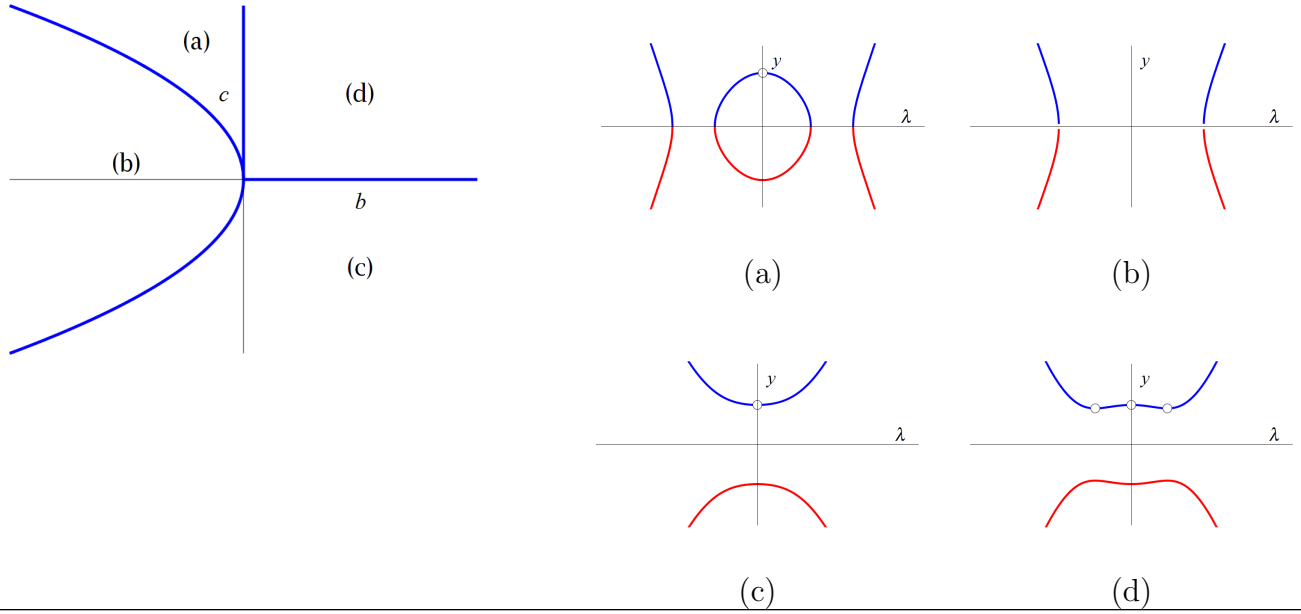

Region $(2)^-$(d) predicts a wide homeostatic plateau.

(3) Simple homeostasis - hysteresis: $-y^3 + \lambda^2 - c + by$

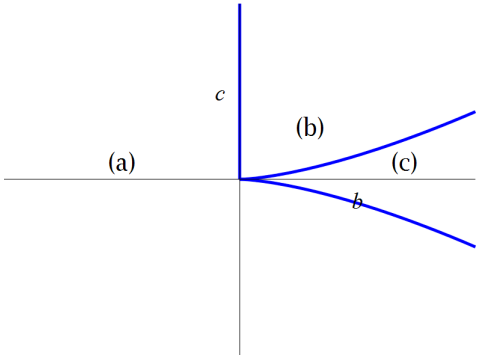

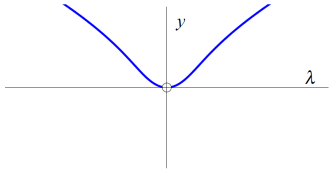

(a)

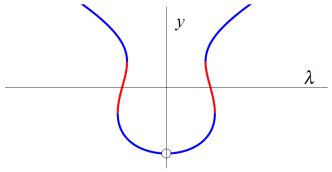

(b)

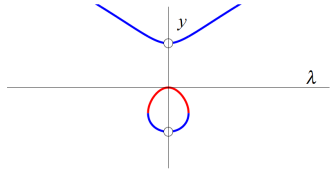

(c)

(4) Chair - limit point: $-y^2 + \lambda^3 + a\lambda - c$

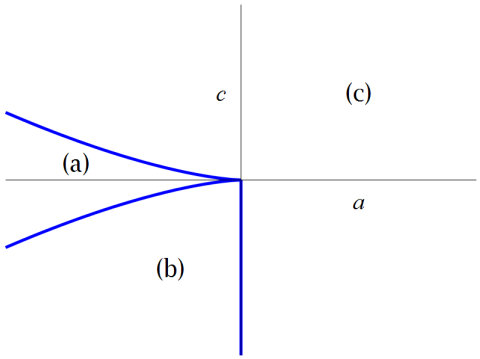

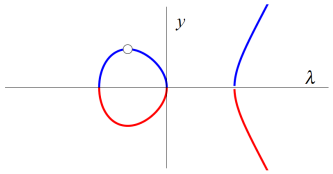

(a)

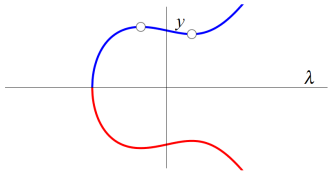

(b)

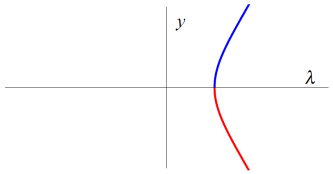

(c)

Transition Variety Σ	Persistent Perturbations

$(5)^+$ Chair - isola: $-y^2 - (\lambda^3 + a\lambda - c)^2 - b$

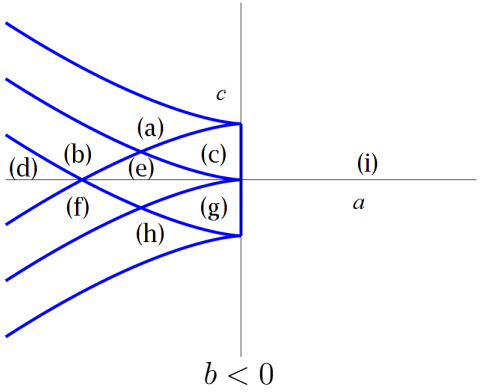

No solutions when $b > 0$.

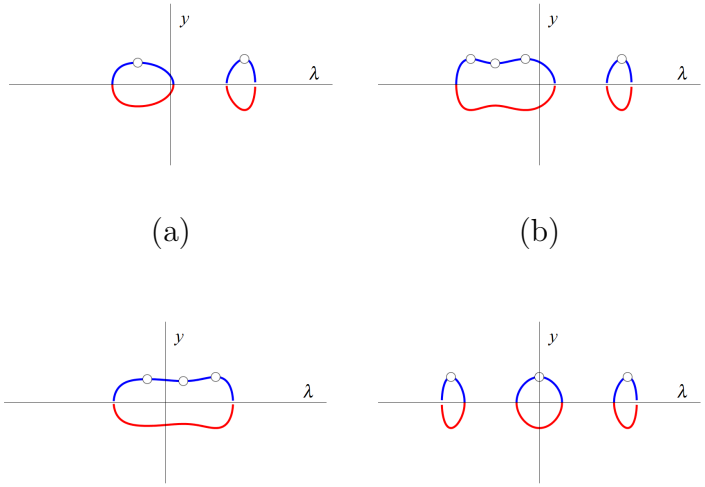

$(5)^+$ has many regions which predict wide plateaus for which leaving the plateau is marked by a loss of steady-state. Region $(5)^+$(e) is exceptionally homeostatic.

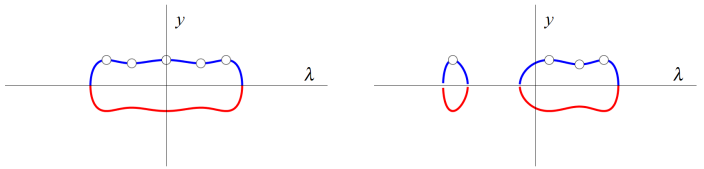

(e) (f)

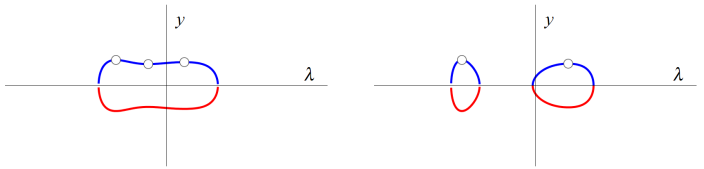

(g) (h)

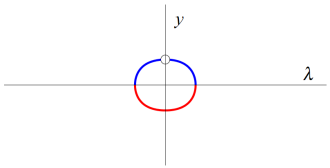

(i)

$(5)^-$ Chair - simple bifurcation: $-y^2 + (\lambda^3 + a\lambda - c)^2 - b$

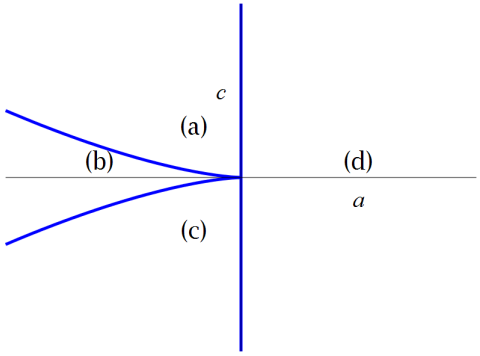

$b < 0$

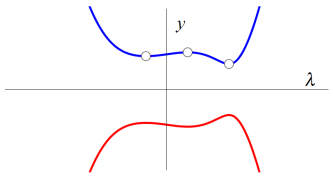

(a)

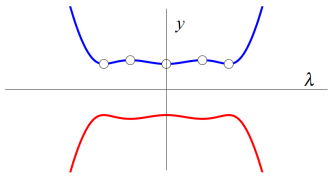

(b)

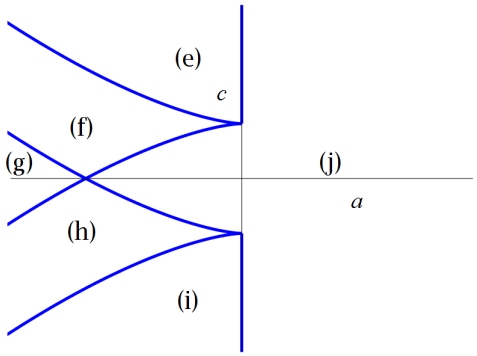

$b > 0$

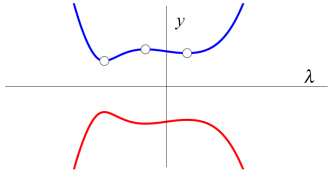

(c)

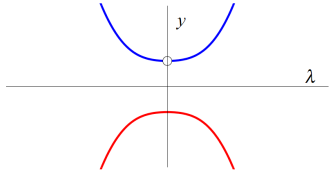

(d)

Transition Variety Σ	Persistent Perturbations

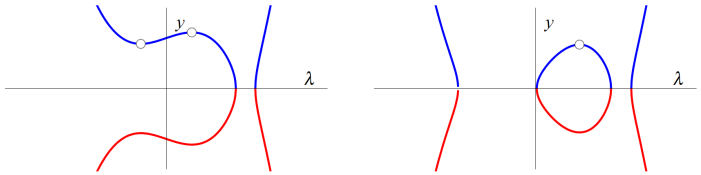

(e)

(f)

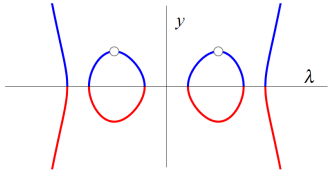

(g)

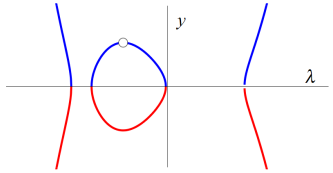

(h)

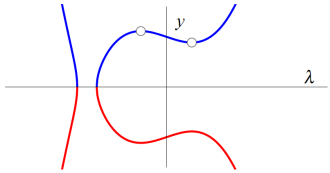

(i)

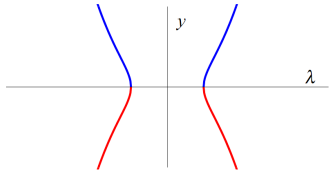

(j)

Region $(5)^{-}$(b) predicts a particularly wide plateau. Regions $(5)^{-}$(e) and $(5)^{-}$(i) predict a plateau for which variation in one direction is marked by loss of steady-state.

(6) Chair - hysteresis: $-y^3 + \lambda^3 + a\lambda - c + by$

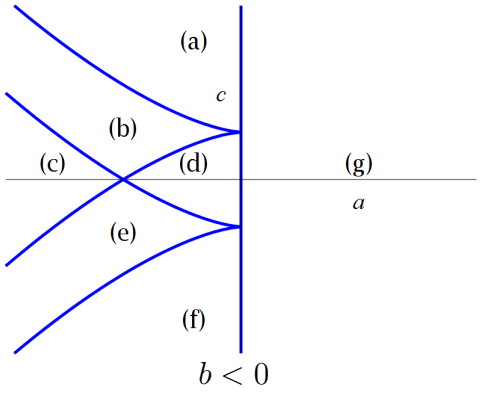

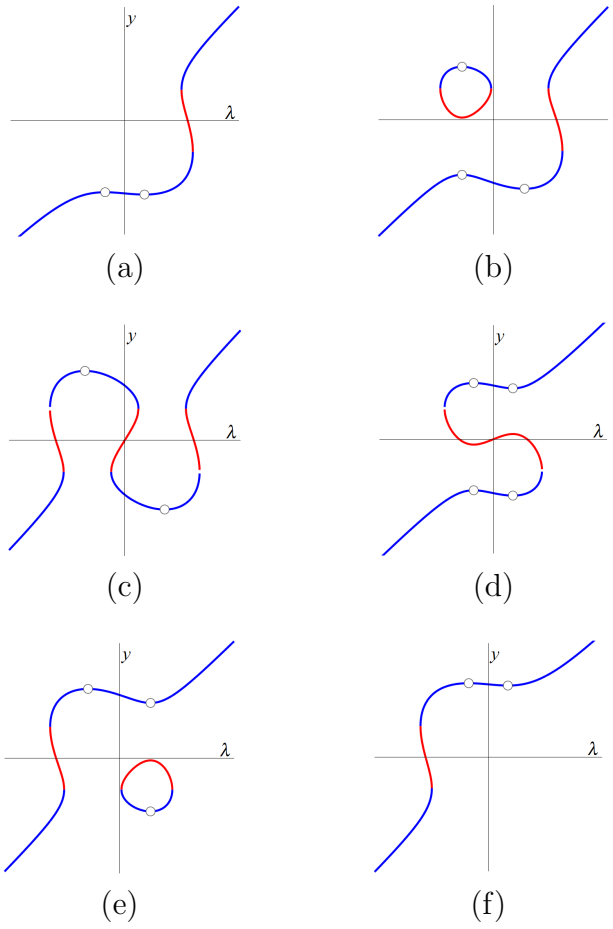

Transition Variety Σ	Persistent Perturbations

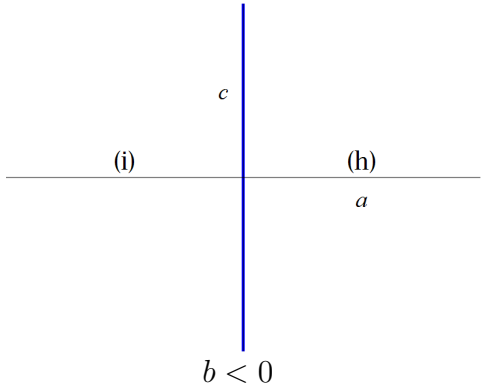

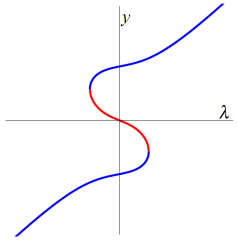

(g)

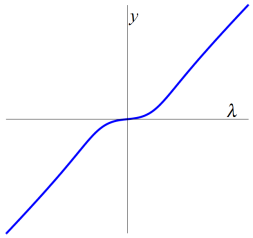

(h)

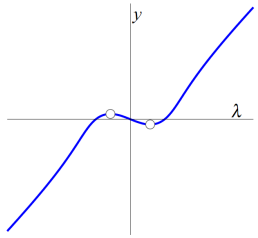

(i)

Regions (6)(c) and (6)(d) are highlighted in Figure 4.7).

Table 4.6: **Persistent perturbations of homeostasis-Hopf bifurcations**
Blue (red) curves indicate stable (unstable) equilibria. Green (orange) curves indicate stable (unstable) limit cycles. Black solid (dashed) curves indicate amplitudes of stable (unstable) limit cycles. Homeostasis points of equilibria and amplitude are marked. Diagrams with particularly interesting features are noted within the table. The numbers link information between tables with (+) or (−) indicating the sign of δ where appropriate. $\delta = 1$ otherwise. We choose $\varepsilon = -1$ and $\eta = 1$.

Transition Variety Σ	Persistent Perturbations
(7)$^+$ Simple homeostasis - simple Hopf: $-y^3 - (\lambda^2 - c)y$ (a) (b) 0 c	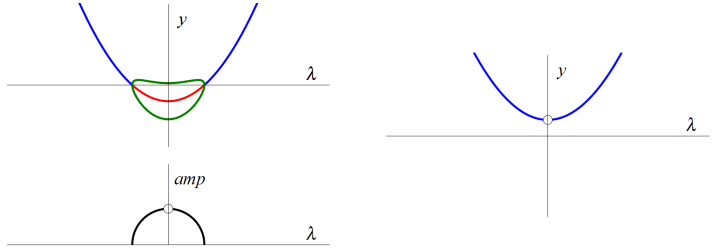 (a) (b)
(7)$^-$ Simple homeostasis - simple Hopf: $-y^3 + (\lambda^2 - c)y$ (a) (b) 0 c	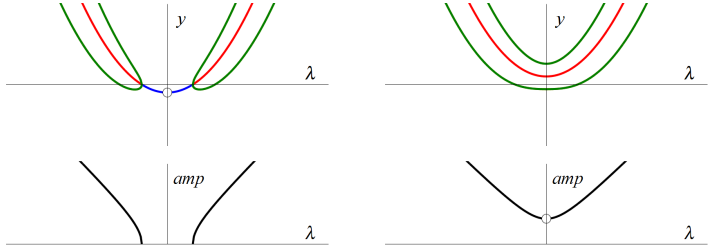 (a) (b)

$(8)^+$ Simple homeostasis - isola Hopf: $-y^3 - (\lambda^2 - c)^2 y - by$

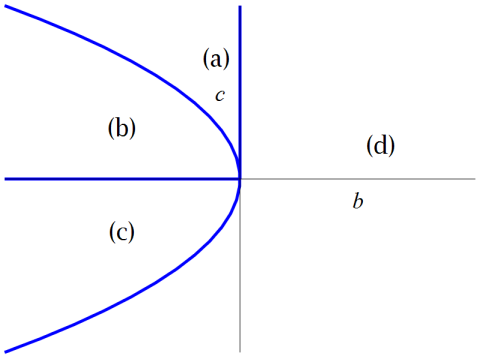

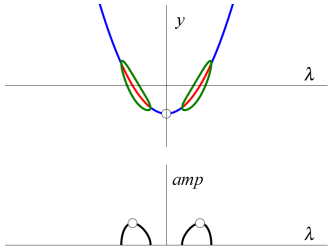

(c)

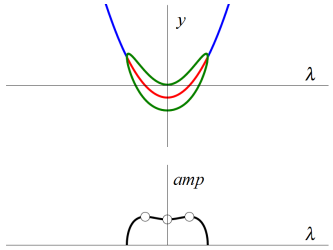

(d)

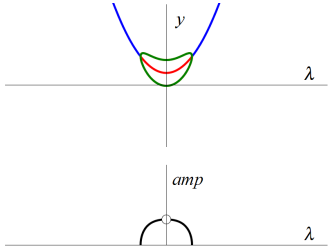

(e)

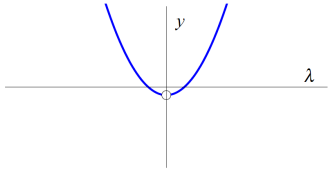

(f)

Transition Variety Σ	Persistent Perturbations
$(8)^-$ $-y^3 + (\lambda^2 - c)^2 y + by$	

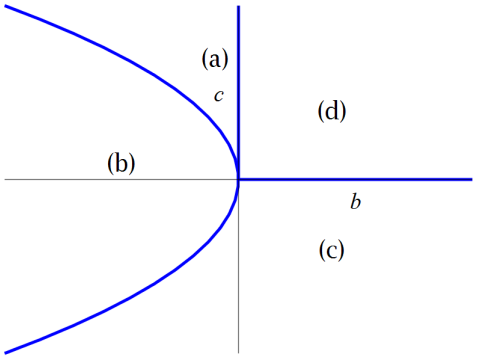

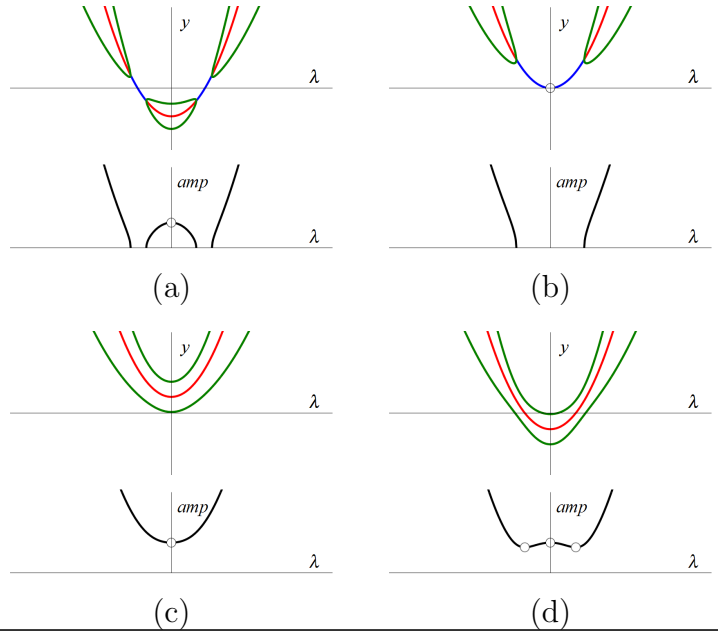

Regions $(8)^+$ and $(8)^-$(j) predict wide homeostatic plateaus in amplitude.

Transition Variety Σ	Persistent Perturbations
(9) $-y^5 + (\lambda^2 - c)y + by^3$	

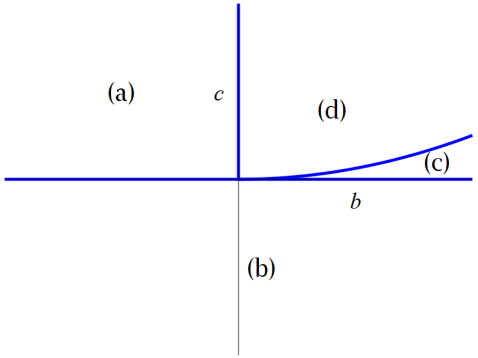

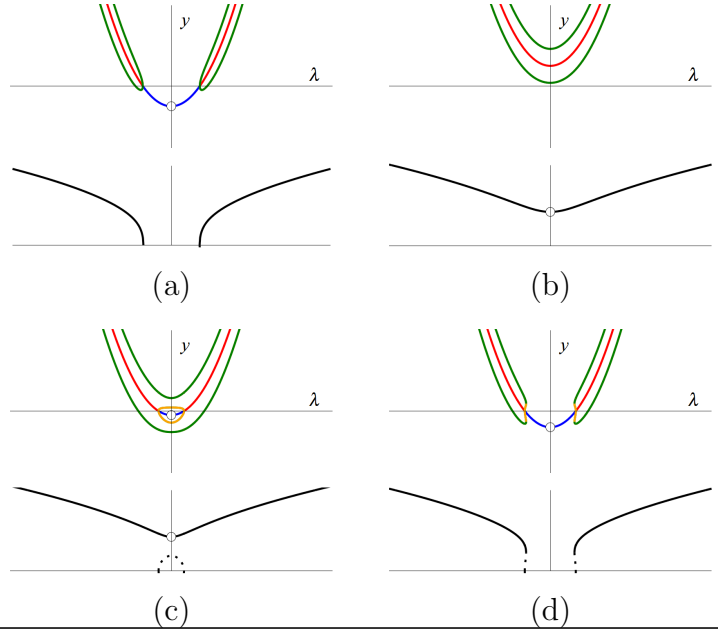

Transition Variety Σ	Persistent Perturbations

(10) Chair - simple Hopf: $-y^3 + (\lambda^3 + a\lambda - c)y$

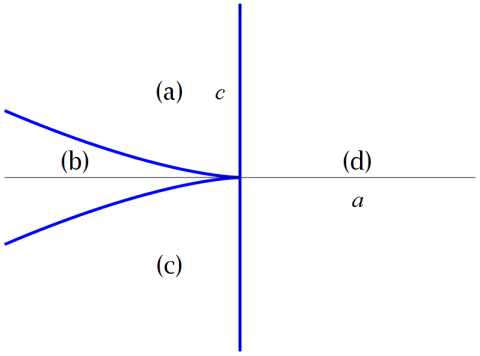

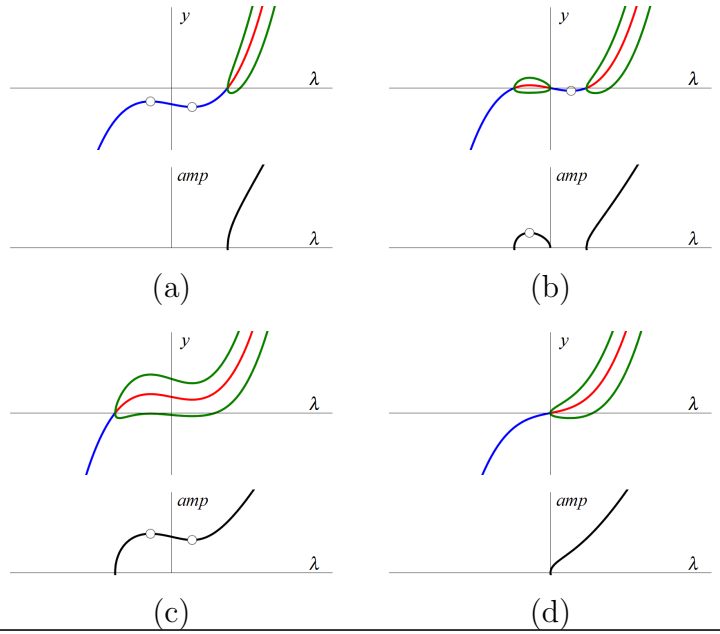

$(11)^+$ Chair - isola Hopf: $-y^3 - (\lambda^3 + a\lambda - c)^2 y - by$

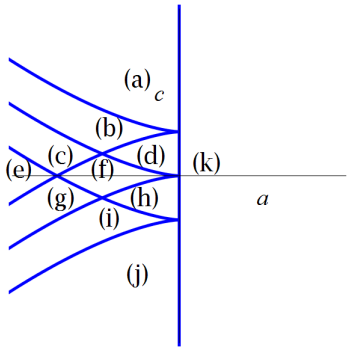

$b < 0$

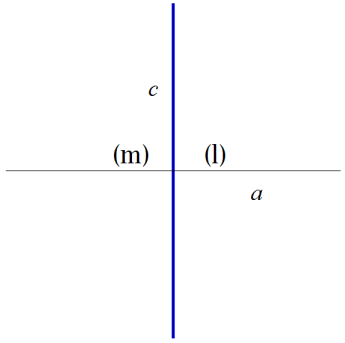

$b > 0$

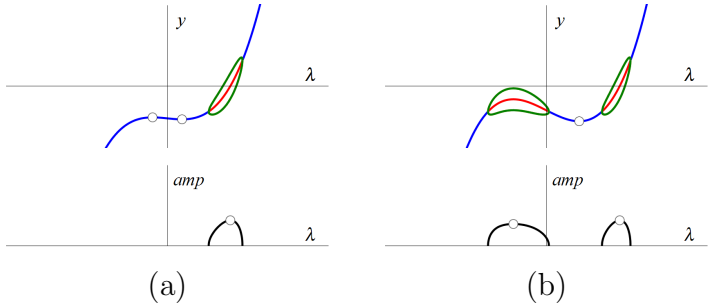

(a) (b)

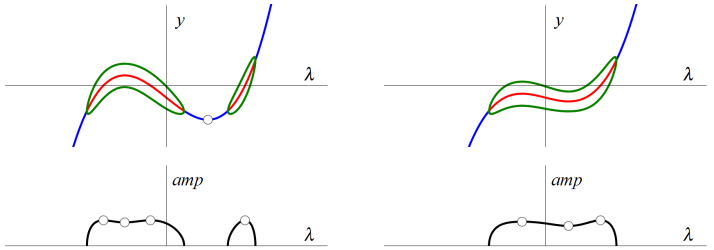

(c) (d)

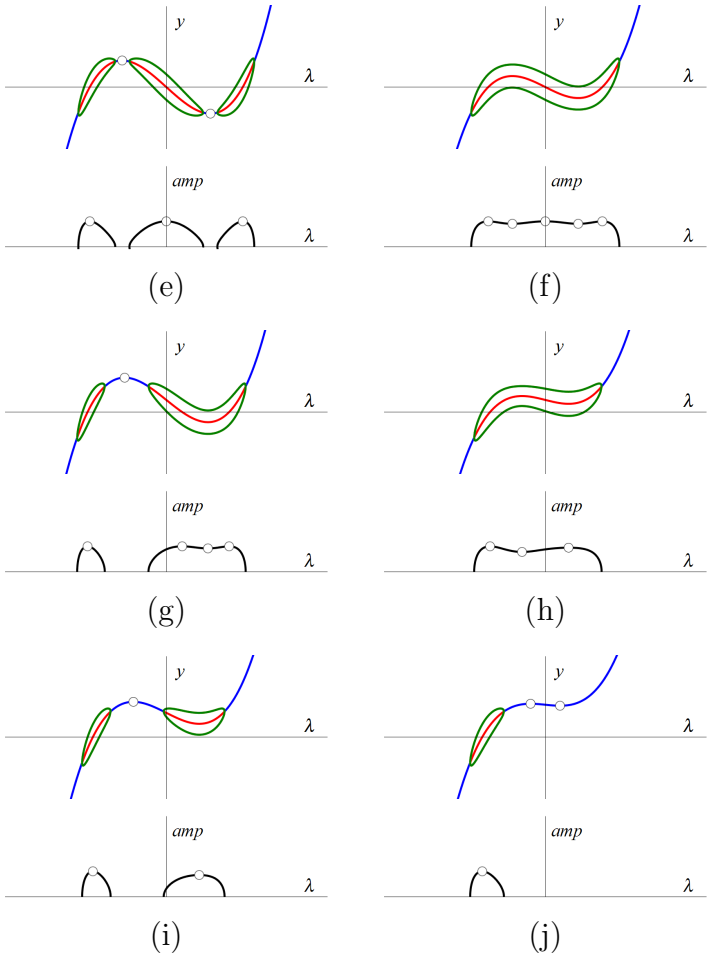
y
λ
amp
λ
(e)
(f)
(g)
(h)
(i)
(j)

Transition Variety Σ	Persistent Perturbations
	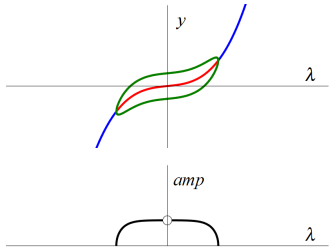 (k) 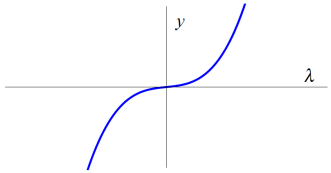 (l) 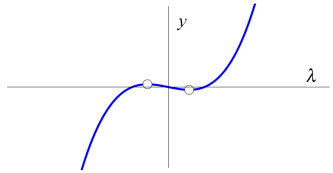 (m)
Regions $(11)^+$(f), $(11)^+$(h), and $(11)^+$(d) are highlighted in Figure 4.9.	

Transition Variety Σ	Persistent Perturbations

$(11)^-$ $-y^3 + (\lambda^3 + a\lambda - c)^2 y + by$

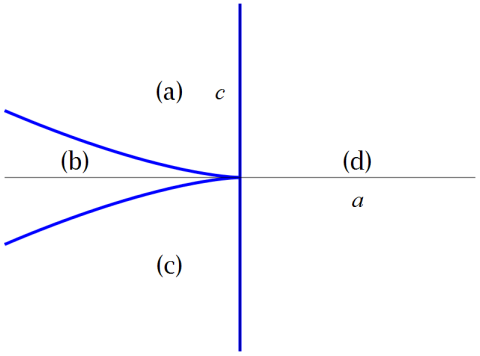

$b < 0$

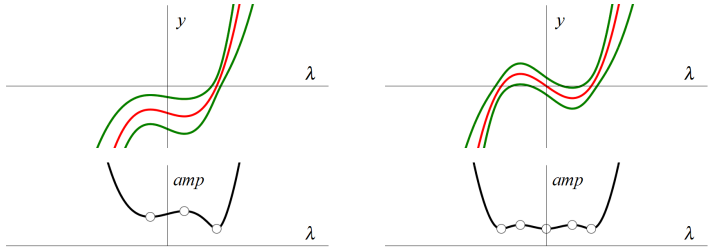

(a) (b)

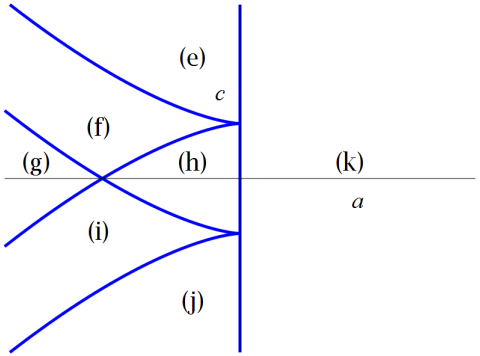

$b > 0$

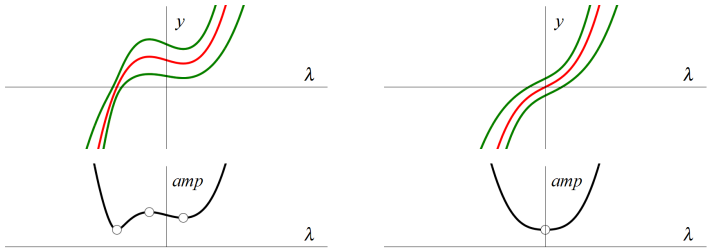

(c) (d)

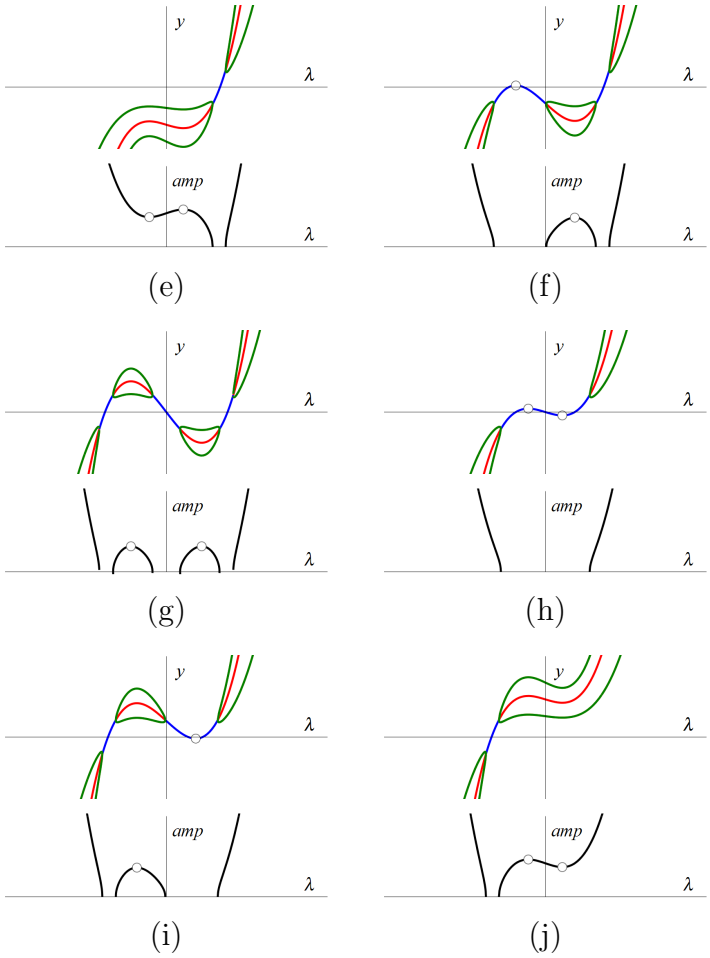
y
λ
amp
λ
(e)
(f)
(g)
(h)
(i)
(j)

Transition Variety Σ	Persistent Perturbations
	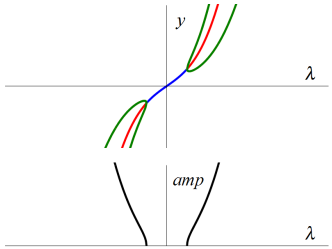 (k)

Regions (11)$^-$(a), (11)$^-$(b), (11)$^-$(c) predict wide homeostatic plateaus in amplitude and period.

(12) $-y^5 + (\lambda^3 + a\lambda - c)y + by^3$

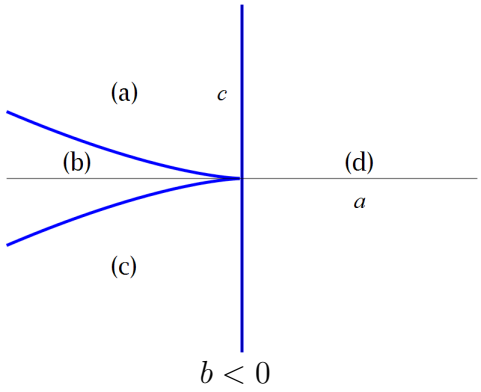

$b < 0$

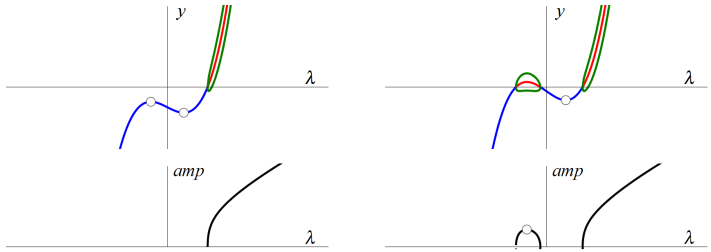

(a) (b)

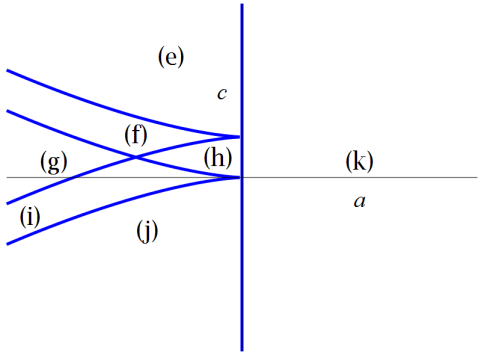

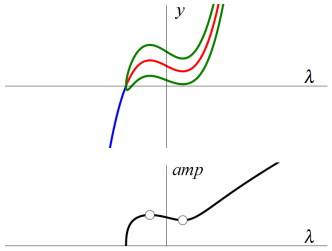

(c)

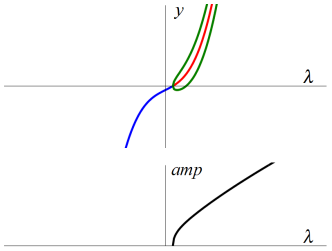

(d)

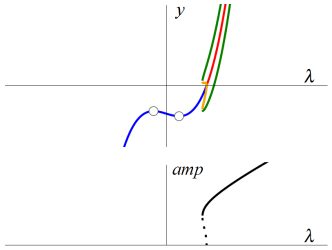

(e)

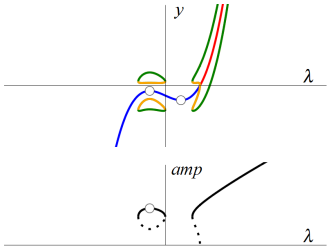

(f)

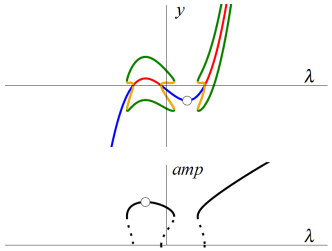

(g)

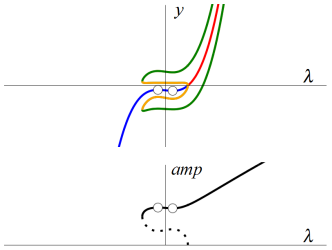

(h)

Transition Variety Σ	Persistent Perturbations

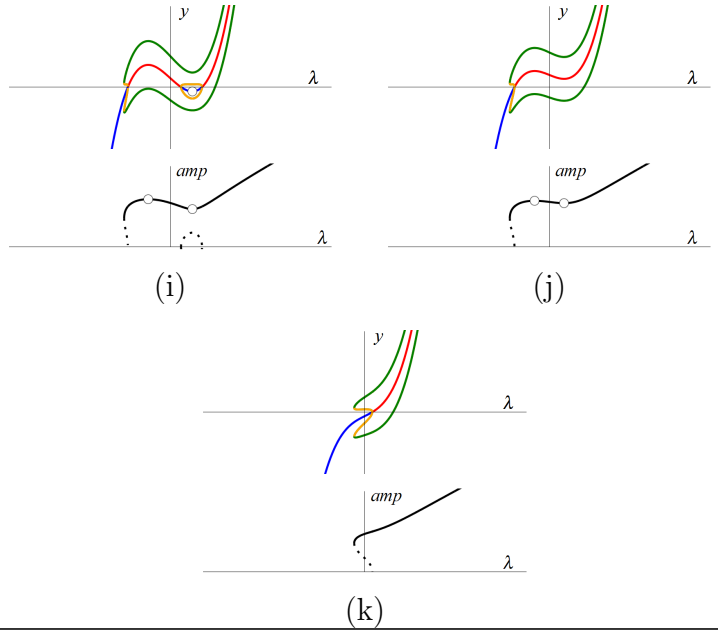

Region (12)(h) predicts coexistence of homeostatic steady-states and homeostatic limit-cycles. Varying λ will switch between the two types of solutions.

4.7 Two Networks with Homeostasis-Bifurcation Points

In this section, two examples of networks with homeostasis-bifurcation points are presented. In section 4.7.1, a network with a chair-hysteresis point is studied and in section 4.7.2 a network with a chair-isola Hopf point is studied. All persistent behaviors listed in the corresponding parts of Table 4.5 and 4.6 are found to be realized by the networks.

4.7.1 A Network with a Chair-Hysteresis Point

Consider the network depicted in Figure 4.1. The X network is the feedforward excitation network of [RBG$^+$17]. We assume mass action kinetics in the X component except for the degradation rate of X_3, which is determined by the feedforward function, η. In the Y network, Y_1 catalyzes the reaction $Y_2 \to \widetilde{Y}_2$ and Y_2 catalyzes the degradation of Y_1. Y_1 is also degraded at a basal rate independent of Y_2. We assume Michaelis-Menten kinetics in the reactions between Y_2 and $\widetilde{Y}_2$ but mass action otherwise. Letting x_i and y_i denote the concentration of X_i and Y_i, respectively, the differential equations for the network are given by

$$\begin{aligned} \dot{x}_1 &= \lambda - 2x_1 \\ \dot{x}_2 &= x_1 - 2x_2 \\ \dot{x}_3 &= x_2 - (1+\eta(x_1))x_3 \end{aligned} \tag{4.7.1}$$

$$\begin{aligned} \dot{y}_1 &= x_3 - 2y_1y_2 - y_1 \\ \dot{y}_2 &= -\frac{y_1y_2}{1+y_2} + \frac{\widetilde{y}_2}{b+\widetilde{y}_2} \\ \dot{\widetilde{y}}_2 &= \frac{y_1y_2}{1+y_2} - \frac{\widetilde{y}_2}{b+\widetilde{y}_2} \end{aligned} \tag{4.7.2}$$

where $\eta(x) = \frac{1}{1+\gamma(x)}$ and $\gamma(x) = e^{\frac{c-x}{a}}$. λ is the input parameter while a, c, and b are auxiliary parameters. The output variable of the X network is x_3. The steady states also depend on the initial condition $y_2(0) + \widetilde{y}_2(0)$, which we set to 5.

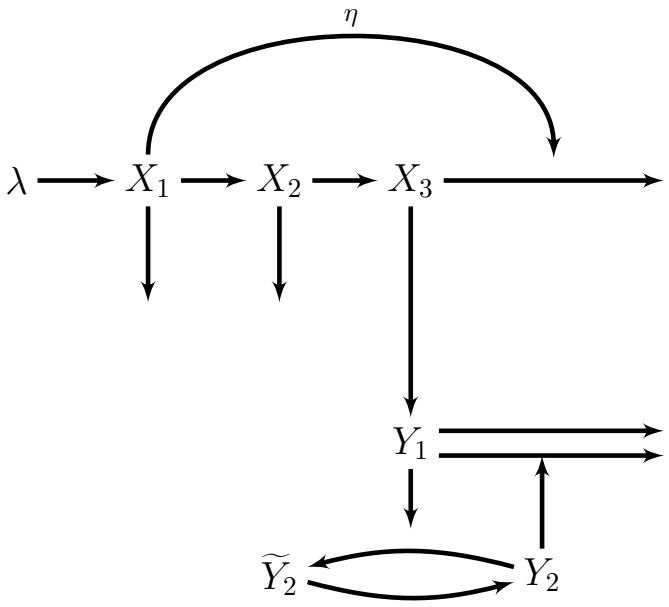

Figure 4.1: **A biochemical network with a chair-hysteresis point.** X_3 has a chair point in λ and acts as input to the Y system, which has a hysteresis point.

Repeating the analysis in [RBG+17] shows that if $a = c/6$ then $x_3(\lambda)$ has a chair point at $\lambda_0 = 2c$ with $x_3(\lambda_0) = c/3$. For the Y network, if we treat x_3 as the bifurcation parameter, then we find a hysteresis point when $b = b^* \approx 16.91$ by using the numerical continuation software MatCont [DGK+08]. Fix b at b^*, and let x_3^h be the value of x_3 at the hysteresis point. The network will have a chair-hysteresis point if $x_3(\lambda_0) = x_3^h$. Choosing $c = 3x_3^h$ therefore produces a chair-hysteresis point. Figure 4.2 shows $x_3(\lambda)$, the equilibria of y_1 as a function of x_3, and the equilibria of y_1 as a function of λ at the chair-hysteresis point.

There are nine persistent perturbations of a chair-hysteresis point which are enumerated in Table 4.5 item (6). By choosing the parameters a, b, and c in (4.7.1) and (4.7.2) appropriately, we can reproduce all of these behaviors in the network

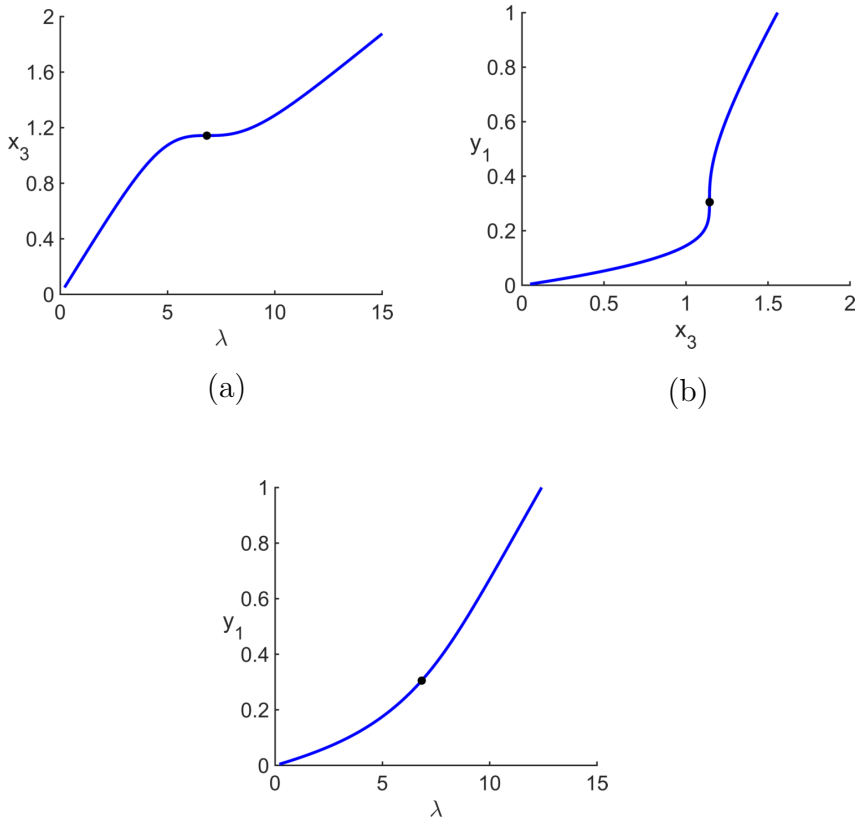

Figure 4.2: **The diagrams of x_3 and y_1 at the chair-hysteresis point. (a):** The marked point indicates the chair point for $x_3(\lambda)$. **(b):** The marked point indicates the hysteresis point of the Y network with x_3 as the bifurcation parameter. **(c):** The chair-hysteresis point is marked. Neither homeostasis nor hysteresis is visible because the two singularities annihilate each other when they coincide.

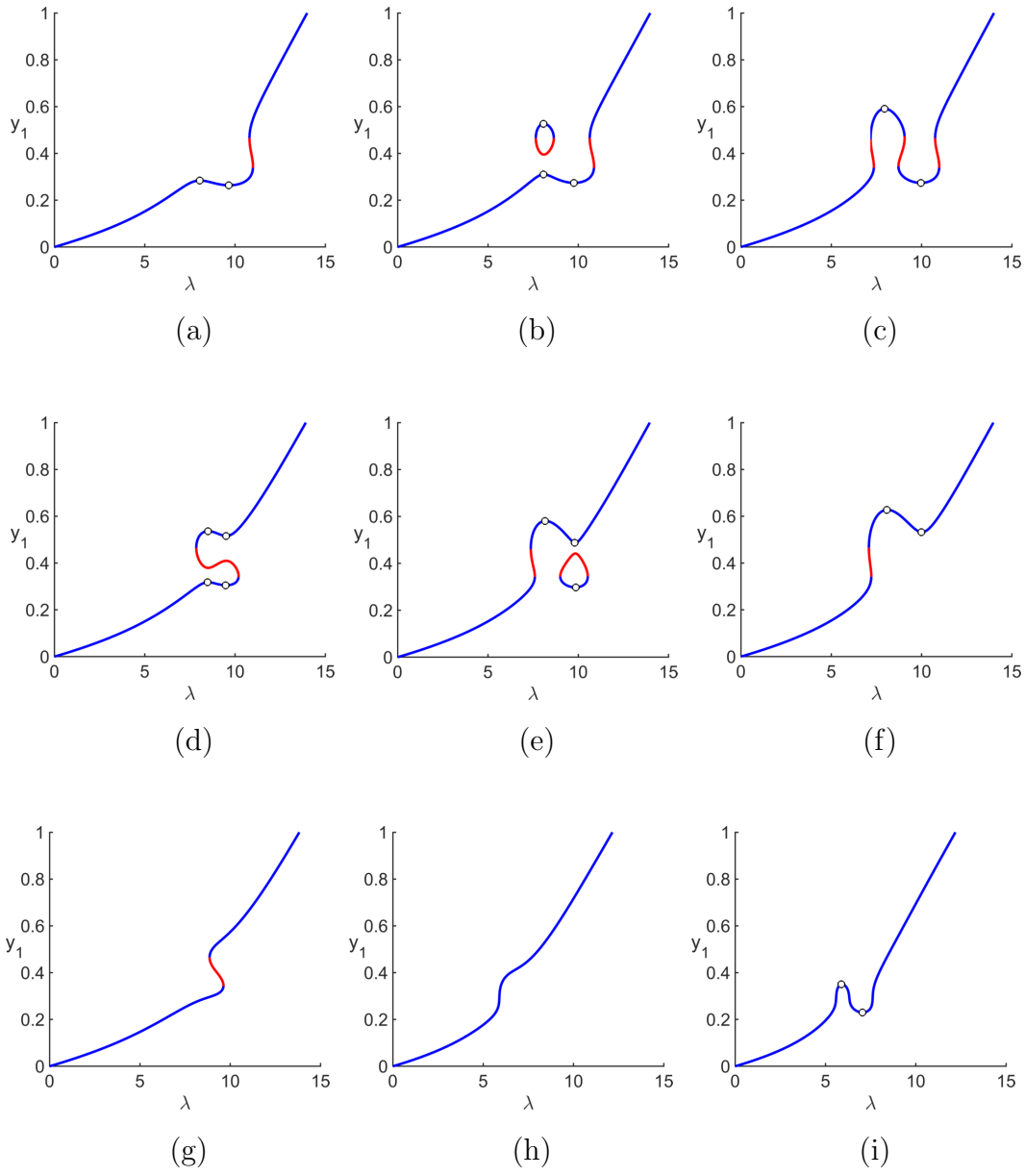

Figure 4.3: **Behavior of the chair-hysteresis network of Figure 4.1.** Each diagram corresponds to a persistent perturbation in Table 4.5 item (6). The blue (red) curves indicate stable (unstable) equilibria and homeostasis points are marked. The parameters chosen to construct each diagram are **(a):** $a = .68$, $b = 12$, $c = 4.45$; **(b):** $a = .68$, $b = 12$, $c = 4.5$; **(c):** $a = .65$, $b = 12$,$c = 4.5$; **(d):** $a = .73$, $b = 12$, $c = 4.51$; **(e):** $a = .67$, $b = 12$, $c = 4.52$; **(f):** $a = .67$, $b = 12$, $c = 4.55$; **(g):** $a = .8$, $b = 12$, $c = 4.5$; **(h):** $a = .6$, $b = 18$, $c = 3.3$; **(i):** $a = .5$, $b = 18$, $c = 3.25$.

(Figure 4.3). The behaviors shown in Figures 4.3(c) and 4.3(d) (and highlighted in Figure 4.7) are of particular interest because each has two stable homeostatic plateaus corresponding to a low state and a high state. In the parameter region corresponding to Figure 4.3(c), there are three hysteretic switches. The middle switch allows for switching between the two homeostatic plateaus while the outer switches define where the system escapes homeostasis. In the parameter region corresponding to Figure 4.3(d), the low and high plateaus coexist over the same range of λ. In this case the state of the system would depend on the history of the input rather than its current value. This behavior could be desirable if it takes energy to move λ outside of the plateau region and without any external forcing λ remains near the center of the plateau. The state of y_1 could then be controlled by bumping λ in the appropriate direction and then letting it relax back to center.

4.7.2 A Network with a Chair-Isola Hopf Point

Consider the network depicted in Figure 4.4. The X network is the same as is used in Section 4.7.1 , and the Y network is adapted from the feedback inhibition network studied in Chapter 3. We assume mass action kinetics for the Y network except for the reaction $Y_1 \to Y_2$, which is controlled by the feedback function ζ. The differential equations for the X network are given by (4.7.1), and the equations for the Y network are

$$\begin{aligned} \dot{y}_1 &= x_3 - \zeta(y_4)y_1 \\ \dot{y}_2 &= \zeta(y_4)y_1 - y_2 \\ \dot{y}_3 &= y_2 - y_3 \\ \dot{y}_4 &= y_3 - y_4 \end{aligned} \tag{4.7.3}$$

where we take $\zeta(y) = 10/(1 + y^{10}) + b$. Using MatCont [DGK$^+$08], we find that there is an isola Hopf bifurcation when $b = b^* \approx .011$. There are two simple Hopf

bifurcations connected by a branch of stable limit cycles when $0 < b < b^*$ and there are no Hopf bifurcations when $b > b^*$.

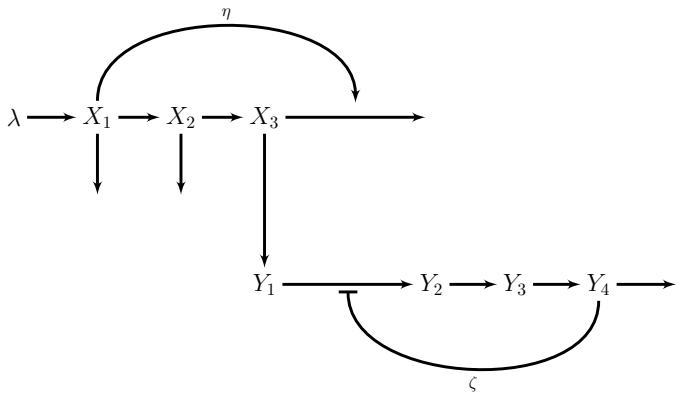

Figure 4.4: **A biochemical network exhibiting a chair-isola Hopf point.** X_3 has a chair point in λ and acts as input to the Y system, which has an isola-Hopf point.

As before, the input-output function is $x_3(\lambda)$. We take the distinguished Y variable to be y_4. Letting x_3^H be the value of x_3 at the isola Hopf bifurcation, there is a chair-isola Hopf point at $\lambda_0 = 2c$ if $c = 3x_3^H$ and $a = c/6$. Figure 4.5 shows the equilibrium values of y_4 at the singularity.

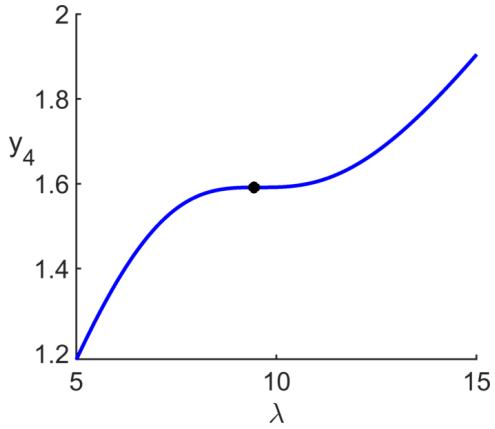

Figure 4.5: **Diagram of y_4 at the chair-isola Hopf point.** The singularity is marked. y_4 inherits the chair point from x_3.

There are 13 persistent perturbations of the chair-isola Hopf which are enumerated

in Table 4.6 item $(11)^+$. The corresponding diagrams for the network are shown in Figure 4.6. The behaviors shown in Figures 4.6(d), 4.6(f), 4.6(h) (and highlighted in Figure 4.9) are particularly interesting from the perspective of homeostasis. In Figure 4.6(f), the limit cycle amplitudes are exceptionally homeostatic with 5 homeostasis points between the two Hopf bifurcations. In each of Figures 4.6(d), 4.6(f), and 4.6(h) the limit cycle periods are homeostatic with two homeostasis points. Homeostatic period of limit cycles is desirable in biological clocks, for example.

4.8 Biologically Relevant Persistent Phenomena

A natural question is whether homeostasis-bifurcation points actually occur in biological systems. Currently, other than the constructed examples of Section 4.7, no singularities of this form have been found (although it would not be hard to construct more artificial networks with homeostasis-bifurcation points of different types). We suggest two reasons for why this is the case: 1. the theory is new and there has been limited opportunity to look for homeostasis-bifurcations; 2. the feedforward structure assumed in the definition is restrictive and may be difficult to satisfy. The first issue is unavoidable, while the second issue of removing the feedforward assumption is the subject of future work. This section highlights some of the persistent behavior from Table 4.5 that is interesting from a biological perspective. Two examples from biology are provided which exhibit behavior similar to these persistent diagrams. This is not to suggest that these behaviors certainly arise as a result of homeostasis-bifurcation, but rather that homeostasis-bifurcation is worth considering as a mechanism when studying these systems.

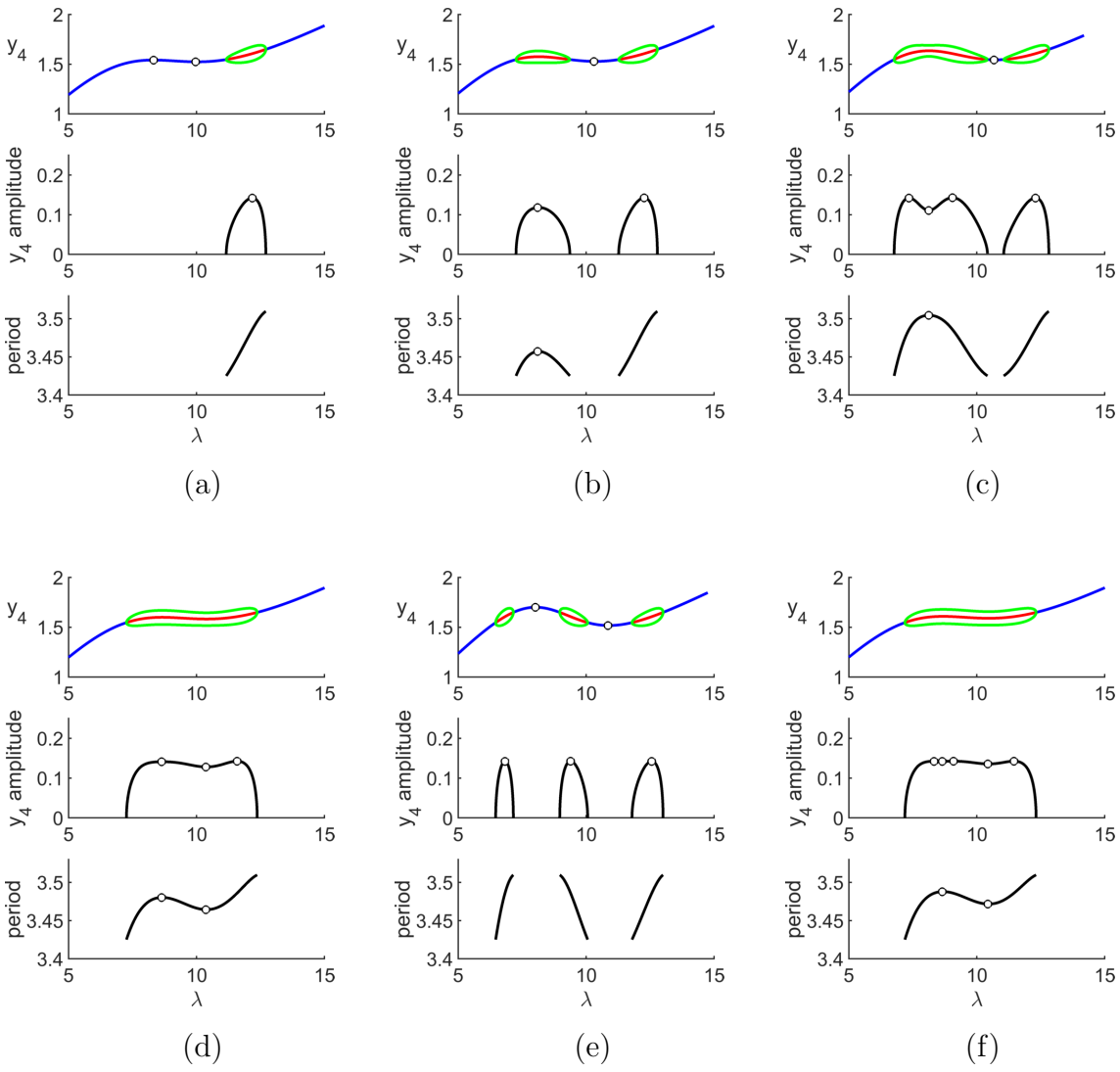

Figure 4.6: **Behavior of the chair-isola Hopf network in Figure 4.4.** Each diagram corresponds to a persistent perturbation in Table 4.6 item $(11)^+$. The blue (red) curves indicate stable (unstable) equilibria. The green curves indicate the maxima and minima of the stable limit cycles. The middle and bottom graphs show the amplitude and period of the limit cycles, respectively. Homeostasis points are marked. The parameters chosen to construct each diagram are **(a):** $a = .7$, $b = .01$, $c = 4.6$; **(b):** $a = .65$, $b = .01$; **(c):** $a = .6$, $b = .01$, $c = 4.75$; **(d):** $a = .73$, $b = .01$, $c = 4.78$; **(e):** $a = .73$, $b = .01$, $c = 4.78$; **(f):** $a = .73$, $b = .01$, $c = 4.8$.

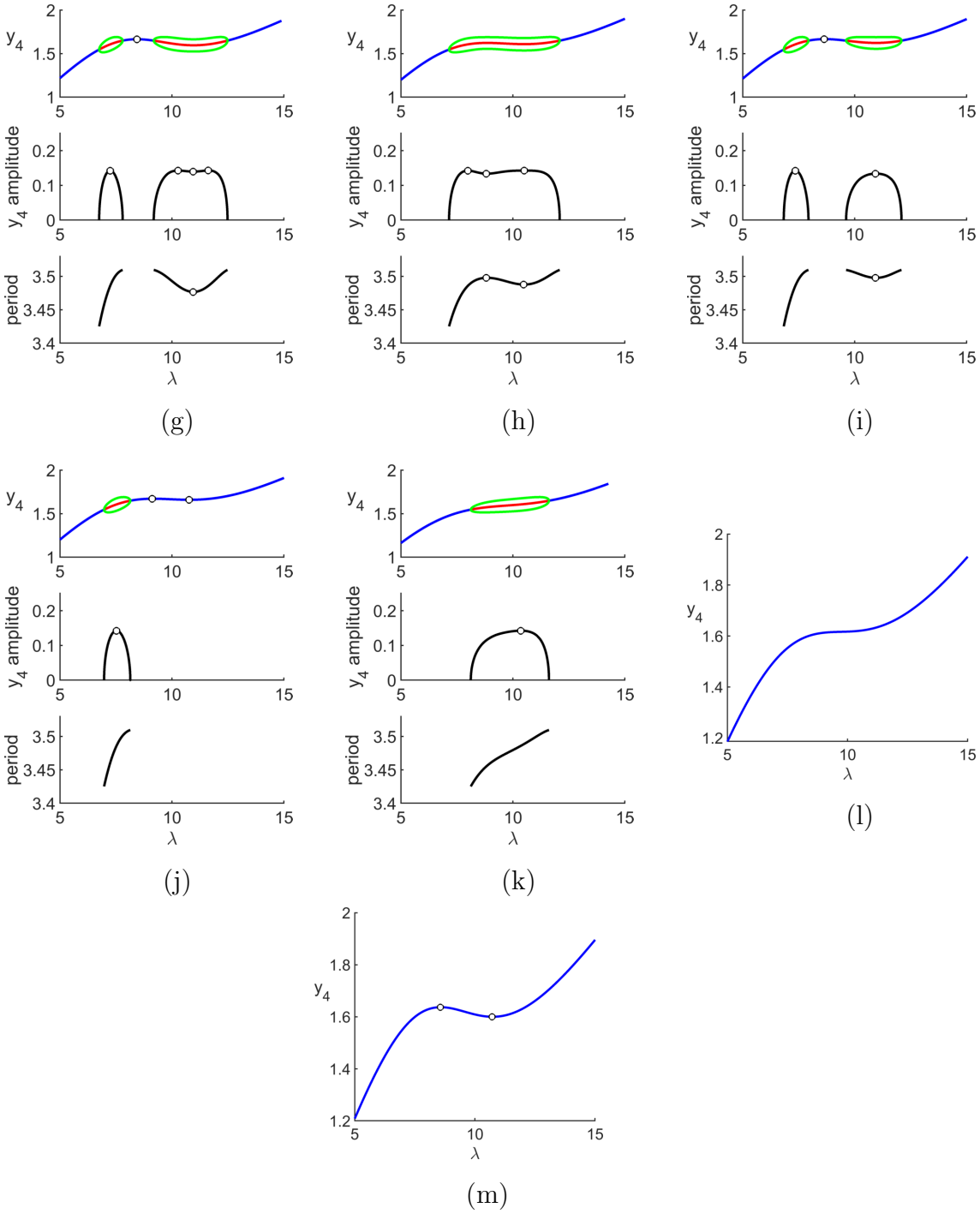

Figure 4.6: **Behavior of the chair-isola Hopf network in Figure 4.4.** The parameters are **(g):** $a = .65$, $b = .01$, $c = 4.88$; **(h):** $a = .75$, $b = .01$, $c = 4.85$; **(i):** $a = .7$, $b = .01$, $c = 4.93$; **(j):** $a = .78$, $b = .01$, $c = 5$; **(k):** $a = .9$, $b = .01$, $c = 4.78$; **(l):** $a = .82$, $b = .11$, $c = 4.78$; **(m):** $a = .7$, $b = .11$, $c = 4.78$.

4.8.1 Multiple Homeostatic Plateaus in Chair-Hysteresis and Glycolysis

The first phenomena we highlight come from chair-hysteresis (item (6) in Section 4.6). In perturbations of the chair-hysteresis point, there are two persistent behaviors which have two homeostatic plateaus separated by hysteretic switches. These are regions (c) and (d) in Table 4.5 item (6) and are reproduced here in Figure 4.7. In both cases, over a large range of λ, the behavior of the distinguished Y variable, y, is essentially binary. In Figure 4.7(a), the homeostatic plateaus largely occur over different values of λ so that whether y is in the high or low state is determined by the current value of λ. The system can switch into the other state by changing λ to the appropriate value and maintaining it there. In Figure 4.7(b), the homeostatic plateaus coexist over the same values of λ so that the state of y depends on the history of λ. This could be a desirable property if it takes energy to move λ outside of the plateau region so that without any external forcing λ remains near the center of the plateau. Each plateau is homeostatic so small, incidental perturbations of λ will not change the state of y. However, large, purposeful changes in λ in the appropriate direction will cause y to fall off one plateau and jump to the other. Letting λ relax back to the center will then stabilize the new state.

The behavior of Figure 4.7(b) can be observed in glycolysis. In [MYDH14], Mulukutla and colleagues cultured HeLa cells in either a low glucose or high glucose environment. The cells were then resuspended in mediums with various glucose concentrations. After letting the cells acclimate to the new environment, the glucose consumption rate of the cells was measured. The results are presented in Figure 4.8, which is reproduced from [MYDH14]. The lower branch of their results is suggestive of the existence of two homeostasis points. The first is evident, while the second would be expected if the lower branch were continued up to the limit point bifurcation. Figure 4.7(b) would suggest homeostasis points in the upper branch which

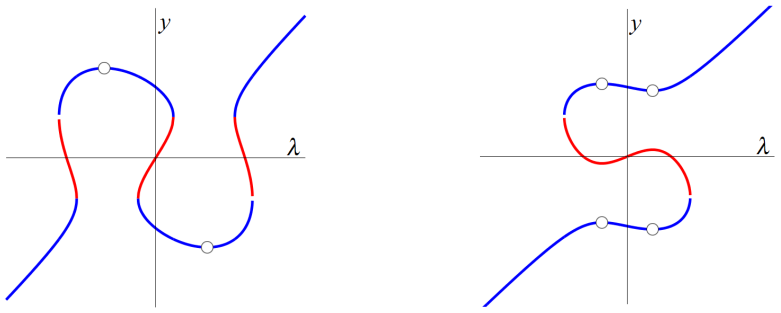

(n) (o)

Figure 4.7: **Examples of multiple homeostatic plateaus in chair-hysteresis.** These diagrams arise from perturbations of the chair-hysteresis point. All perturbation types can be seen in Table 4.5 item (6). The blue (red) curves indicate stable (unstable) equilibria and homeostasis points are marked. These perturbations are particularly interesting because each has two homeostatic plateaus. In **(a)**, the plateau that y lies in is predominantly determined by the current value of λ, while in **(b)** the choice of plateau is determined by the history of λ.

coincide with those in the upper branch, which is not the case in Figure 4.8. This discrepancy is likely because glycolysis is not a feedforward network.

4.8.2 Homeostatic Amplitudes and Periods in Chair-Isola Hopf and Circadian Rhythms

In perturbations of the Chair-Isola Hopf point (item $(11)^+$ in Section 4.6), there are limit cycles which have homeostatic periods and exceptionally homeostatic amplitudes. Regions (f) and (h) from Table 4.6 item $(11)^+$ are highlighted in Figure 4.9. In these regions, the limit cycle amplitudes are exceptionally homeostatic with either three or five homeostasis points within the plateau. The limit cycle periods inherit homeostasis from the input-output function so the periods are also homeostatic. Many of the other homeostasis-Hopf bifurcations considered in Section 4.6 also have homeostatic amplitudes and periods, so this is not limited to the chair-isola Hopf.

Homeostatic limit cycles can be seen biologically in circadian rhythms, for ex-

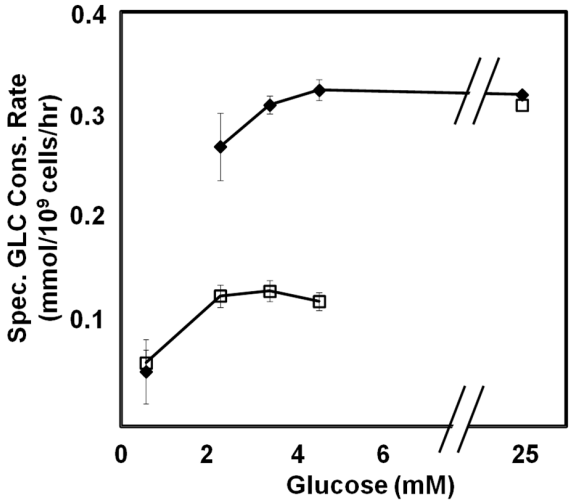

Figure 4.8: **Bistability in cultured HeLa cells (reproduced from [MYDH14]).** Cells were initially cultured in high glucose (⧫) or low glucose (□) and then resuspended in a medium with the indicated glucose concentration. The data suggests the existence of two homeostasis points on the lower branch: one which is apparent in the figure, and one which we would expect to see if it were extended further. The similar glucose consumption rates of both types of cells in very high and very low glucose environments indicate two switches on the border of the plateaus. The homeostasis points and the bistable behavior is suggestive of the behavior depicted in Figure 4.7(a).

ample. Circadian rhythms have been shown to maintain a period of about 24 hours despite large changes in gene expression levels or variation in temperature [DSU+08, BT10, ZKE+15]. Homeostasis-Hopf bifurcation is therefore a mechanism by which this can be achieved.

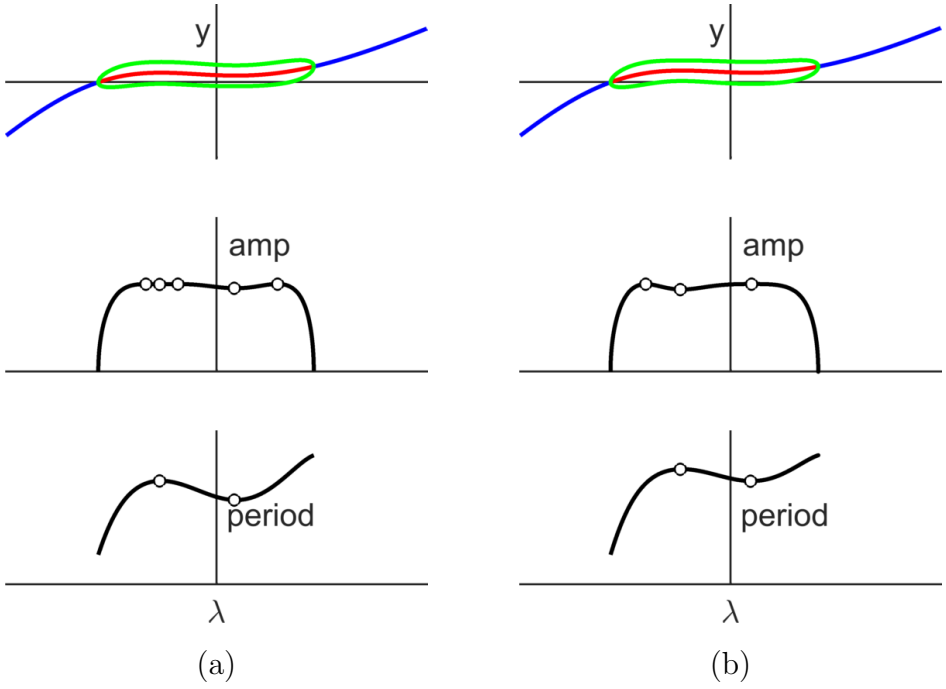

Figure 4.9: **Examples of homeostatic amplitude and period in the chair-isola Hopf**. These diagrams arise from perturbations of the chair-isola Hopf point. All perturbation types can be seen in table 6 item $(11)^+$. The blue (red) curves indicate stable (unstable) equilibria. Green curves indicate the maxima and minima of stable limit cycles. Homeostasis points are marked.

Chapter 5

Identifiability of Feedforward Networks

This chapter studies the identifiability of feedforward networks. With linear kinetics, we show that the rate parameters are locally identifiable. In particular, the solutions to the identifiability problem have a permutation structure.

In Section 5.1, feedforward networks are defined and we associate linear dynamics to these networks. Section 5.2 characterizes the input-output equations for linear feedforward networks and Section 5.3 uses the input-output equation to solve the identifiability problem. In Section 5.4, we extend the results for linear kinetics to identifiability results for feedforward networks with Michaelis-Menten kinetics.

5.1 Linear Feedforward Networks

In this section we define linear feedforward networks, and provide some examples. We begin by defining what we mean by feedforward, which differs from how it was used in Chapter 4.

Definition 5.1. A *tree* is an undirected acyclic graph. A *directed tree* is a directed graph whose underlying undirected graph is a tree.

We will represent a graph as a set of vertices, V, and edges, E: $\mathcal{G} = \{V, E\}$. If there is an edge from $j \in V$ to $i \in V$ we write $(j \to i) \in E$. For the purpose of identifiability, the input and output nodes need to be specified.

Definition 5.2. A *network*, $\mathcal{N} = \{\mathcal{G}, \mathcal{I}, \mathcal{O}\}$, is a directed graph, $\mathcal{G}$, with a set of input vertices, $\mathcal{I}$, and output vertices, $\mathcal{O}$. A *feedforward network* is a network whose graph is a directed tree.

A simple example of a feedforward network is the linear chain which is depicted in Figure 5.1. In this network the first node is the input (square) and the last node is the output (diamond). Each vertex has an edge directed towards it from the previous vertex. Explicitly, a linear chain is the network $\mathcal{N} = \{\mathcal{G}, \mathcal{I}, \mathcal{O}\}$ where $\mathcal{G} = \{\{1, 2, \ldots, n\}, \{1 \to 2, 2 \to 3, \ldots, (n-1) \to n\}\}$, $\mathcal{I} = \{1\}$, and $\mathcal{O} = \{n\}$. Other examples of feedforward networks include those pictured in Figure 5.2.

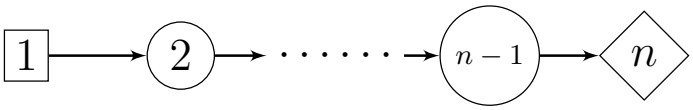

Figure 5.1: **The linear chain: a simple feedforward network.** The linear chain is a feedforward network with n nodes and $n-1$ edges. The first node is the input (denoted by the square), and the last node is the output (denoted by the diamond).

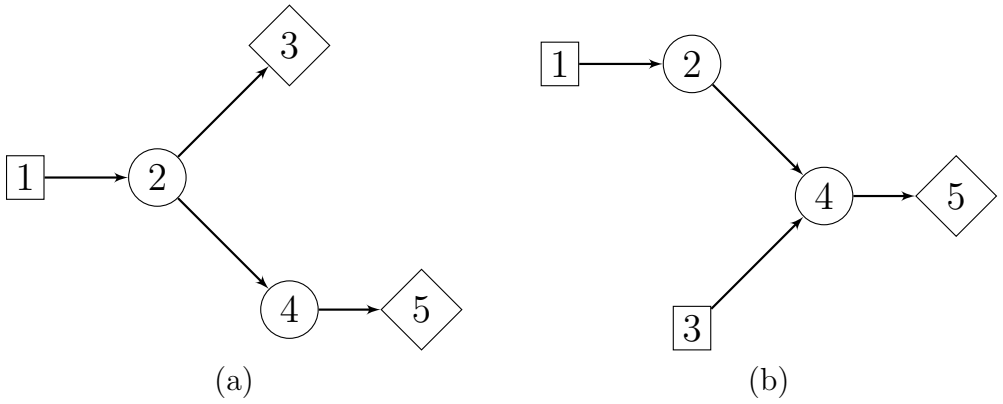

Figure 5.2: **Two simple feedforward networks.** Inputs are denoted by squares and outputs are denoted by diamonds.

Although we will be restricting our attention to feedforward networks, a linear system of differential equations can be associated to any network. Let $\mathcal{G}$ be a directed graph. A matrix, $A(\mathcal{G})$, or simply A when the graph is implicitly clear, is defined by

the graph via

$$A(\mathcal{G})_{ij} = \begin{cases} a_{ii} & \text{if } i = j \\ a_{ij} & \text{if } j \to i \text{ is an edge of G} \\ 0 & \text{otherwise,} \end{cases} \tag{5.1.1}$$

where each a_{ij} is a parameter. The off diagonal entries are always positive and represent the instantaneous rate at which material from j is transferred to i. The diagonal entries are always negative and are the negative sum of the other entries in the same column. In addition, we will typically assume that each output node, $j \in O$, has a leak parameterized by b_j. The diagonal entries can therefore be written as

$$a_{ii} = \begin{cases} -b_i - \sum_{j \neq i} a_{ji} & \text{if } j \in O \\ -\sum_{j \neq i} a_{ji} & \text{otherwise.} \end{cases} \tag{5.1.2}$$

From the input vertices, $\mathcal{I}$, we create an input function

$$(u(t))_j = \begin{cases} u_j(t) & \text{if } j \in I \\ 0 & \text{otherwise.} \end{cases} \tag{5.1.3}$$

For the purpose of identifiability analysis, $U_j(t)$ will be the functions assumed to be under the experimenter's control. Similarly, the observed variables are defined by $\mathcal{O}$:

$$Y = \{x_j \mid j \in O\}. \tag{5.1.4}$$

The system of differential equations for the network $\mathcal{N} = \{\mathcal{G}, \mathcal{I}, \mathcal{O}\}$ is then given by

$$\dot{x}(t) = Ax(t) + u(t). \tag{5.1.5}$$

Definition 5.3. A *linear feedforward network* is a feedforward network whose dynamics are given by (5.1.5).

Example 5.1. The dynamics for the linear chain of figure 5.1 with $n = 3$ and output leaks are defined by $u(t) = (u_1(t), 0, 0)^T$ and

$$A = \begin{pmatrix} -a_{21} & & \\ a_{21} & -a_{32} & \\ & a_{32} & -b_3 \end{pmatrix}.$$

Example 5.2. The dynamics for the networks in figure 5.2 with output leaks are defined by

(a). $u(t) = (u_1(t), 0, 0, 0, 0)^T$ and

$$A = \begin{pmatrix} -a_{21} & & & & \\ a_{21} & -a_{32} - a_{42} & & & \\ & a_{32} & -b_3 & & \\ & a_{42} & & -a_{54} & \\ & & & a_{54} & -b_5 \end{pmatrix}$$

(b). $u(t) = (u_1(t), 0, u_3(t), 0, 0)^T$ and

$$A = \begin{pmatrix} -a_{21} & & & & \\ a_{21} & -a_{42} & & & \\ & & -a_{43} & & \\ & a_{42} & a_{43} & -a_{54} & \\ & & & a_{54} & -b_5 \end{pmatrix}$$

5.2 The Input-Output Equations

The key to determining the identifiability of a network are the input-output equations (see Section 2.3). This section is devoted to finding the input-output equations for linear feedforward networks. With linear dynamics, we are able to take advantage of the relationship between cycles on a graph, $\mathcal{G}$, and the coefficients of the characteristic

polynomial of $A(\mathcal{G})$. This idea is also used in [MS14, MSE15] to find identifiable reparameterizations for networks with a strongly connected graph.

For each output, $j \in \mathcal{O}$, there is exactly one input-output equation. These can be constructed independently of each other. The following theorem is Theorem 2.4 in [MSE15].

Theorem 5.1. *Let $\mathcal{N} = \{\mathcal{G}, \mathcal{I}, \mathcal{O}\}$ be a linear network. Let $j \in \mathcal{O}$. For each $k \in \mathcal{I}$, let $A_{kj}(\lambda)$ be the matrix obtained by deleting the jth column and kth row of $(\lambda I - A)$. Let $\widetilde{f}$ be the characteristic polynomial of A, $\widetilde{f}_{kj}(\lambda) = \det(A_{kj}(\lambda))$, $g_j = gcd\left(\widetilde{f}, \{\widetilde{f}_{kj} \mid k \in I, \widetilde{f}_{kj} \neq 0\}\right)$, $f_j = \widetilde{f}/g_j$, and $f_{kj} = \widetilde{f}_{kj}/g_j$. Then the input-output equation corresponding to output j is given by*

$$f_j\left(\frac{d}{dt}\right) x_j = \sum_{k \in \mathcal{I}} (-1)^{j+k} f_{kj}\left(\frac{d}{dt}\right) u_k. \tag{5.2.1}$$

Proof. Denote the Laplace transform of x and u as $\hat{x}$ and $\hat{u}$ respectively. Applying the Laplace transform to (5.1.5) we have

$$(sI - A)\hat{x} = \hat{u}.$$

Applying Cramer's rule to solve for x_j

$$\hat{x}_j = \frac{\det(A_j)}{\det(sI - A)}$$

where A_j is the matrix obtained be replacing the jth column of $(sI - A)$ with u. Expanding the determinant of A_0 along the jth column we have

$$\det(sI - A)\hat{x}_j = \sum_{k \in I} (-1)^{j+k} \det(A_{kj}(s)).$$

Recognizing $\det(sI - A)$ as $\widetilde{f}(s)$ and applying the inverse Laplace transform,

$$\widetilde{f}\left(\frac{d}{dt}\right)(x_j) = \sum_{k \in I} (-1)^{j+k} \widetilde{f}_{kj}\left(\frac{d}{dt}\right) u_k.$$

Dividing both sides by g gives the result. ∎

The remainder of this section is concerned with understanding the coefficients of the input-output equation, (5.2.1). We will need the following definitions.

Definition 5.4. (Observability).

1. Given an output, $y \in \mathcal{O}$, a vertex, $v \in V$, is *y-observable* if there is a path from v to y.

2. A vertex, v, is *observable* if it is y-observable for some $y \in \mathcal{O}$.

3. A network, $\mathcal{N}$, is *y-observable* if for every vertex $v \in V$, v is y-observable.

4. A network, $\mathcal{N}$, is *observable* if every vertex $v \in V$ is observable.

5. The *y-observable subgraph* of $\mathcal{G}$ is defined by $\mathcal{G}_y = \{V_y, E_y\}$ where

$$V_y = \{v \in V \mid v \text{ is } y\text{-observable}\}$$

and

$$E_y = \{v \to w \in E \mid v \in V_y, w \in V_y\}.$$

The coefficient matrix $A(\mathcal{G}_y)$ is obtained by removing all the rows and columns in $A(\mathcal{G})$ which correspond to vertices not in $\mathcal{G}_y$.

Note that $A(\mathcal{G}_y)$ may still incorporate rate parameters associated to edges from $v \in V_y$ to $w \notin V_y$ in the diagonal entries. That is $A(\mathcal{G}_y)_{vv} = A(\mathcal{G})_{vv}$ for all $v \in V_y$.

Definition 5.5. (Controllability).

1. Given an input, $k \in \mathcal{I}$, a vertex, $v \in V$ is *k-controllable* if there is a path from k to v.

2. A vertex, v, is *controllable* if it is k-controllable for some $k \in \mathcal{I}$.

3. A network, $\mathcal{N}$, is controllable if for every vertex $v \in V$, v is controllable.

Example 5.3. The linear chain of Figure 5.1 is observable and controllable because given any $k \in \{1, 2, \ldots, n\}$, $1 \to 2 \to \cdots \to k$ and $k \to k+1 \to \cdots \to n$ are paths.

Example 5.4. Consider the networks in Figure 5.2. Both networks are observable and controllable.

(a). The 3-observable subgraph is the subgraph consisting only of the vertices 1, 2, and 3. $A(\mathcal{G}_3)$ is given by

$$A(\mathcal{G}_3) = \begin{pmatrix} -a_{21} & & \\ a_{21} & -a_{32} - a_{42} & \\ & a_{32} & -b_3 \end{pmatrix}$$

Note that a_{42} still appears as a parameter in $A(\mathcal{G}_3)$ even though 4 is not 3-observable. The 5-observable subgraph is the graph consisting of 1, 2, 4, and 5. Every vertex is 1-controllable.

(b). The 5-observable subgraph is the original graph. 2 is 1-controllable but not 3-controllable.

Lemma 5.2. *Let $\mathcal{N} = \{\mathcal{G}, \mathcal{I}, \mathcal{O}\}$ be a linear feedforward network with $y \in \mathcal{O}$. The vertices of $\mathcal{G}$ may be labeled so that $A(\mathcal{G})$ is lower triangular. Additionally, the labeling may be chosen so that $A(\mathcal{G}_y)$ is the first $|V_y|$ rows and columns of $A(\mathcal{G})$.*

Proof. $\mathcal{G}_y$ is a directed, acyclic graph so we may place a total order on the vertices such that $n < m$ only if there is not a path from m to n. Said another way, $n < m$ only if m is not n-observable. Labeling the vertices based on this ordering, $a_{nm} = 0$ for $n < m$ so $A(\mathcal{G}_y)$ must be lower triangular. Given this ordering on V_y, we can choose an ordering on $\mathcal{G}$ that respects the ordering on V_y by first ordering the vertices according to the order on V_y and then labeling the remaining vertices using the same rule. This is possible because if v is not y-observable then necessarily it is not w-observable for

any $w \in V_y$. Any such ordering will satisfy $n < m$ only if there is not a path from m to n for the whole graph, $\mathcal{G}$. Under this ordering, $A(\mathcal{G})$ will therefore be lower triangular as well. ■

Example 5.5. Consider the network in Figure 5.2(a). The vertices have been labeled so that $A(\mathcal{G})$ is lower triangular, as shown in Example 5.2(a). $A(\mathcal{G}_3)$ is the first 3 rows and columns of $A(\mathcal{G})$.

Lemma 5.3. *Suppose A is lower triangular and B is the matrix obtained by deleting the jth column and kth row of A where $j < k$. Then B is lower triangular with $B_{jj} = 0$.*

Proof. A is lower triangular so $A_{i\ell} = 0$ if $i < \ell$. We need to show that if $i < \ell$ then $B_{i\ell} = 0$. Suppose $i < \ell$. If $i < k$ and $\ell < j$ then $B_{i\ell} = A_{i\ell} = 0$. If $i < k$, and $\ell > j$ $B_{i\ell} = A_{i(\ell+1)} = 0$. If $i > k$ then we must have $\ell > j$ and then $B_{i\ell} = A_{(i+1)(\ell+1)} = 0$. So B is upper triangular. Noticing $B_{jj} = A_{j(j+1)} = 0$ completes the proof. ■

Proposition 5.4. *Let $\mathcal{N} = \{\mathcal{G}, \mathcal{I}, \mathcal{O}\}$ be a linear feedforward network. Let $j \in \mathcal{O}$ and $k \in \mathcal{I}$. Suppose k is not j-observable. Then $\widetilde{f}_{kj} \equiv 0$.*

Proof. Label the vertices according to Lemma 5.2. k is not j observable and so we must have $j < k$. A is lower triangular so $(\lambda I - A)$ is as well. A_{kj} is formed by removing the jth column and kth row of $(\lambda I - A)$. By Lemma 5.3, A_{kj} is lower triangular with $(A_{kj})_{jj} = 0$. A_{kj} is thus singular and $\widetilde{f}_{kj}(\lambda) = \det(A_{kj}(\lambda)) \equiv 0$. ■

The coefficient of the input-output equations can be related to the topology of the graph. To make this relationship precise, we need the following definitions.

Definition 5.6. A *path* in $\mathcal{G}$ is a sequence of vertices $i_0, i_1, \ldots, i_m$ such that $i_j \to i_{j+1} \in E$ for all $j = 0, \ldots, m-1$. In acyclic graphs, if a path exists between i_0 and i_m it is unique so it can be unambiguously identified by i_0 and i_m. Given the

path, we let $P(i_0, i_m)$ denote the set of vertices on the path and $i_0 \dashrightarrow i_m$ denote the sequence of vertices. To the sequence of vertices we associate the monomial $a^{i_0 \dashrightarrow i_m} = a_{i_1 i_0} a_{i_2 i_1} \cdots a_{i_m i_{m-1}}$ which we refer to as a *monomial path*.

Definition 5.7. A *cycle* in $\mathcal{G}$ is a sequence of vertices $i_0, i_1, \ldots, i_m$ with $i_m = i_0$ such that $i_j \to i_{j+1} \in E$ for all $j = 0, \ldots, m-1$. To a cycle, $C = i_0, i_1, \ldots, i_m$, we associate the monomial $a^C = a_{i_1 i_0} a_{i_2 i_1} \cdots a_{i_m i_{m-1}} = a_{i_1 i_0} a_{i_2 i_1} \cdots a_{i_0 i_{m-1}}$ which we refer to as a *monomial cycle*.

Note that we include 1-cycles (cycles formed by a single vertex) in this definition. The monomial 1-cycles form the diagonal entries of $A(\mathcal{G})$.

Lemma 5.5. *Let $\mathcal{G}$ be a graph with n vertices and $A(\mathcal{G})$ be the associated matrix. Then we can write the determinant in the following way.*

$$\det(A) = \sum_{C_1, C_2, \ldots, C_k \in \mathcal{C}(\mathcal{G})} \prod_{j=1}^{k} \operatorname{sign}(C_j) a^{C_j}$$

where the sum is over collections of vertex disjoint cycles involving exactly n edges of $\mathcal{G}$, and $\operatorname{sign}(C) = 1$ if C has odd length and $\operatorname{sign}(C) = -1$ if C has even length.

Proof. The lemma follows from rewriting the usual definition of the determinant by breaking each permutation into its disjoint cycle decomposition. Explicitly,

$$\det(A) = \sum_{\sigma \in S_n} \operatorname{sign}(\sigma) \prod_{i=1}^{n} a_{i\sigma(i)}.$$

Write $\sigma \in S_n$ as a disjoint cycle decomposition: $\sigma = C_1 C_2 \cdots C_k$. Notice that $\operatorname{sign}(\sigma) = \operatorname{sign}(C_1) \operatorname{sign}(C_2) \cdots \operatorname{sign}(C_k)$. Given $\sigma \in S_n$, we can use this cycle decomposition and the definition of monomial cycles to write

$$\operatorname{sign}(\sigma) \prod_{i=1}^{n} a_{i\sigma(i)} = \prod_{j=1}^{k} \operatorname{sign}(C_j) a^{C_j}.$$

Now, $a_{i\sigma(i)} \neq 0$ if and only if $\sigma(i) \to i$ is an edge of $\mathcal{G}$ or $\sigma(i) = i$. So, given $\sigma \in S_n$, the corresponding term in the sum is non-zero if and only if each cycle in the cycle

decomposition is a cycle of $\mathcal{G}$. This reduces the number of terms in the sum to those given in the statement of the lemma. ■

Using the cycle decomposition of Lemma 5.5, it is now possible to identify the form of $\widetilde{f}_k j$.

Proposition 5.6. *Let $\mathcal{N} = \{\mathcal{G}, \mathcal{I}, \mathcal{O}\}$ be a linear feedforward network. Let $y \in \mathcal{O}$ and $k \in \mathcal{I}$ be y-observable. Then*

$$\widetilde{f}_{ky}(\lambda) = a^{k \dashrightarrow y} \prod_{v \notin P(k,y)} (\lambda - a_{vv}).$$

Proof. Recall that $\widetilde{f}_{ky}(\lambda) = \det(A_{ky}(\lambda))$ where $A_{ky}(\lambda)$ is obtained by deleting the kth row and jth column of $(\lambda I - A)$. Assume that the vertices are labeled as in Lemma 5.2. Let $\widetilde{\mathcal{G}}$ be the graph $\mathcal{G}$ with $y \to k$ added as an edge. Then $(A(\widetilde{\mathcal{G}}))_{ky} = a_{ky}$ and we have the relationship

$$\det(A_{ky}(\lambda)) = \frac{\partial}{\partial a_{yk}} \det(\lambda I - A(\widetilde{\mathcal{G}}))$$

Using Lemma 5.5 and noticing $(k \dashrightarrow y, k)$ is the only cycle with length greater than 1,

$$\det(\lambda I - A(\widetilde{\mathcal{G}})) = \prod_{v \in V} (\lambda - a_{vv}) \; + \; (-1)^{|P(k,y)|} \operatorname{sign}(k \dashrightarrow y, k) a_{ky} a^{k \dashrightarrow y} \prod_{v \notin P(k,y)} (\lambda - a_{vv}).$$

Taking the derivative of the right hand side with respect to a_{ky} and noticing $\operatorname{sign}(k \dashrightarrow y, k) = (-1)^{|P(k,y)|}$ gives the result.

■

The following proposition identifies the greatest common denominator, g_y for an output, y. This allows for f_y and f_{kj} to be written explicitly.

Proposition 5.7. *Let $\mathcal{N} = \{\mathcal{G}, \mathcal{I}, \mathcal{O}\}$ be a linear feedforward network. Let $y \in \mathcal{O}$ and suppose $\mathcal{G}_y$ is controllable. Then*

$$g_y = \prod_{v \notin V_y} (\lambda - a_{vv}) \tag{5.2.2}$$

$$f_y = \prod_{v \in V_y} (\lambda - a_{vv}) \tag{5.2.3}$$

$$f_{ky} = a^{k \dashrightarrow y} \prod_{\substack{v \in V_y \\ v \notin P(k,y)}} (\lambda - a_{vv}) \tag{5.2.4}$$

Proof. We have $\widetilde{f} = \prod_{v \in V} (\lambda - a_{vv})$ because A is lower triangular with diagonal entries a_{vv}. $\mathcal{G}_y$ is controllable so given $w \in V_y$, there is an input $k \in \mathcal{I}$ so that $w \in P(k, y)$. By Proposition 5.6 $(\lambda - a_{ww})$ is not a factor of $\widetilde{f}_{kj}$. For $w \notin V_y$, there is no path from an input to y which passes through w, so $(\lambda - a_{ww})$ is a factor of $\widetilde{f}_{kj}$ for each $k \in \mathcal{I}$ that is y-observable by Proposition 5.6. The right hand side of g_y in the statement above is therefore exactly the greatest common divisor and the equations for f_y and f_{ky} follow by division of $\widetilde{f}_y$ and $\widetilde{f}_{ky}$. ■

To simplify the expression of the coefficients of the input-output equation we use the elementary symmetric polynomials.

Definition 5.8. The *elementary symmetric polynomial* of degree $k \geq 1$ in n variables is defined by

$$\pi_n^k(z_1, z_2, \ldots, z_n) = \sum_{i_1 < i_2 < \cdots < i_k} z_{i_1} z_{i_2} \cdots z_{i_k}.$$

For $k = 0$, we define $\pi_n^k(z_1, \ldots, z_n) = 1$. For a set of variables, $Z = \{z_1, z_2, \ldots, z_n\}$, we define

$$\pi^k(Z) = \pi_n^k(z_1, z_2, \ldots, z_n)$$

where we have dropped the subscript n because the number of variables is implicit. We further define $\Pi(Z)$ to be the set of all elementary symmetric polynomials up to

degree n:

$$\Pi(Z) = \{\pi^k(Z) \mid 1 \leq k \leq |Z|\}.$$

Theorem 5.8. *Let $\mathcal{N} = \{\mathcal{G}, \mathcal{I}, \mathcal{O}\}$ be a linear feedforward network. Let $n_j = |V_j|$, and $n_{kj} = |V_j \setminus P(k,j)|$. Suppose $j \in \mathcal{O}$ and $\mathcal{G}_j$ is controllable. Then*

$$f_j\left(\frac{d}{dt}\right) x_j = \sum_{i=0}^{n_j} (-1)^{n_j - i} \pi^{n_j - i}(\{a_{vv} \mid v \in V_j\}) x_j^{(i)} \tag{5.2.5}$$

and

$$f_{kj}\left(\frac{d}{dt}\right) u_k = a^{k \dashrightarrow j} \sum_{i=0}^{n_{kj}} (-1)^{n_{kj} - i} \pi^{n_{kj} - i}(\{a_{vv} \mid v \in V_j \setminus P(k,j)\}) u_k^{(i)}. \tag{5.2.6}$$

Proof. These equations are found by expanding the expressions in (5.2.3) and (5.2.4). ■

Substituting (5.2.5) and (5.2.6) into (5.2.1) gives the expanded input-output equation.

Example 5.6. Consider the linear chain of Figure 5.1. The input-output equation is given by

$$\begin{aligned} &y^{(n)} + \pi^1(a_{21}, a_{32}, \ldots, a_{n(n-1)}, b_n) + \pi^2(a_{21}, a_{32}, \ldots, a_{n(n-1)}, b_n) y^{(n-2)} \\ &\quad + \cdots + \pi^n(a_{21} a_{32} \cdots a_{n(n-1)} b_n) y = \pi^{(n-1)}(a_{21} a_{32} \cdots a_{n(n-1)}) u_1 \end{aligned}$$

where $y = x_n$.

Example 5.7. Consider the linear feedforward networks of Figure 5.2.

(a). There are two outputs so there are two input-output equations given by

$$\begin{aligned} &\dddot{x}_3 + (a_{21} + a_{32} + a_{42} + b_3)\ddot{x}_3 + (a_{21}(a_{32} + a_{42}) + a_{21} b_3 + (a_{32} + a_{42}) b_3)\dot{x}_3 \\ &\quad + (a_{21}(a_{32} + a_{42}) b_3) x_3 = a_{21} a_{32} u_1 \end{aligned}$$

and

$$x_5^{(4)} + \pi^1(a_{21}, a_{32} + a_{42}, a_{54}, b_5)x_5^{(3)} + \cdots + \pi^4(a_{21}, a_{32} + a_{42}, a_{54}, b_5)x_5 = a_{21}a_{42}a_{54}u_1.$$

(b). There is one input-output equation given by

$$y^{(5)} + \pi^1(a_{21}, a_{42}, a_{43}, a_{54}, b_5)y^{(4)} + \cdots + \pi^5(a_{21}, a_{42}, a_{43}, a_{54}, b_5)y = a_{21}a_{42}a_{54}(\dot{u}_1 + a_{43}u_1) + a_{43}a_{54}(\ddot{u}_2 + (a_{21} + a_{42})\dot{u}_2 + a_{21}a_{42}u_2$$

where $y = x_5$.

5.3 Identifiability Results

Given that we have the input-output equations and a nice way to write their coefficients, we would now like to use the coefficients to study the identifiability of individual parameters. We begin by giving a necessary condition for identifiability.

Proposition 5.9. *Let $\mathcal{N} = \{\mathcal{G}, \mathcal{I}, \mathcal{O}\}$ be a linear feedforward network. Suppose that $v \in V$ is not observable or not controllable. Then a_{vv} is unidentifiable.*

Proof. First suppose that v is not observable. Then by Proposition 5.7, $v \notin P(k, j)$ and $(\lambda - a_{vv})$ is not a factor of f_j or f_{kj} for any $j \in \mathcal{O}$, $k \in \mathcal{I}$. Therefore, a_{vv} does not appear in the input-output equation.

Now, suppose that v is not controllable. Clearly $v \notin P(k, j)$ for any $j \in \mathcal{O}$ or $k \in \mathcal{I}$. By Proposition 5.6, $(\lambda - a_{vv})$ is a factor of $\widetilde{f}_{kj}$ for every $j \in \mathcal{O}$ and $k \in \mathcal{I}$. Therefore $(\lambda - a_{vv})$ is a factor of g_j for every j and a_{vv} does not appear in the input-output equation.

■

Proposition 5.9 shows that we can only hope to identify parameters associated with observable and controllable vertices. Given a graph, $\mathcal{G}$, it is natural to study the corresponding network with the minimum number of input and output vertices that make the the network controllable and observable. Proposition 5.10 shows what this network must be.

Definition 5.9. A *root* of a directed graph, $\mathcal{G}$, is a vertex that is not the terminal vertex of any edge. A *leaf* of $\mathcal{G}$ is a vertex that is not the origin vertex of any edge.

Proposition 5.10. *Let $\mathcal{N} = \{\mathcal{G}, \mathcal{I}, \mathcal{O}\}$ be a linear feedforward network. Let R be the set of roots of $\mathcal{G}$ and L be the set of leaves. $\mathcal{N}$ is controllable if and only if $R \subset \mathcal{I}$. $\mathcal{N}$ is observable if and only if $L \subset \mathcal{O}$.*

Proof. Let $v \in V$. We can find a path from a root, $r \in R$, to v using the following recursive algorithm.

1. Check if v is a root. If it is, then $r = v$ and we are done. If not, go to step 2.
2. v is the terminal vertex of an edge, $w \to v$. Set $v = w$ and go to step 1.

This algorithm is guaranteed to terminate because $\mathcal{G}$ is finite. This shows that for every $v \in V$ there is a root, r_v such that $r_v \dashrightarrow v$ is a path. If $R \subset \mathcal{I}$, then $r_v \in \mathcal{I}$ and v is controllable. If there is a $w \in V$ that is not controllable, then there is a path $r_w \dashrightarrow w$ so $r_w \in R$ must not be an input vertex. This proves $\mathcal{N}$ is controllable if and only if $R \subset I$.

A similar argument works to prove that $\mathcal{N}$ is observable if and only if $L \subset \mathcal{O}$. Let $v \in V$. We can find a path from v to a leaf, $\ell \in L$ using the following recursive algorithm.

1. Check if v is a leaf. If it is, then $\ell = v$ and we are done. If not, go to step 2.
2. v is the origin of an edge, $v \to w$. Set $v = w$ and go to step 1.

Again, the algorithm is guaranteed to terminate because $\mathcal{G}$ is finite. This shows that for every $v \in V$ there is a leaf, ℓ_v such that $v \dashrightarrow \ell_v$ is a path. If $L \subset \mathcal{O}$, then $\ell_v \in \mathcal{O}$ and v is observable. If there is a $w \in V$ that is not observable, then there is a path $w \dashrightarrow \ell_w$ so ℓ_w must not be an output vertex. ■

Definition 5.10. Given a directed tree, $\mathcal{G}$, the *minimal network*, $\mathcal{N}(\mathcal{G})$, is the feed-forward network defined by $\mathcal{N}(\mathcal{G}) = \{\mathcal{G}, \mathcal{I} = R, \mathcal{O} = L\}$ where R is the set of roots of $\mathcal{G}$ and L is the set of leaves.

Definition 5.11. Let $Z = \{z_1, \ldots, z_n\}$ be a set of unknown parameters and $\{\zeta_1, \ldots, \zeta_n\}$ the true, unobserved values of these parameters. Z is *identifiable up to permutations* if the solutions to the identifiability problem is a subset of $\{(z_k = \zeta_{\sigma(k)})_{k=1}^n \mid \sigma \in S_n\}$ where S_n is the symmetric group of order n.

Note that if $\Pi(C)$ is identifiable, then C is identifiable up to permutations. From Theorem 5.8, we know that $\Pi(V_j)$ is identifiable for every $j \in \mathcal{O}$ and $\Pi(V_j \setminus P(k, j))$ is identifiable for every connected $j \in \mathcal{O}$ and $k \in \mathcal{I}$. These sets are then identifiable up to permutation. The following proposition tells us how to use this information to identify other sets which are identifiable up to permutation.

Proposition 5.11. *Let Z_1, Z_2, and Z be sets of parameters with $Z_1 \subset Z$. Suppose Z_1, Z_2, and Z are identifiable up to permutations. Then $Z \setminus Z_1$, $Z_1 \cup Z_2$, and $Z_1 \cap Z_2$ are identifiable up to permutations.*

Proof. First we show $Z \setminus Z_1$ is identifiable up to permutations. Let $Z_1 = \{z_1, \ldots, z_{n_1}\}$ and $Z = \{z_1, \ldots, z_{n_1}, z_{n_1+1}, \ldots, z_n\}$. Suppose the corresponding true, unobserved values of the parameters are $\{\zeta_1, \ldots, \zeta_n\}$. Z is identifiable up to permutations so the solution set is a subset of $\{(z_k = \zeta_{\sigma(k)})_{k=1}^n \mid \sigma \in S_n\}$. Z_1 is identifiable up to permutations so these solutions are restricted to those which respect permutations of Z_1:

$$\{(z_k = \zeta_{\sigma_1(k)})_{k=1}^{n_1} \times (z_k = \zeta_{\sigma_0(k)})_{k=n_1+1}^{n} \mid (\sigma_1, \sigma_0) \in S_{n_1} \times S_{n-n_1}\}.$$

These solutions respect permutations of $Z \setminus Z_1$ so $Z \setminus Z_1$ is identifiable up to permutations.

If Z_1 and Z_2 are identifiable up to permutations, then solutions are restricted to permutations which respect both Z_1 and Z_2. If $Z_1 \cap Z_2$ were not identifiable up to permutation, then there must be an element, $z \in Z_1 \cap Z_2$ and a permutation, σ, corresponding to a solutions so that $\sigma(z) \notin Z_1 \cap Z_2$. But then $\sigma(z) \notin Z_1$ or $\sigma(z) \notin Z_2$ which contradicts that Z_1 and Z_2 are identifiable up to permutation.

To see that $Z_1 \cup Z_2$ are identifiable up to permutation, notice that

$$Z_1 \cup Z_2 = (Z_1 \setminus (Z_1 \cap Z_2)) \cup (Z_2 \setminus (Z_1 \cap Z_2)) \cup (Z_1 \cap Z_2)\,.$$

This is a disjoint union of sets which are identifiable by permutation. The set of permutations of $Z_1 \cup Z_2$ must therefore be a superset of the union of the permutations of each of these sets so that $Z_1 \cup Z_2$ is identifiable up to permutation.

■

We now partition the graph into subsets of parameters that are identifiable up to permutation.

Definition 5.12. The *in-degree* of a vertex, v, is the number of edges which terminate in v and is denoted $\text{indeg}(v)$. The *out-degree* of v is the number of edges which originate from v and is denoted $\text{outdeg}(v)$.

Definition 5.13. A sequence of vertices, $C = v_1, v_2, \ldots, v_\ell$, is a *chain* of $\mathcal{G}$ if for each $2 < j < \ell$, $v_{j-1} \to v_j$ is an edge and $\text{indeg}(v_j) = \text{outdeg}(v_j) = 1$. C is a *maximal chain* of G if the sequence is maximal: no vertex can be added to the sequence so that the sequence remains a chain.

To simplify notation, it is convenient to have a way to refer to the parameters associated with a set of vertices. Given $V_0 \subset V$, define $a(V) = \{a_{vv} \mid v \in V_0\}$.

Theorem 5.12. *Let $\mathcal{N} = \{\mathcal{G}, \mathcal{I}, \mathcal{O}\}$ be a minimal linear feedforward network. Let C be a maximal chain of $\mathcal{G}$. Then $a(C)$ is identifiable up to permutations in $\mathcal{N}(\mathcal{G})$.*

Proof. To prove the theorem, we will use all the coefficients of the input-output equation given in Theorem 5.8 except for the $a^{k\dashrightarrow j}$ terms. The remaining coefficients are the elementary symmetric polynomials in sets of parameters. In particular, for each $y \in \mathcal{O}$, $\Pi(\{a_{vv} \mid v \in V_y\})$ is identifiable and for each $y \in \mathcal{O}$ and $u \in \mathcal{I}$ that are connected in $\mathcal{G}$, $\Pi(\{a_{vv} \mid v \in V_j \setminus P(u,y)\})$ is identifiable. Therefore, $\{a_{vv} \mid v \in V_y\}$ is identifiable up to permutation and $\{a_{vv} \mid v \in V_j \setminus P(u,y)\}$ is identifiable up to permutation. It then immediately follows from Proposition 5.11 that for each input-output path, the parameters corresponding to vertices along the path are identifiable up to permutation. That is, $\{a_{vv} \mid v \in P(u,y)\}$ is identifiable up to permutation for each input-output path $P(u,y)$.

Let $C = v_1, v_2, \ldots, v_\ell$. We separate the proof into the 9 cases that arise from all combinations of $\text{indeg}(v_1) = 0, 1$ or > 1 and $\text{outdeg}(v_\ell) = 0, 1$ or > 1. The case of $\text{indeg}(v_1) > 1$ and $\text{outdeg}(v_\ell) = 1$ (case 7) is illustrated in Figure 5.3.

Case 1: $\text{indeg}(v_1) = \text{outdeg}(v_\ell) = 0$.

If $\text{outdeg}(v_\ell) = 0$, then v_ℓ is a leaf and therefore an output. We have $a(V_{v_\ell})$ is identifiable up to permutation. But $V_{v_\ell} = C$ because $\text{outdeg}(v_j) = 1$ for $j < \ell$. So $a(C)$ is identifiable up to permutation.

Case 2: $\text{indeg}(v_1) = 1$ and $\text{outdeg}(v_\ell) = 0$.

v_ℓ is a leaf so v_ℓ is an output. Let w_0 be the vertex which has an edge $w_0 \to v_1$. w_0 is not in C so $\text{outdeg}(w_0) > 1$ else C would not be maximal. Let w_1 be a vertex with edge $w_0 \to w_1$ and let u be an output connected to w_0. Let y be an output connected to w_1. $a(P(u,y))$ and $a(P(u,v_\ell))$ are identifiable up to

permutation. We have

$$P(u, y) \cap P(u, v_\ell) = P(u, w_0)$$
$$P(u, v_\ell) \setminus P(u, w_0) = C.$$

$P(u, w_0) \subset P(u, v_\ell)$ so by Proposition 5.11 $a(C)$ is identifiable up to permutation.

Case 3: $\text{indeg}(v_1) > 1$ and $\text{outdeg}(v_\ell) = 0$.

v_ℓ is a leaf so v_ℓ is an output. $\text{indeg}(v_1) > 1$ so there are two vertices, w_1 and w_2 so that $w_1 \to v_1$ and $w_2 \to v_1$ are edges. There is no path between w_1 and w_2 because $\mathcal{G}$ is acyclic. Therefore, there are distinct inputs, u_1 and u_2 so that there is a path between u_i and w_i for $i = 1, 2$. $a(P(u_1, v_\ell))$ and $a(P(u_2, v_\ell))$ are identifiable up to permutation and $P(u_1, v_\ell) \cap P(u_2, v_\ell) = C$. By Proposition 5.11, $a(C)$ is identifiable up to permutation.

Case 4: $\text{indeg}(v_1) = 0$ and $\text{outdeg}(v_\ell) = 1$.

v_1 is a root so v_1 is an input. Let ν_1 be the vertex with edge $v_\ell \to \nu_1$. ν_1 is not in the chain so there is a second edge for which ν_1 is the terminal vertex: $\nu_0 \to \nu_1$. Let y be an output connected to ν_1 and u an input connected to ν_0. $a(P(v_1, y))$ and $a(P(u, y))$ are identifiable up to permutation. We have

$$P(v_1, y) \cap P(u, y) = P(\nu_1, y)$$
$$P(v_1, y) \setminus P(\nu_1, y) = C.$$

$P(\nu_1, y) \subset P(v_1, y)$ so by Proposition 5.11, $a(C)$ is identifiable up to permutation.

Case 5: $\text{indeg}(v_1) = 0$ and $\text{outdeg}(v_\ell) > 1$.

v_1 is a root so v_1 is an input. Let ν_1 and ν_2 be vertices with edges $v_\ell \to \nu_1$ and $v_\ell \to \nu_2$. Let y_i be an output connected to ν_i for $i = 1, 2$. $a(P(v_1, y_i))$ is

identifiable up to permutation for $i = 1, 2$ and $P(v_1, y_1) \cap P(v_1, y_2) = C$ so $a(C)$ is identifiable up to permutation by Proposition 5.11.

Case 6: $\text{indeg}(v_1) = \text{outdeg}(v_\ell) = 1$.

Let w_0 be the vertex so that $w_0 \to v_1$ is an edge. There is a vertex, w_1 with edge $w_0 \to w_1$ else C is not maximal. Let ν_1 be the vertex with edge $v_\ell \to \nu_1$. There is a vertex, ν_0 with edge $\nu_0 \to \nu_1$ else C is not maximal. Let u_1 and u_2 be inputs with u_1 connected to w_0 and u_2 connected to ν_0. Let y_1 and y_2 be outputs with y_1 connected to w_1 and y_2 connected to ν_1. $a(P(u_1, y_1))$, $a(P(u_1, y_2))$, and $a(P(u_2, y_2))$ are identifiable up to permutation. We have

$$P(u_1, y_1) \cap P(u_1, y_2) = P(u_1, w_0)$$
$$P(u_1, y_2) \cap P(u_2, y_2) = P(\nu_1, y_2)$$
$$P(u_1, y_2) \setminus P(u_1, w_0) = P(v_1, y_2)$$
$$P(v_1, y_2) \setminus P(\nu_1, y_2) = C.$$

$P(u_1, w_0) \subset P(u_1, y_2)$ and $P(\nu_1, y_2) \subset P(v_1, y_2)$ so by Proposition 5.11, $a(C)$ is identifiable up to permutation.

Case 7: $\text{indeg}(v_1) > 1$ and $\text{outdeg}(v_\ell) = 1$.

This case is illustrated in Figure 5.3. Let w_i be a vertex with edge $w_i \to v_1$ for $i = 1, 2$. Let ν_1 be a vertex with edge $v_\ell \to \nu_1$. There is a vertex, ν_0, with edge $\nu_0 \to \nu_1$ else C is not maximal. Let u_i be an input connected to w_i for $i = 1, 2$ and u_3 be an input connected to ν_0. Let y be an output connected to ν_1. $a(P(u_i, y))$ is identifiable up to permutation for each $i = 1, 2, 3$. We have

$$P(u_1, y) \cap P(u_2, y) = P(v_1, y)$$
$$P(u_1, y) \cap P(u_3, y) = P(\nu_1, y)$$
$$P(v_1, y) \setminus P(\nu_1, y) = C.$$

$P(\nu_1, y) \subset P(v_1, y)$ so $a(C)$ is identifiable up to permutation by Proposition 5.11.

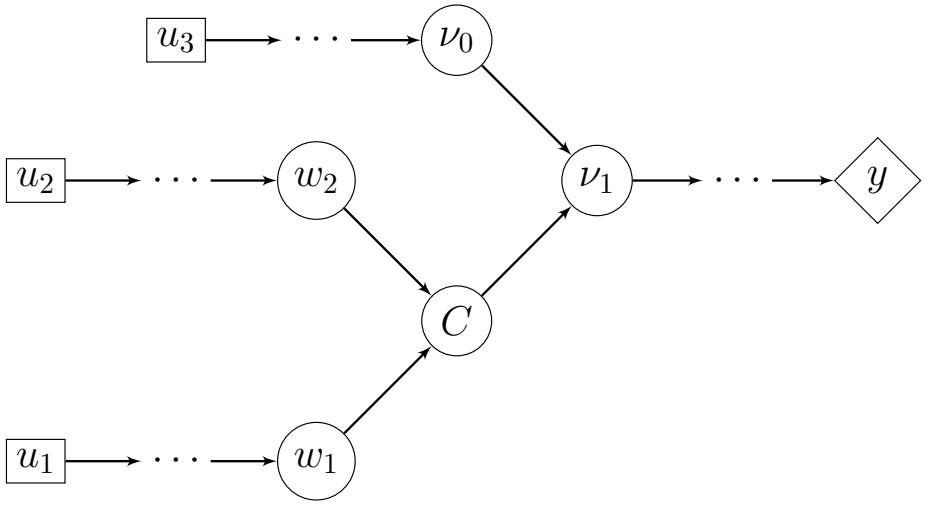

Figure 5.3: **Case 7 in the proof of Theorem 5.12.** The labels of the vertices match those used in the proof. Dots indicate where the graph is unspecified. Only the edges and vertices considered in the proof are drawn.

Case 8: $\text{indeg}(v_1) = 1$ and $\text{outdeg}(v_\ell) > 1$.

Let w_0 be the vertex with edge $w_0 \to v_1$. There must be a vertex w_1 with edge $w_0 \to w_1$ else C is not maximal. Let ν_1 and ν_2 be vertices with edges $v_\ell \to \nu_1$ and $v_\ell \to \nu_2$. Let u be an input connected to w_0. Let y_1, y_2, and y_3 be outputs with y_1 connected to w_1, y_2 connected to ν_1, and y_3 connected to ν_2. $a(P(u, y_i))$is identifiable up to permutation for $i = 1, 2, 3$. We have

$$P(u, y_1) \cap P(u, y_2) = P(u, w_0)$$
$$P(u, y_2) \cap P(u, y_3) = P(u, v_\ell)$$
$$P(u, v_\ell) \setminus P(u, w_0) = C.$$

$P(u, w_0) \subset P(u, v_\ell)$ so $a(C)$ is identifiable up to permutation by Proposition 5.11.

Case 9: $\text{indeg}(v_1) > 1$ and $\text{outdeg}(v_\ell) > 1$.

Let w_1, w_2, ν_1, and ν_2 be vertices with edges $w_1 \to v_1$, $w_2 \to v_1$, $v_\ell \to \nu_1$, and $v_\ell \to \nu_2$. Let u_i be an input connected to w_i for $i = 1, 2$. Let y_i be an output connected to ν_i for $i = 1, 2$. $a(P(u_i, y_j))$ is identifiable up to permutation for $i = 1, 2$, $j = 1, 2$. We have

$$P(u_1, y_1) \cap P(u_2, y_2) = C$$

so $a(C)$ is identifiable up to permutation by Proposition 5.11.

■

Theorem 5.13. *Let $\mathcal{N} = \{\mathcal{G}, \mathcal{I}, \mathcal{O}\}$ be a minimal linear feedforward network and let $y \in \mathcal{O}$. Then a_{yy} is globally identifiable.*

Proof. Let C_y be the maximal chain containing y. By Theorem 5.12, $a(C_y)$ is identifiable up to permutation. Let u be an input connected to y. $a^{u \dashrightarrow y}$ is identifiable and we will show that this term rules out solutions that permute a_{yy}.

Let $C_1, C_2, \ldots, C_k$ be the sequence of maximal chains in $u \dashrightarrow y$. Note that $C_k = C_y$. Let v_{if} and $v_{i\ell}$ be the first and last vertex in C_i respectively. Let $n_i = |C_i|$. Then $a^{u \dashrightarrow y}$ can be written as

$$a^{u \dashrightarrow y} = \left(\prod_{i=1}^{k} \pi^{n_i}(a(C)) / a_{v_{i\ell} v_{i\ell}} \right) \prod_{i=1}^{k-1} a_{v_{(i+1)f} v_{i\ell}}. \tag{5.3.1}$$

The product outside of the parentheses are terms corresponding to edges connecting chains, while the product in the parentheses are the terms corresponding to edges internal to the chains. In particular, $\pi^{n_k - 1}(a(C_k)/a_{v_{k\ell} v_{k\ell}}) = \pi^{n_k - 1}(a(C_y)/a_{yy})$ so that a_{vv} for $v \in C$ is a factor of (5.3.1) if and only if $v \neq y$. Therefore permutations of $a(C_y)$ must fix a_{yy} to be a solution.

■

The global identifiability of a_{yy} means that the leak parameters, b_y, are globally identifiable.

Noticing that there are no other terms in the input-output equation that break the permutation symmetries of the maximal chains shows that Theorem 5.12 and Theorem 5.13 is the best that we can do. That is, the maximal chains are identifiable up to permutation, a_{yy} is globally identifiable for $y \in \mathcal{O}$ and every permutation that respects this corresponds to a solution to the identifiability problem.

The maximal chains are identifiable up to permutation, but there is a question of what that means when a_{vv} may be the sum of multiple parameters when v is the terminal vertex of a chain. The following proposition shows what identifiability up to permutation of $\{a_{vv}\}$ means for the underlying parameters, $\{a_{wv}\}$.

Proposition 5.14. *Let $\mathcal{N} = \{\mathcal{G}, \mathcal{I}, \mathcal{O}\}$ be a minimal linear feedforward network and $C = 1, 2, \ldots, k$ be a maximal chain with $k \notin \mathcal{O}$. Let $\sigma \in S_k$. Then*

$$(a_{ii} = \alpha_{\sigma(i)\sigma(i)} \mid i = 1, \ldots, k-1) \times \left(a_{vk} = \frac{\alpha_{vk}}{\sum_{w,\, k \to w \in E} \alpha_{wk}} \alpha_{\sigma(k)\sigma(k)} \;\middle|\; k \to v \in E \right) \tag{5.3.2}$$

is a solution to the identifiability problem for $a(C)$.

Proof. C is identifiable up to permutation by Theorem 5.12. Therefore any solution must be contained in

$$\{(a_{ii} = \alpha_{\sigma(i)\sigma(i)}) \mid \sigma \in S_k\}. \tag{5.3.3}$$

Let $\sigma \in S_k$. We have that $a_{kk} = \sum_{k \to v \in E} a_{vk}$. Applying this to the proposed solution given in (5.3.2),

$$a_{kk} = \sum_{v,\, k \to v \in E} \frac{\alpha_{vk}}{\sum_{w,\, k \to w \in E} \alpha_{wv}} \alpha_{\sigma(k)\sigma(k)} = \alpha_{\sigma(k)\sigma(k)}$$

so that (5.3.2) is contained in (5.3.3).

Let u be an input and y be an output with u and y connected to C. It remains to show that (5.3.2) is consistent with the identifiability of the path $a^{u\dashrightarrow y}$. Let v be the vertex on the path with edge $k \to v$. Then

$$\begin{aligned} a^{u\dashrightarrow y} &= f(a(V \setminus C))a_{vk}\prod_{i=1}^{k-1} a_{(i+1)i} \\ &= f(a(V \setminus C))a_{vk}\prod_{i=1}^{k-1} a_{ii} \end{aligned}$$

where $f(a(V \setminus C))$ is a product of parameters corresponding to vertices not in C. For (5.3.2) to be consistent with $a^{u\dashrightarrow y}$ we need to show

$$a_{vk}\prod_{i=1}^{k-1} a_{ii} = \alpha_{vk}\prod_{i=1}^{k-1} \alpha_{ii}.$$

Plugging in (5.3.2),

$$\begin{aligned} a_{vk}\prod_{i=1}^{k-1} a_{(i+1)i} &= \frac{\alpha_{vk}}{\sum_{k\to w\in E}\alpha_{wk}}\alpha_{\sigma(k)\sigma(k)}\prod_{i=1}^{k-1}\alpha_{\sigma(i)\sigma(i)} \\ &= \frac{\alpha_{vk}}{\sum_{w,\ k\to w\in E}\alpha_{wk}}\alpha_{kk}\prod_{i=1}^{k-1}\alpha_{ii} \\ &= \frac{\alpha_{vk}}{\sum_{w,\ k\to w\in E}\alpha_{wk}}\left(\sum_{w,\ k\to w\in E}\alpha_{wk}\right)\prod_{i=1}^{k-1} a_{ii} \\ &= \alpha_{vk}\prod_{i=1}^{k-1}\alpha_{ii} \end{aligned}$$

as desired. ■

Example 5.8. Consider the linear chain of Figure 5.1. This graph is a maximal chain. $a_{nn} = b_n$ is globally identifiable by Theorem 5.13. By Theorem 5.12 solutions to the identifiability problem for the remaining parameters are

$$a_{(i+1)i} = \alpha_{(\sigma(i)+1)\sigma(i)}, \quad i = 1, 2, \ldots, n-1$$

where $\sigma \in S_{n-1}$.

Example 5.9. Consider the networks in Figure 5.2. Using Theorems 5.12 and 5.13 and Proposition 5.14 we solve the identifiability problem.

(a). 3 and 5 are the outputs so $a_{33} = b_3$ and $a_{55} = b_5$ are globally identifiable. The maximal chains are $C_1 = 1, 2$, $C_2 = 3$ and $C_3 = 4, 5$. Within C_1 the solutions are

$$(a_{21} = \alpha_{21}, a_{32} = \alpha_{32}, a_{42} = \alpha_{42}) \quad \text{and}$$
$$(a_{21} = \alpha_{32} + \alpha_{42},\ a_{32} = \frac{\alpha_{21}}{\alpha_{32} + \alpha_{42}}\alpha_{32},\ a_{42} = \frac{\alpha_{21}}{\alpha_{32} + \alpha_{42}}\alpha_{42}).$$

a_{44} is globally identifiable so $a_{54} = \alpha_{54}$.

(b). 5 is the output so $a_{55} = b_5$ is globally identifiable. The maximal chains are $C_1 = 1, 2$, $C_2 = 3$, and $C_3 = 4, 5$. $a_{33} = a_{43}$ and $a_{44} = a_{54}$ are thus globally identifiable. Within C_1 the solutions are

$$(a_{21} = \alpha_{21}, a_{42} = \alpha_{42}) \quad \text{and}$$
$$(a_{21} = \alpha_{42}, a_{42} = \alpha_{21}).$$

5.4 Michaelis-Menten Kinetics

The results of the previous sections are for linear kinetics. In this section, we show how they may be extended to Michaelis-Menten kinetics using small amplitude inputs.

Consider a reaction, $w_1 \to w_2$. With linear kinetics, the rate at which w_1 is converted to w_2 is proportional to the concentration of w_1 so that the reaction rate is given by $a_{w_2w_1}x_{w_1}$. Mechaelis-Menten kinetics assigns a nonlinear reaction rate given by

$$M_{w_2w_1}(x_{w_1}) = V_{w_2w_1}\frac{x_{w_1}}{K_{w_2w_1} + x_{w_1}} \tag{5.4.1}$$

where $V_{w_2w_1}$ is a parameter describing the maximum possible reaction rate and $K_{w_2w_1}$ is a parameter which describes the value of x_{w_1} at which the reaction rate is half maximal. Typically these parameters are denoted the $V_{\max}$ and K_M of the reaction, respectively. We can rewrite (5.4.1) as

$$M_{w_2w_1}(x_{w_1}) = \frac{V_{w_2w_1}}{K_{w_2w_1}} \frac{x_{w_1}}{1 + \frac{x_{w_1}}{K_{w_2w_1}}} \tag{5.4.2}$$

which shows that as

$$\frac{x_{w_1}}{K_{w_2w_1}} \to 0,$$

the reaction rate approaches

$$\frac{V_{w_2w_1}}{K_{w_2w_1}} x_{w_1},$$

a linear rate. We will be using this observation to relate the identifiability of a network with Michaelis-Menten kinetics to the identifiability of the network with linear kinetics. Specifically, the quotient $V_{w_2w_1}/K_{w_2w_1}$ has the same identifiability properties as $a_{w_2w_1}$.

Definition 5.14. A *Michaelis-Menten feedforward network* is a feedforward network where for each edge the reaction rate is given by (5.4.1) and for each output y, there is a leak rate given by

$$M_y(x_y) = V_y \frac{x_y}{K_y + x_y}.$$

Explicitly, the differential equation for the concentration of node j, x_j, in a Michaelis-Menten feedforward network is given by

$$\dot{x}_j = \chi_{j\in\mathcal{I}} u_j(t) + \sum_{i,\, i\to j\in E} M_{ji}(x_i) - \sum_{k,\, j\to k\in E} M_{kj}(x_j) - \chi_{j\in\mathcal{O}} M_j(x_j) \tag{5.4.3}$$

where for a set D, $\chi_{j\in D} = 1$ if $j \in D$ and is 0 otherwise. We first show that for a Michaelis-Menten feedforward network, if the size of the inputs are bounded, then the

concentrations are also bounded. Intuitively, this is obvious because the maximum flux out of a vertex cannot exceed the maximum flux into the vertex. Define

$$N_j = |\{i \in \mathcal{I} \mid \text{there is a path from } i \text{ to } j\}|. \tag{5.4.4}$$

and

$$K_j^{\max} = \max_{k,k\to j}\{K_{jk}\}. \tag{5.4.5}$$

Proposition 5.15. *Let $\mathcal{N}$ be a minimal network with Michaelis-Menten kinetics and suppose $u_i(t) \le \varepsilon < N_j^{-1}\sum_{k,\,k\to j} V_{jk}$ for each $i \in \mathcal{I}$, $j \in V$. Then*

$$x_j \le \frac{\varepsilon N_j K_j^{\max}}{\sum_{k,\,k\to j} V_{jk} - \varepsilon N_j}. \tag{5.4.6}$$

Proof. The statement follows from a trapping region argument. Let $j \in V$. To simplify notation, define

$$\overline{M}_j(x) = \sum_{k,j\to k} M_{kj}(x) + \chi_{j\in\mathcal{O}} M_j(x). \tag{5.4.7}$$

Now, define Ω by

$$\Omega = \{x \in \mathbb{R}^{|V|} \mid \overline{M}_j(x_j) \le \varepsilon N_j\}. \tag{5.4.8}$$

We claim that Ω is a trapping region. Given this claim,

$$\begin{aligned}\varepsilon N_j \ge \overline{M}_j(x_j) &= \sum_{k,\,k\to j} \frac{V_{jk}x_j}{K_{jk}+x_j} \\ &\ge \frac{x_j}{K_j^{\max}+x_j}\sum_{k,\,k\to j} V_{jk}.\end{aligned}$$

Rearranging the final inequality gives (5.4.6).

Now, we complete the proof by showing Ω is a trapping region. If j is an input vertex then j is a root so that $N_j = 1$ and

$$\chi_{j\in\mathcal{I}} u_j(t) + \sum_{i,\,i\to j} M_{ji}(x_i) = u_j(t) \le \varepsilon = \varepsilon N_j.$$

If j is not an input then

$$\begin{aligned}\chi_{j\in\mathcal{I}}u_j(t) + \sum_{i,\, i\to j} M_{ji}(x_i) &= \sum_{i,\, i\to j} M_{ji}(x_i)\\ &\leq \sum_{i,\, i\to j} \overline{M}_i(x_i)\\ &\leq \sum_{i,\, i\to j} \varepsilon N_i\\ &= \varepsilon N_j.\end{aligned}$$

So, on the boundary of Ω with $\overline{M}_j(x_j) = \varepsilon N_j$,

$$\begin{aligned}\dot{x}_j &= \chi_{j\in\mathcal{I}}u_j(t) + \sum_{i,\, i\to j\in E} M_{ji}(x_i) - \overline{M}_j(x_j)\\ &\leq \varepsilon N_j - \overline{M}_j(x_j) = 0.\end{aligned}$$

■

For $j \neq i$ let $c_{ji} = V_{ji}/K_{ji}$ when $i \to j \in E$ and $c_{ji} = 0$ otherwise. Define

$$c_{ii} = \begin{cases} -V_i/K_i - \sum_{j\neq i} c_{ji} & \text{if } j \in \mathcal{O} \\ -\sum_{j\neq i} c_{ji} & \text{otherwise.}\end{cases} \tag{5.4.9}$$

For $V_0 \subset V$ let $c(V_0) = \{c_{vv} \mid v \in V_0\}$. As a consequence of Theorem 5.12, we can prove the following.

Theorem 5.16. *Let C be a maximal chain of a directed tree $\mathcal{G}$. Then $c(C)$ is identifiable up to permutations in $\mathcal{N}(\mathcal{G})$ under Michaelis-Menten kinetics.*

Proof. For $j, i \in V$ let x_j denote the concentration of j in $\mathcal{N}(\mathcal{G})$ under linear kinetics with $a_{ji} = c_{ji}$ and $b_j = V_j/K_j$. Let z_j denote the concentration under Michaelis-Menten kinetics. Define $R_{ji}(x)$ by

$$R_{ji}(x) = \frac{V_{ji}x^2}{K_{ji}(K_{ji} + x)} \tag{5.4.10}$$

and notice that

$$M_{ji}(x) = \frac{V_{ji}}{K_{ji}}x + R_{ji}(x) = c_{ji}x + R_{ji}(x).$$

Similarly define $R_j(x) = \frac{V_j x^2}{K_j(K_j+x)}$.

Let $e_j = z_j - x_j$ and notice that

$$\begin{aligned}\dot{e}_j &= \dot{z}_j - \dot{x}_j \\ &= \sum_{i\ ,i\to j} a_{ji}e_i - \sum_{k,\ j\to k} a_{kj}e_j - \chi_{j\in\mathcal{O}} b_j e_j + \sum_{i,\ i\to j} R_{ji}(z_i) - \sum_{k,\ j\to k} R_{kj}(z_j) - \chi_{j\in\mathcal{O}} R_j(z_j).\end{aligned}$$

That is, letting $e = (e_1, \ldots, e_n)^T$,

$$\dot{e} = Ae + R(z) \tag{5.4.11}$$

where $R(z)$ is the vector defined by

$$R(z)_j = \sum_{i,\ i\to j} R_{ji}(z_i) - \sum_{k,\ j\to k} R_{kj}(z_j) - \chi_{j\in\mathcal{O}} R_j(z_j).$$

Therefore,

$$e(t) = \int_0^t \exp(A(t-s))R(z(s))\ ds. \tag{5.4.12}$$

Let $u(t)$ be an input vector with $u_i(t) \le \varepsilon \ll N_j^{-1}\sum_{k,\ k\to j} V_{jk}$ for each j. By Proposition 5.15, the corresponding solutions satisfy $z(t) = O(\varepsilon)$. Define the vector $R^+(z)$ by

$$R(z)_j^+ = \sum_{i,\ i\to j} R_{ji}(z_i) + \sum_{k,\ j\to k} R_{kj}(z_j) + \chi_{j\in\mathcal{O}} R_j(z_j), \tag{5.4.13}$$

and note that $|R^+(z(t))| = O(\varepsilon^2)$ for all t. Taking the absolute value of (5.4.12), and

letting $||\cdot||$ denote the matrix norm,

$$\begin{aligned}
|e(t)| &\leq \int_0^t ||\exp(A(t-s))||\ |R^+(z(s))|\ ds \\
&\leq \int_0^t ||\exp(A(t-s))||\ ds\ \max_{0\leq s\leq t} |R^+(z(s))| \\
&\leq \int_0^t \exp(-\min_i |a_{ii}|(t-s))\ ds\ \max_{0\leq s\leq t} |R^+(z(s))| \\
&= \frac{1}{\min_i |a_{ii}|}(1-\exp(-\min_i |a_{ii}|\ t))\max_{0\leq s\leq t} |R^+(z(s))| \\
&= O(\varepsilon^2).
\end{aligned}$$

By Theorem 5.1, the input-output equations for $\mathcal{N}$ with linear kinetics is given by (5.2.1):

$$f_j\left(\frac{d}{dt}\right)x_j = \sum_{k\in\mathcal{I}}(-1)^{j+k}f_{kj}\left(\frac{d}{dt}\right)u_k.$$

Now, $x_j = z_j - e_j$ so we may rewrite the input-output equations as

$$f_j\left(\frac{d}{dt}\right)(z_j - e_j) = \sum_{k\in\mathcal{I}}(-1)^{j+k}f_{kj}\left(\frac{d}{dt}\right)u_k. \tag{5.4.14}$$

However, $z_j = O(\varepsilon)$, $u_k = O(\varepsilon)$, while $e_j = O(\varepsilon^2)$. Therefore, we can choose a sequence of inputs, $u^n(t)$ with $u_j^n(t) \leq \varepsilon_n$ for each j and $\varepsilon_n \to 0$ to recover the identifiability of the coefficients of (5.4.14). Theorem 5.12 then applies with $c(C)$ replacing $a(C)$ in the statement of the theorem.

■

Chapter 6

Conclusion

In this dissertation, we defined a new type of singularity and studied the identifiability properties of feedforward networks. We summarize the results here.

Chapter 3 studied the feedback inhibition motif and showed that the stability properties of this network were proven to be heavily dependent on the network length, the feedback function, and a leakage parameter. We showed that feedback inhibtion is an example of a system in which a single mechanism could produce both homeostasis and Hopf bifurcations within the homeostatic plateau. This served as motivation to study the interaction of homeostasis and bifurcation more generally in the following chapter. In Chapter 4, we defined the homeostasis-bifurcation singularity for feedforward networks and characterized the unfoldings of these singularities. We found the transition varieties and classified all persistent phenomena of homeostasis-bifurcation points arising from codimension 0 or 1 homeostasis points and steady-state or Hopf bifurcations. Examples of artificial networks with homeostasis-bifurcation points were given and examples of biological systems with behavior similar to phenomena observed in the unfoldings of homeostasis-bifurcation points were given.

Chapter 5 studied the identifiability of linear feedforward networks associated to directed trees. We gave the minimal set of inputs and outputs required for local identifiability of the rate parameters. We proved that the graph could be decomposed into subgraphs in which the parameters were identifiable up to permutation of the rate parameters within each subgraph. We show how identifiability results for the network with linear reaction rates can be extended to a network with nonlinear kinetics.

Bibliography

[AEJ14] David F Anderson, Germán A Enciso, and Matthew D Johnston. Stochastic analysis of biochemical reaction networks with absolute concentration robustness. *Journal of The Royal Society Interface*, 11(93):20130943, 2014.

[BT10] J. Bass and J. S. Takahashi. Circadian integration of metabolism and energetics. *Science*, 330(6009):1349–1354, dec 2010.

[DBG+18] W. Duncan, J. Best, M. Golubitsky, H.F. Nijhout, and M. Reed. Homeostasis despite instability. *Mathematical Biosciences*, 300:130–137, jun 2018.

[DG19] William Duncan and Martin Golubitsky. Coincidence of homeostasis and bifurcation in feedforward networks. *International Journal of Bifurcation and Chaos*, 29(13):1930037, 2019.

[DGK+08] A. Dhooge, W. Govaerts, Yu. A. Kuznetsov, H. G.E. Meijer, and B. Sautois. New features of the software matcont for bifurcation analysis of dynamical systems. *Mathematical and Computer Modelling of Dynamical Systems*, 14(2):147–175, 2008.

[DSU+08] Charna Dibner, Daniel Sage, Michael Unser, Christoph Bauer, Thomas d'Eysmond, Felix Naef, and Ueli Schibler. Circadian gene expression is resilient to large fluctuations in overall transcription rates. *The EMBO Journal*, 28(2):123–134, dec 2008.

[Eis13] Marisa Eisenberg. Generalizing the differential algebra approach to input-output equations in structural identifiability. *arXiv preprint arXiv:1302.5484*, 2013.

[EMKO+16] Jeanne MO Eloundou-Mbebi, Anika Küken, Nooshin Omranian, Sabrina Kleessen, Jost Neigenfind, Georg Basler, and Zoran Nikoloski. A network property necessary for concentration robustness. *Nature communications*, 7(1):1–7, 2016.

[ERT13] Marisa C Eisenberg, Suzanne L Robertson, and Joseph H Tien. Identifiability and estimation of multiple transmission pathways in cholera and waterborne disease. *Journal of theoretical biology*, 324:84–102, 2013.

[GS85] M. Golubitsky and D. Schaeffer. *Singularities and Groups in Bifurcation Theory: Vol. I.* Applied Mathematical Sciences 51. Springer-Verlag, New York, NY, 1985.

[GS16] M. Golubitsky and I. Stewart. Homeostasis, singularities and networks. *J. Math. Biol.*, 1:DOI 10.1007/s00285–016–1024–2, 2016.

[KUAG17] Hiroyuki Kuwahara, Ramzan Umarov, Islam Almasri, and Xin Gao. Acre: Absolute concentration robustness exploration in module-based combinatorial networks. *Synthetic Biology*, 2(1), 2017.

[Mos86] R. Mosier. Root neighborhoods of a polynomial. *Mathematics of Computation*, 47:265–273, 1986.

[MS14] Nicolette Meshkat and Seth Sullivant. Identifiable reparametrizations of linear compartment models. *Journal of Symbolic Computation*, 63:46–67, 2014.

[MSE15] Nicolette Meshkat, Seth Sullivant, and Marisa Eisenberg. Identifiability results for several classes of linear compartment models. *Bulletin of mathematical biology*, 77(8):1620–1651, 2015.

[MYDH14] Bhanu Chandra Mulukutla, Andrew Yongky, Prodromos Daoutidis, and Wei-Shou Hu. Bistability in glycolysis pathway as a physiological switch in energy metabolism. *PLOS ONE*, 9(6):1–12, 06 2014.

[NBR14] H. F. Nijhout, J. Best, and M. Reed. Escape from homeostasis. *Math. Biosci.*, 257:104–110, 2014.

[RBG+17] M. Reed, J. Best, M. Golubitsky, I. Stewart, and H. F. Nijhout. Analysis of homeostatic mechanisms in biochemical networks. *Bulletin of Mathemtical Biology*, 79:2534–2557, 2017.

[SF10] Guy Shinar and Martin Feinberg. Structural sources of robustness in biochemical reaction networks. *Science*, 327(5971):1389–1391, 2010.

[Var00] Richard S. Varga. *Matrix Iterative Analysis*. Computational Mathematics. Springer, New York, NY, 2000.

[ZKE+15] Min Zhou, Jae Kyoung Kim, Gracie Wee Ling Eng, Daniel B Forger, and David M Virshup. A period2 phosphoswitch regulates and temperature compensates circadian period. *Molecular cell*, 60(1):77–88, 2015.

Biography

William Duncan earned a B.S. in Applied and Computational Mathematics with a minor in Computational Biology from Carnegie Mellon University in May 2015. In August 2015 he moved to Durham, North Carolina to begin graduate school as a PhD student studying mathematical biology at Duke University. William was a SAMSI graduate fellow from Fall 2018 through Spring 2019 in the Model Uncertainty: Mathematical and Statistical program. Upon completiion of his PhD in May 2020, he will take up a postdoctoral position in the Mathematics Department at Montana State University.